

DISS. ETH NO. 22498

**ANALYTICAL STRATEGIES FOR A SYSTEMATIC CHARACTERIZATION OF NANO-
PARTICLE RELEASE FROM COMMERCIAL SPRAY PRODUCTS**

A thesis submitted to attain the degree of

DOCTOR OF SCIENCES of ETH ZURICH
(Dr. sc. ETH Zurich)

presented by

SABRINA LOSERT

Master of Chemistry, Technical University of Munich

born on 04th March, 1987

citizen of Germany

accepted on the recommendation of

Prof. Dr. Konrad Hungerbühler, Examiner

Prof. Dr. Alexander Wokaun, Co-examiner

Prof. Dr. Christian Ludwig, Co-examiner

2015

„Darin besteht das Wesen der Wissenschaft. Zuerst denkt man an etwas, das wahr sein könnte. Dann sieht man nach, ob es der Fall ist und im Allgemeinen ist es nicht der Fall.“

Bertrand Russell (1872-1970), brit. Philosoph u. Mathematiker

Für meine Eltern.

Abstract

Nanomaterials exhibit rich physical and chemical phenomena and their fascinating and unusual properties have opened up a myriad of applications in various fields resulting in a tremendous increase in the use of engineered nanoparticles (ENP) in consumer products during the last years. In spite of the superior properties, ENP also raise concerns about adverse effects on biological systems and the human health. In particular, spray products containing ENP deserve closer attention with respect to the very critical exposure pathway.

Compared to nanoparticle-containing sprays, the release of pesticides from conventional spray products has been investigated in depth. Suitable analytical techniques detecting the mass of the released substances are well developed. On the other hand, nanoparticle-containing sprays are much less studied though they are perceived as critical for consumers. A few recent published studies presented analytical concepts/techniques for exposure experiments and generated data for exposure assessment. In the first part of this work, other publications were reviewed and the current approaches to characterize nanosprays were compared. Deficiencies were identified and ideas for future research were created. In addition, experimental setups used for exposure assessment from conventional sprays were reviewed and compared to setups used for nanoparticle-containing sprays. National and international norms and standards dealing with nanoparticle characterization in general, spray characterization, and exposure experiments were inspected with regard to their usefulness for standardizing spray experiments. It was determined that, due to largely varying experimental setups, it is not possible to compare exposure values for nanosprays. All studies were conducted with a limited batch of sprays and no systematic evaluation of the study conditions is available. A suitable set of experimental setups as well as minimum reporting requirements should

be agreed upon to enable systematic evaluation of consumer sprays in the future. Indispensable features of such experimental setups were developed and tested in this work specifically different spray durations as well as different spray directions were compared. Particle number concentration and size distribution was determined at different positions inside a spray chamber. Thus, different spray scenarios were re-enacted and a worst case scenario was identified. This scenario was then applied for the analysis of real consumer spray samples.

For the analysis of spray products next to aerosol analysis, the original spray suspension is important. Therefore we tried to improve an already existing method: asymmetric flow field flow fractionation (A4F). A drawback of this technique is particle-membrane interactions which can lead to unpredictable channel recoveries. Consequently, quantification of nanoparticles cannot be performed reliably, which degrades the A4F technique to a very sophisticated but rather qualitative tool for unknown nanoparticle dispersions. To elucidate the main mechanisms and identify major parameters responsible for particle-membrane interactions, systematic experiments were conducted. The influence of the membrane material, homogeneity, hydrophobicity, the ζ -potential, pH, ionic strength of the carrier solution, salts, and commonly used surfactants for A4F nanoparticle separation was discussed. To keep the parameters simple for the nanoparticle system, investigations were performed with standardized polystyrene particles. On the membrane side, three different membranes often used in literature were analyzed.

In case of two membranes, results indicated that recovery can be maximized with careful matching of membrane and particle charge. For the third membrane, the assumption of better recovery adjusting the ζ -potential did not hold through. Therefore we also studied the morphology of the membrane surface, which seems to be another major influencing factor of

particle-membrane interaction. In addition, next to these parameters the results show that also the hydrophobicity of the membrane surface and the particles plays an important role in particle-membrane interactions. As a result these new findings can improve the quality of results produced with A4F.

But as the matching of the carrier liquid, the particles, and the membrane material is very time consuming and even harder for real samples, we decided not to use A4F for the characterization of consumer spray suspensions.

In this work the suspension and the released aerosol of six different commercially available consumer spray products were analyzed and a broad spectrum of analytical methods were tested and compared. In addition, the already mentioned standardized setup for analysis of the aerosol was tested. A new online coupling technique (SMPS-ICPMS) for the simultaneous analysis of particle size and elemental composition of aerosol particles was applied. Results obtained with this new method are comparable to other, well established techniques. Comparison of particles in the original suspensions and in the generated aerosol showed that during spraying, single particles smaller than 20 nm were formed, even though in none of the suspensions single particle particles, just agglomerates with the smallest size of 280 nm were present. Both pump sprays and propellant gas sprays were analyzed and both potentially release particles in the nm size range. Both water-based and organic solvent-based sprays potentially release nanoparticles. However, an aqueous suspension in a pump spray dispenser seemed to deliver bigger agglomerates than organic suspensions in propellant gas dispensers.

Zusammenfassung

Nanomaterialien weisen aussergewöhnliche physikalische und chemische Eigenschaften auf; diese faszinierenden und ungewöhnlichen Charakteristiken haben eine Unzahl von Anwendungsmöglichkeiten in den unterschiedlichsten Bereichen hervorgerufen. Daraus resultierend ist der Gebrauch von technisch hergestellten Nanopartikeln in Konsumentenprodukten in den letzten Jahren drastisch angestiegen. Trotz all der positiven Eigenschaften von Nanopartikeln wurden in der letzten Zeit immer mehr Bedenken bezüglich negativer Auswirkungen auf biologische Systeme und die menschliche Gesundheit geäussert. Ganz besonders Spray Produkte, die Nanopartikel enthalten, verdienen hier genauerer Betrachtung bedingt durch ihren sehr kritischen Wirkungspfad durch die Aufnahme der Partikel über die Lunge.

Im Vergleich zu Nanopartikel haltigen Sprays wurde die Freisetzung von Pestiziden aus konventionellen Spray Produkten bereits tiefgründig untersucht und studiert. Geeignete analytische Messmethoden, welche die Masse der freigesetzten Substanzen bestimmen sind seit Jahren bekannt und daher auf einem sehr hohen Entwicklungsstand. Nanopartikel haltige Sprays sind hingegen deutlich weniger gut untersucht obwohl sie als kritisch für Konsumenten eingeschätzt werden. Ein paar aktuelle Studien zeigen analytische Konzepte und Messmethoden für Expositionsversuche auf und generieren gleichzeitig Daten für eine Expositionsabschätzung.

Im ersten Teil dieser Arbeit wurden diese Arbeiten kritisch rezensiert und aktuelle Ansätze zur „NanoSpray“ Charakterisierung wurden verglichen. Defizite wurden aufgedeckt und daraus resultierend wurden Ideen für zukünftige Untersuchungen erzeugt. Zusätzlich wurde der experimentelle Aufbau, welche für die Analyse von konventionellen Sprays verwendet wurde,

mit dem für die Analyse von Nanopartikel haltigen Sprays verglichen. Nationale und internationale Normen und Standards, welche sich mit der Charakterisierung von Nanopartikeln im Allgemeinen, Spray Charakterisierung und Expositions Experimenten befassen wurden hinsichtlich ihrer Verwendbarkeit für eine Standardisierung der Spray Experimente bewertet. Es wurde festgestellt, dass bedingt durch grosse Unterschiede im experimentellen Aufbau ein Vergleich der bisherigen Expositions Werte, welche in den verschiedenen bisherigen Studien ermittelt wurde nicht möglich ist. Alle Studien wurden mit einer begrenzten Anzahl an Proben durchgeführt und keine systematische Bewertung der Versuchs Konditionen ist vorhanden. Eine angemessene Zusammenstellung der analytischen Methoden, sprich des experimentellen Aufbaus, sowie ein Minimum an Dokumentations-Voraussetzung sollte erfüllt sein, um eine systematische Untersuchung von Nanopartikel haltigen Konsumenten Sprays in Zukunft möglich zu machen. Unabdingbare Charakteristika wie der experimentelle Messaufbau wurden daher weiterentwickelt und getestet. Besonders verschiedenen Spray Dauern und Richtungen wurden untersucht und die Ergebnisse verglichen. Die Partikel Anzahl sowie die Partikel Grösse wurden an unterschiedlichen Positionen innerhalb einer Spray Kammer bestimmt. Dadurch wurden verschiedenen Szenarien konstruiert und ein „Worst-Case“ Szenario wurde konstruiert. Diese Versuchsbedingungen wurden dann für die Analyse von Realproben herangezogen.

Für die Analyse von Spray Produkten ist neben der Analyse des Aerosols auch die Analyse der original Spray Suspension von Interesse. Hierzu haben wir versucht eine bereits existierende Methode, nämlich Asymmetrische Fluss Feld Fluss Fraktionierung (A4F), zu verbessern. Ein Manko dieser Methode sind die Partikel Membran Interaktionen welche zu unvorhersehbaren Wiederfindungen im Analysekanal führen. Folglich ist eine Quantifizierung der Nanopartikel

nicht möglich, wodurch A4F zu einer zwar durchdachten, aber wenig quantitativen Analysemethode für unbekannte Nanopartikel Suspensionen herabgestuft wird. Um den Mechanismus dieser Interaktionen und die grössten Einflussfaktoren aufzuklären, wurden systematische Experimente durchgeführt. Sowohl der Einfluss des Membran Materials, als auch die Homogenität, die Wasserabweisung und, das ζ - Potenzial sowie der Einfluss des pH Werts, der Ionenstärke des Trägermediums und die Zugabe von Salzen und Zusatzstoffen auf die Trennbarkeit von Nanopartikeln wurden untersucht. Um die diversen Parameter so einfach wie möglich zu halten wurden standardisierte Polystyrol Nanopartikel untersucht. Hinsichtlich der Membran wurden drei verschiedene Materialien, welche häufig in der Literatur vorkommen und verwendet werden untersucht. Auch die Auswahl der Salze und der Zusatzstoffe hat sich nach deren häufigen Anwendung in der Literatur orientiert.

Im Fall zweier Membranen zeigen die Resultate, dass die Wiederfindung durch vorsichtiges Anpassen der Ladungen der Membran und der Partikel optimiert werden kann. Für die dritte Membran allerdings hielt diese These, der Anpassung des ζ - Potentials nicht stand, weswegen wir zu dem Schluss gekommen sind, dass es noch andere oder zumindest einen anderen Einflussfaktor geben muss. Daher wurde zusätzlich die Morphologie der Membran Oberfläche analysiert, welche der zweite grosse Einfluss gebende Faktor der Partikel Membran Interaktionen zu sein scheint. Zusätzlich zu diesen Ergebnissen, haben Studien zur Wasserabweisung der Membranen gezeigt, dass auch dieser Faktor einen grossen Einfluss auf die Wiederfindung der Partikel hat. Diese neuen Erkenntnisse führen dazu, dass die Qualität der Messergebnisse, produziert mittels A4F, deutlich verbessert werden können.

Da das Abstimmen des Trägermediums auf die Partikel und das Membran Material enorm zeitaufwändig ist und für Realproben mit einer hohen Matrix nur noch schwieriger wird ha-

ben wir entschlossen, A4F nicht als Analysemethode für die Analyse der Spray Suspensionen heranzuziehen. Für die vorliegende Arbeit wurden die Suspensionen und das freigesetzte Aerosol von sechs verschiedenen kommerziell erhältlichen Konsumenten Sprayprodukten untersucht und ein breites Spektrum an analytischen Methoden getestet und verglichen. Zusätzlich wurde das im ersten Teil der Arbeit neu entwickelte standardisierte Setup zur Aerosolanalyse getestet. Weiter wurde eine neue online Kopplung von einem SMPS mit einem ICPMS zur simultanen Analyse der Partikel Grösse und der chemischen Zusammensetzung angewendet. Die Ergebnisse, welche mit dieser neuen Methode gewonnen wurden, wurden mit alten, etablierten Methoden verglichen. Ein Vergleich der Partikelgrösse in der original Suspension mit der Partikelgrösse, freigesetzt nach dem Sprühen zeigt, dass während des Sprayvorgangs einzelne Partikel kleiner 20 nm gebildet werden, obwohl in der Suspension keine einzelnen Partikel, sondern nur Agglomerate mit einer kleinsten Grösse von 280 nm zu finden sind. Sowohl Pumpsprays, als auch Druckgas-Spraydosen wurden untersucht und es wurde gezeigt, dass beide Partikel im Nanometer Grössenbereich emittieren können. Wasser basierende und organische Lösungsmittel basierende Sprays können potenziell Nanopartikel freisetzen. Allerdings scheint es, als ob eine Kombination aus wässriger Lösung abgefüllt in einer Pumpflasche grössere Agglomerate freisetzt als eine Druckgas-Spraydose gefüllt mit einer auf organischer Basis bestehenden Nanopartikelsuspension.

Danksagung

An erster Stelle möchte ich Prof. Konrad Hungerbühler danken, welcher mir die Möglichkeit gab meine Arbeit in seiner Arbeitsgruppe anzufertigen. In vielen Gesprächen und Diskussionen hatte er immer ein offenes Ohr für meine Ideen und Wünsche. Auch durch seine unvergleichbare hilfsbereite Art hat er mir auch über schwere Phasen während meiner Promotion hinweggeholfen. Vielen Dank Konrad.

An dieser Stelle sollte der Dank an den Betreuer der Dissertation folgen. Leider kann ich mich bei Dr. Andrea Ulrich nicht mehr bedanken, da sie während der Anfertigung der Arbeit einen tragischen Unfall hatte. Daher möchte ich ihr hier an dieser Stelle gedenken. Sie war eine fabelhafte Wissenschaftlerin und eine mindestens genauso gute Mentorin. Andrea du hast eine grosse Lücke hinterlassen und wir werden dich nie vergessen.

Dr. Natalie von Goetz gilt daher mein innigster Dank, da Sie die unvorhergesehen Lücke als Betreuerin meiner Arbeit übernommen hat. Danke Natalie, dass du dich sofort dazu bereit erklärt hast und mir mit deinem Wissen und deiner Erfahrung immer hilfsbereit und mit Rat und Tat zur Seite gestanden hast.

Prof. Alexander Wokaun und Prof. Christian Ludwig danke ich sehr für die Übernahme des Koreferats.

Dem Bundesamt für Gesundheit möchte ich für die grosszügige finanzielle Unterstützung danken. Zudem danke ich Christoph Studer, Martine Bourqui-Pittet und Tobias Walser für die regelmässigen Diskussionen und Meetings.

Heinz Vonmont möchte ich dafür danken, dass ich meine Arbeit in seiner Abteilung anfertigen durfte.

Einen enormen Dank möchte ich an Dr. Harald Hagendorfer richten, der immer ein offenes Ohr hatte, wenn es um Probleme bei der Laborarbeit ging. Ohne deine Hilfe und Unterstützung wären manche Hürden sicher etwas höher gewesen.

Meinen beiden Büro-Kollegen Adrian (der kleine) und Adrian (der grosse) möchte ich für die tollen 3 ½ Jahre danken. Ihr hattet immer ein offenes Ohr, sei es in privater als auch in beruflicher Hinsicht gewesen. Auch meinen ganzen anderen Kollegen an der EMPA möchte ich herzlich für die tolle Zeit danken. Ganz besonders Julian, Regula, Conny, Beni, Pascal, Mustafa und allen anderen „Cafe-Raum-Pausenmacher“. Ihr habt die Pausen nie langweilig werden lassen.

Zusätzlich zu den Kollegen von der EMPA möchte ich mich auch bei den Kollegen an der ETH bedanken, ganz besonders der Gruppe „Human Exposure Analysis“ und Isabelle für ihre Unterstützung, wenn es um organisatorische Fragen ging.

I would like to thank all past collaboration partners at Empa and Eawag. Thanks to the particle laboratory at Eawag, the electron microscopy center at Empa, the Laboratory for Air Pollution/Environmental Technology and the Applied Wood Materials laboratory.

Weiter möchte ich mich bei meinem Freund Lucas für die Unterstützung jeglicher Art bedanken.

Der grösste Dank geht an meine Eltern. Durch euch allein wurde all das möglich. Danke, dass ihr mich zu der Person gemacht habt, die ich heute bin. Ich bin stolz und dankbar so tolle Eltern zu haben.

Abbreviations

A4F	Asymmetric Flow Field Flow Fractionation
AISE	Int. Association for Soaps, Detergents and Maintenance Product
APS	Aerosol Particle Sizer
ART	Advanced Research Tool
ASTM	American Society for Testing and Materials
BAMA	British Aerosol Manufacturers Association
CPC	Condensation Particle Counter
DIN	Deutsches Institut für Normen
DLS	Dynamic Light Scattering
DMA	Differential Mobility Analyzer
ECETOC	European Centre for Ecotoxicology and Toxicology of Chemicals
EDX	Energy Dispersive X-Ray
EGRET	ESIG GES (Generic Exposure Scenario) Risk and Exposure Tool
ENP	Engineered Nanoparticles
ESIG	European Solvents Industry Group
FE-SEM	Field Emission Scanning Electron Microscopy
FMPS	Fast Mobility Particle Sizer
GC/ECD	Gas Chromatography/Electron Capture Detector
GC/FID	Gas Chromatography/Flame Ionization Detector
GC/MS	Gas Chromatography/Mass Spectrometry
HR-SEM	High Resolution Scanning Electron Microscopy
ICPMS	Inductively Coupled Plasma Mass Spectrometry
ISO	International Organization for Standardization
mNOAA	manufactured Nano Objects and their Agglomerates and Aggregates
NIST	National Institute of Standards and Technology
OECD	Organization for Economic Co-operation and Development

OPC	Optical Particle Counter
PBPK	Physiologically based pharmacokinetic modeling
PMP	Particle Measurement Program
RDD	Rotating Disc Diluter
REACH	Registration, Evaluation, Authorization and Restriction of Chemicals
SEM	Scanning Electron Microscopy
SMPS	Scanning Mobility Particle Sizer
spICPMS	single particle ICPMS
STEM	Scanning Transmission Electron Microscopy
TEM	Transmission Electron Microscopy
VDI	Verein Deutscher Ingenieure
VOC	Volatile Organic Carbon
WHO	World Health Organization
ENM	Engineered Nanomaterial
PDI	Polydispersity Index
UV/Vis	Ultraviolet-Visible Spectrophotometry
PES	Polyethylensulfone
PSS	Polysulfon Sulfonate
kDa	Kilo Dalton
RC	Regenerated Cellulose
PVDF	Polyvinylidifluoride
AFM	Atomic Force Microscopy
UCPC	Ultrafine Condensation Particle Counter
SDS	Sodium Dodecyl Sulfate
HPLC	High Performance Liquid Chromatography
PE-LD	Low-Density Polyethylene
DI water	De ionized water

Table of contents

1	General Introduction.....	24
1.1	Engineered Nanoparticles.....	25
1.2	State of research and positioning of the own work.....	26
1.3	Objectives and structure of the thesis.....	29
2	Classification of Nanosprays – Literature Review.....	32
2.1	Introduction.....	32
2.2	Review of spray experiments.....	36
2.3	National and international standards and guidelines.....	37
2.4	Conventional spray products: experimental and analytical setup.....	39
2.5	NOAA – containing sprays: experimental and analytical setup.....	46
3	Investigation of appropriate analytical concepts for nanoparticle analysis in suspensions	58
3.1	Overview over hyphenated techniques for nanoparticle analysis.....	58
3.2	Evaluation of membrane surface characteristics on particle-membrane interaction in field-flow-fractionation analysis.....	61
3.3	Experimental Section.....	65
3.4	Results and Discussion.....	69
4	Investigation of appropriate analytical concepts for nanoparticle analysis in aerosols.....	82
4.1	Introduction.....	82
4.2	Classification of nano sprays.....	83
4.2.1	General categorization.....	83
4.2.2	Application.....	84
4.3	Experimental Section.....	85
4.4	Results.....	87
5	Real consumer spray process assessment.....	102

5.1	Introduction.....	102
5.2	Experimental section.....	106
5.3	Results	113
5.4	Discussion	126
6	Conclusion and Outlook.....	132
7	Appendix.....	142
7.1	Critical aspects of sample handling for direct nanoparticle analysis and analytical challenges using asymmetric field flow fractionation in a multi-detector approach.....	142
7.1.1	Introduction.....	142
7.1.2	Prospects and limitations of spICPMS and A4F-ICPMS.....	147
7.1.3	Results and Discussion.....	154
7.1.4	Assumed theory of particle –particle and particle-membrane interaction	165
7.1.5	Conclusion	169
7.2	Membrane-particle interactions in an asymmetric flow field flow fractionation channel studied with titanium dioxide nanoparticles.....	172
7.2.1	Introduction.....	172
7.2.2	Material and Methods.....	177
7.2.3	Results and Discussion.....	180
7.2.4	Summary and Conclusion.....	195
7.2.5	Outlook.....	197
7.3	General supplementary material	199
8	References.....	202

Chapter 1

1 General Introduction

The application and amount of consumer products in industrial countries has risen significantly during the last decades. Along with that, a constant development of new materials and products can be observed. To improve the quality, the stability, and the functionality of these products, newly developed compounds are added. These compounds can then get in contact with the human body or the environment when they are released from the products.

One group of these compounds is engineered nanoparticles (ENPs). As ENPs exhibit rich physical and chemical phenomena, they are used more and more in consumer products. ENPs of different properties including shape, coating, or diameter have entered the market and are added to consumer products. During the last years, the questions about adverse health effects and toxicity of ENPs appear more and more. Therefore analytical techniques need to be developed detecting the quantity of these compounds to guarantee a proper risk assessment.

1.1 Engineered Nanoparticles

Experts from ISO and ASTM provide different definitions for the word nanoparticle. Both define a nanoparticle in the scale from 1 – 100 nm. Since particles are three dimensional, standards define that two or three dimensions must be between 1 – 100 nm. (ISO 2008, ASTM 2012)

Other definitions also exist, like the one from the Scientific Committee on Emerging and Newly Identified Health Risks (SCENIHR), offers a more complex approach which divides nanoparticles into three categories: category 1: size > 500 nm; category 2: 500 nm > size >100 nm; category 3: 100 nm > size >1 nm. The category of nanoparticle defines here the recommended approach for risk assessment. (SCENIHR 2010)

Next to these definitions, one can distinguish between three different types of nanoparticles: natural, anthropogenic, and engineered nanoparticles. Naturally occurring nanoparticles can be found in volcanic ash, ocean spray, and fine sand and dust. Biological matter, like viruses, can also be defined as natural nanoparticles. The other two types of nanoparticles can also be called “man-made” nanoparticles whereupon anthropogenic nanoparticles are by-products of human activities and have generally poorly controlled size and shape. Engineered nanoparticles on the other hand have very precisely controlled sizes, shapes, and compositions. They can even contain layers made of different chemical compositions, so called core-shell particles.

1.2 State of research and positioning of the own work

The number of nanoparticle-containing consumer products increased over the last 10 years from a few to several hundreds and their number is expected to increase in the future. Sprays which contain nanoparticles were identified as a most critical class due to the direct exposure pathway via lungs which implies an enhanced health risk.

Safety and health effects of ultra-fine particles (nanoparticles) are well known in emission control of combustion generated nanoparticles and adequate monitoring concepts for emission control were already developed and recently implemented by the PMP protocol for particle measurements. (UNESCO 2007) For the assessment of air quality, first analytical concepts for the implementation of particle number analysis in air quality monitoring networks are in the test phase. (Wiedensohler 2010) However, similar concepts need to be implemented also in the assessment of engineered nanoparticles.

In a prior work performed by Lorenz, an initial analytical approach was applied for a preliminary investigation of the behavior of nanosilver in aqueous spray suspensions and primarily applied also to selected commercial consumer sprays. (Hagendorfer, Lorenz et al. 2010, Lorenz, Hagendorfer et al. 2011) The study identified the importance of the size distribution of the generated spray aerosols which is mainly dispenser-dependent as the main influencing factor for the fate of the nanoparticles. Figure 1.1 describes this first postulated hypothesis. (Ulrich and Hagendorfer 2009, Hagendorfer, Lorenz et al. 2010)

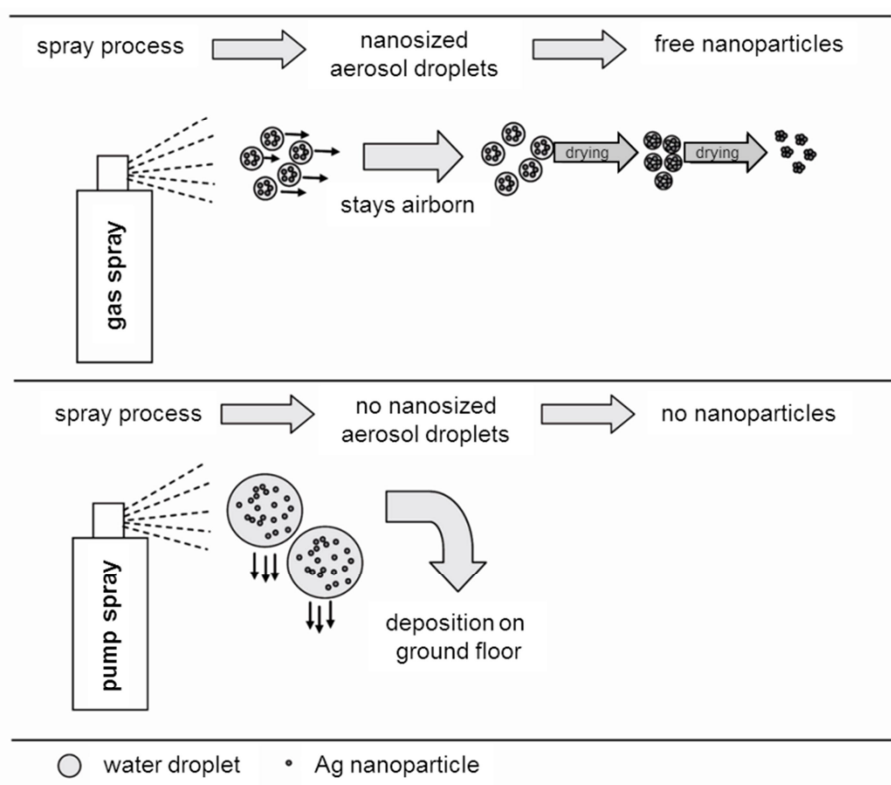


Figure 1.1: Scheme of understanding of the spray process, subsequent nanoparticle transport, and release using a propellant gas spray or a pump spray dispenser. (Hagendorfer, Lorenz et al. 2010)

A critical review of the literature and the used approach already showed that there is still a lack of systematic approaches and analytical concepts for appropriate exposure simulation as well as a lack of analytical concepts. Also a lack of standardized spray experiments which can provide suitable data for later exposure modeling exists. A need for further development is seen and this thesis will focus on this need.

A standardized validated analytical concept which is appropriate for exposure/risk assessment will be conducted.

1. Based on the already existing analytical basic approach, concepts for aerosol analysis need to be systematically elaborated
 - a. Standardization of the spray chamber experiments
 - b. Enhancement of analytical concept and validation
2. Methods for nanoparticle analysis in suspension need to be tested, compared, and, if necessary, improved
3. Analysis of further consumer spray products

1.3 Objectives and structure of the thesis

The overall aim of this work is to find and compare analytical methods for the assessment of consumer exposure to ENPs caused by the use of consumer spray products.

Accordingly, the results of this thesis are presented in four main chapters:

Chapter 2: "Classification of Nanosprays"

The first chapter is a literature review dealing with conventional and nanoparticle-containing sprays. The major objective of this chapter is to identify most suitable analytical setups as well as a critical evaluation of given information and performances. An optimization by identifying the knowledge gaps and providing concepts how to fill them is given.

Chapter 3: "Appropriate analytical concepts for nanoparticles in suspension"

The aim of this chapter is to improve an already known method for nanoparticle analysis in suspension, A4F. The suitability of this technique for analysis of consumer products is evaluated.

Chapter 4: "Appropriate analytical concepts for nanoparticles in aerosol"

The goal of this chapter is to propose concepts for appropriate analytical setups for nanoparticle analysis in aerosols. In the end, a validated and exactly specified "ready to go" setup should be received, demonstrating a worst-case scenario for consumer exposure.

Chapter 5: "Real consumer spray process assessment"

This chapter will deal with analyzing real consumer spray products in this way that real spray processes are simulated. In this way, a realistic risk assessment can be performed. Therefore the knowledge from Chapter 4 is of importance.

Chapter 2

2006, Sung, Ji et al. 2008, Ganguly, Upadhyay et al. 2011, Semmler-Behnke, Kreyling et al. 2012) However, also potentially harmful organic substances like pesticides and biocides are being used in sprays, (Berger-Preiß, Koch et al. 2004, Berger-Preiß, Boehncke et al. 2005, Berger-Preiß, Gerling et al. 2006, Berger-Preiß, Koch et al. 2006, Vernez, Bruzzi et al. 2006, Berger-Preiß, Koch et al. 2009) so that in the context of both the pesticides and the biocides regulation an assessment of inhalation exposure is mandatory. With the introduction of REACH also consumer sprays have moved into the regulatory focus. (ECHA 2008) On principle, the same approaches can be used for the exposure assessment of classical biocidal and mNOAA-containing sprays, but both with respect to measurement and modeling mNOAA pose special challenges.

The properties that determine nanoparticle activity (and toxicity) are size distribution, agglomeration state, number concentration, chemical composition, particle shape and crystallinity, as well as surface area and surface functionality. (Ulrich, Losert et al. 2012) How nanoparticle properties determine their toxicity is discussed by Krug and Wick (Krug and Wick 2011), but shortly summarized below together with an illustration how these particle properties can change during and after the process of spraying.

One very important metric for toxicity supposedly is the particle size, (Krug and Wick 2011) since it influences nanoparticle uptake into the cell and body tissue. The size distribution of particles directly after spraying, however, is not the same as the size distribution that is available for inhalation. The following processes influence the size distribution during and after spraying (see also Figure 2.1): First, the droplets are moving away from the spray can with a velocity that is defined by the design of the spray can. The distribution of particles along the spraying axis is a function of the velocity of the droplets. It is important to investigate where

the highest number of droplets will be found along this axis, because at that point presumably the highest exposure for consumers will result. Droplets in the size range of a few micrometers will then diffuse and stay up in the air for some time. Larger droplets will sediment, merge with other droplets and grow on their way. When the solvent evaporates, the particles inside the droplets can aggregate so that the resulting aggregates are larger than the initial particles present in the suspension. Also smaller droplets containing only one or few particles can dry, which results in particles in the nanometer size range. In addition, background particles (nano or larger) can influence the droplet size and thereby the final particle size. A high number concentration of background particles induces larger agglomerates because the former act as seed crystals for agglomeration, (Seipenbusch, Binder et al. 2008) thereby reducing the exposure to nanoparticles both by reducing the number concentration and by shifting the size distribution to sizes beyond the nanoscale.

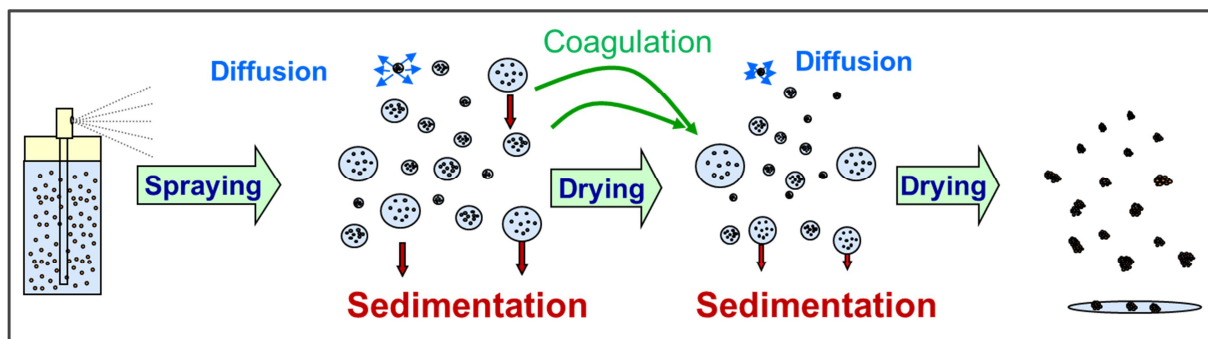


Figure 2.1: Processes influencing nanoparticle size and aggregation status during and after spraying.

A further property that influences the risk from nanoparticles is the number concentration. A high number concentration of particles results in more particles being inhaled and consequently in a higher risk. Also the chemical composition of the particles has a strong influence on the risk, since e.g. some metals (Fe, Cu, Zn) are suspected to promote Alzheimer's disease (González-Domínguez, García-Barrera et al. 2014), while other nanoparticles are readily de-

gradable in the human body and thus pose little risk. They are even used as drug delivery devices. (Soppimath, Aminabhavi et al. 2001) Also the particle shape is of importance as fiber-shaped particles like carbon nanotubes can increase the risk of lung cancer (Toyokuni 2013) whereas e.g. fullerenes, which can have the same chemical composition, do not pose a risk. (Aschberger, Johnston et al. 2010) The same holds true for the crystallinity of particles: rutile is supposed to be less harmful than anatase. (Zhang, Bai et al. 2012) The surface area and functionality influence the toxicity of nanoparticles by modulating the uptake of nanoparticles into the human body. (Hirn, Semmler-Behnke et al. 2011) During spraying the surface of particles can be coated by other ingredients present in the spray product, which results in changes in the surface charge or functionality.

Experimental set-ups to assess human exposure to mNOAA-containing sprays were recently proposed (Nørgaard, Jensen et al. 2009, Chen, Afshari et al. 2010, Hagendorfer, Lorenz et al. 2010, Lorenz, Hagendorfer et al. 2011, Quadros and Marr 2011, Bekker 2014) and the attempt was made to model exposure from consumer sprays on the basis of particle number instead of mass concentration. These new analytical concepts allow measuring some of the properties mentioned above.

This study aimed to review and compare the existing approaches for the exposure assessment of conventional sprays (that e.g. contain biocides) and mNOAA -containing sprays. Special emphasis was given to evaluating data requirements for a reliable exposure assessment and how to improve experimental and analytical setups.

2.2 Review of spray experiments

Concerns related to spray applications exist since some decades. Therefore, in 1984 the group of Gold (Gold, Holcslaw et al. 1984) published the first spray experiments in the US where exposure to ingredients of a biocidal spray product was assessed. Due to the increasing use of manufactured nano-objects in spray products, also risk and exposure assessments for mNOAA -containing sprays became necessary. Thus, about 5 years ago, different research groups started independently to study exposure to mNOAA from sprays, focusing on metallic (Hagendorfer, Lorenz et al. 2010, Lorenz, Hagendorfer et al. 2011, Nazarenko, Han et al. 2011, Quadros and Marr 2011) and organic nanoparticles. (Nørgaard, Jensen et al. 2009) They identified specific requirements for the analysis and later exposure assessment of mNOAA -containing spray products.

Currently, there are no agreed guidelines how to study the release of substances from spray products. Therefore, this chapter reviews the existing literature to give a systematic overview of the different experimental and analytical approaches used for studying exposure to substances in sprays, and how this data subsequently is used for exposure assessment. In order to evaluate and discuss the specific needs for mNOAA containing sprays, we first evaluate the experimental setups for “conventional” sprays (without mNOAA) and mNOAA containing sprays, respectively, and later compare them.

2.3 National and international standards and guidelines

There are standards, norms and guidelines available for the evaluation of exposure and toxicity for different types of sprays and nano-aerosols (Table 2.1). In general, these guidelines are dealing with the instrumental setup and give recommendations for instruments: how to use them, how to calibrate them and which instrument is valid for which application. Also guidelines for assessing spray toxicity have been developed.

To date, there are no norms or standards available for the risk assessment of (consumer) mNOAA -containing spray products. Nevertheless many aspects treated in the guidelines and norms for workplace exposure can be adapted. The standards for measuring aerosols (ASTM 2010, ASTM 2010, ASTM 2012) are mandatory in the publicly funded sector of the USA and could be used in a modified way for mNOAA -containing sprays. The NIST guidelines (NIST 2010, NIST 2011) for mNOAA in solutions are indicative and propose strategies for the characterization of nanoparticles. The same applies for the DIN (ISO 2010, DIN 2012, DIN 2012) and ISO (ISO/TR 2007) norms on the characterization of inhalable mNOAAs. Furthermore, OECD guidelines on inhalation toxicity tests for aerosols, (OECD 2009, OECD 2009, OECD 2009) which are mandatory in the OECD member states (international; government, industry, independent laboratories) could be adapted for mNOAA containing aerosols.

Table 2.1: National and international guidelines for the evaluation of exposure and toxicity for conventional spray products and nanoaerosols.

Valid for	Guideline	Title	Year	Scope	Purpose	Level of regulation
Aerosols in general	ASTM D4532-10 (ASTM 2010)	Standard Test Method for Respirable Dust in Workplace Atmospheres Using Cyclone Samplers	2010	Respirable dust concentrations	Test methods for dust in the range of 0.5 – 10 mg/m ³	mandatory in the US
	ASTM D4336-054 (ASTM 2010)	Standard test method for determination of the output per strokes of a mechanical pump dispenser	2010	Consumer sprays in pump dispenser	Determination of amount per Stroke	mandatory in the US
	ASTM D6062-07 (ASTM 2012)	Standard Guide for Personal Samplers of Health-Related Aerosol Fractions	2012	Respirable dust concentrations	Conventions for personal samplers of specific particle size dependent fractions of aerosols	mandatory in the US
Inhalable NPs	ISO/TR 27628 (ISO/TR 2007)	Workplace atmospheres – Ultrafine, nanoparticle and nanostructured aerosols – Inhalation exposure characterization and assessment	2007	Workplace atmosphere – Inhalation exposure assessment	Background information and sampling guideline to monitor nanoaerosol exposure	mandatory in the US
	DIN EN ISO 10808:2010 (ISO 2010)	Nanotechnologies – Characterization of nanoparticles in inhalation exposure chambers for inhalation toxicity testing	2010	Characterization of nanoparticles for inhalation exposure	Assessment of inhalation toxicity for particle mass, size distribution, number concentration and composition	mandatory in Europe
	DIN 33899-1 (DIN 2012)	Workplace exposure – Guide for the use of direct-reading instruments for aerosol monitoring – Part 1: Choice of monitor for specific applications (Draft)	2012	Strategies for determination of inhalable mNOAAs at workplaces	Evaluation of available direct-reading instruments for aerosol monitoring	mandatory in Germany
	DIN 33899-2 (DIN 2012)	Workplace exposure – Guide for the use of direct-reading instruments for aerosol monitoring – Part 2: Evaluation of airborne particle concentrations using optical particle counters (Draft)	2012	Strategies for determination of inhalable mNOAAs at workplaces using an optical particle counters	Evaluation of an optical particle counters for aerosol monitoring	mandatory in Germany
NP solutions	NIST PCC-7 (NIST 2010)	Measuring the size of nanoparticles using transmission electron microscopy (TEM)	2010	Offline size determination - Image Analysis	Sample preparation and determination of mean size using TEM	indicative
	NIST PCC-15 (NIST 2011)	Measuring the size of colloidal gold nanoparticles using high-resolution scanning electron microscopy	2011	Offline size determination - Image Analysis	Sample preparation and determination of mean size of citrate stabilized Au mNOAAs using HRSEM	indicative
Inhalation toxicity	OECD Test Guideline 403 (OECD 2009)	Acute Inhalation Toxicity	2009	Acute inhalation toxicity of aerosols	Obtaining sufficient information on the acute toxicity of aerosols	mandatory internationally
	OECD Test Guideline 412 (OECD 2009)	Subacute Inhalation toxicity: 28-Day Study	2009	Subacute inhalation toxicity of aerosols	Obtaining sufficient information on the sub-acute toxicity of aerosols	mandatory internationally
	OECD Test Guideline 413 (OECD 2009)	Subchronic inhalation toxicity: 90-Day Study	2009	Subchronic inhalation toxicity of aerosols	Obtaining sufficient information on the sub-acute toxicity of aerosols	mandatory internationally

2.4 Conventional spray products: experimental and analytical setup

Investigated sprays

Several groups investigated the release of insecticides from sprays (Gold, Holcslaw et al. 1984, Class and Kintrup 1991, Llewellyn, Brazier et al. 1996, Berger-Preiß, Koch et al. 2004, Berger-Preiß, Boehncke et al. 2005, Berger-Preiß, Gerling et al. 2006, Berger-Preiß, Koch et al. 2006, Berger-Preiß, Koch et al. 2009) and one group the release of fluorinated acrylate polymers and isoparaffinic hydrocarbons from waterproofing sprays. (Vernez, Bruzzi et al. 2006) In these studies the potential risk of the substances due to inhalation was assessed based on the released mass of the substances. Data are available for sprays based on organic solvents (Gold, Holcslaw et al. 1984, Class and Kintrup 1991, Berger-Preiß, Boehncke et al. 2005, Vernez, Bruzzi et al. 2006, Berger-Preiß, Koch et al. 2009) and for water-based sprays. (Gold, Holcslaw et al. 1984, Class and Kintrup 1991) Also the influence of different spray vessels and dispersion mechanisms (pump vs. propellant spray) on the released mass has been assessed. (Berger-Preiß, Koch et al. 2009) Some groups used aerosol generators for more standardized aerosol formation. (Class and Kintrup 1991, Llewellyn, Brazier et al. 1996, Berger-Preiß, Boehncke et al. 2005)

Experimental Setup

Almost all the experiments were carried out under field conditions, i.e. inside an airplane, (Berger-Preiß, Koch et al. 2004, Berger-Preiß, Boehncke et al. 2005, Berger-Preiß, Gerling et al. 2006) in model rooms (Class and Kintrup 1991, Berger-Preiß, Koch et al. 2006) or outdoors (Gold, Leavitt et al. 1982, Gold, Holcslaw et al. 1984) in order to generate realistic data. One experiment was conducted in a simulation chamber (Vernez, Bruzzi et al. 2006) where the

spray process itself was investigated. Due to the diverging dissipation volumes, ventilation rates and backgrounds of these different locations the size distribution of the substances after spraying will differ considerably.

Samples were sprayed either manually from the original spray vessel (Gold, Holclaw et al. 1984, Llewellyn, Brazier et al. 1996, Berger-Preiß, Koch et al. 2004, Berger-Preiß, Koch et al. 2006, Vernez, Bruzzi et al. 2006, Berger-Preiß, Koch et al. 2009) or with aerosol generators and sprayers. (Class and Kintrup 1991, Llewellyn, Brazier et al. 1996, Berger-Preiß, Boehncke et al. 2005, Berger-Preiß, Koch et al. 2009) The spraying time in the studies ranged from a few seconds (Berger-Preiß, Koch et al. 2004, Berger-Preiß, Boehncke et al. 2005, Berger-Preiß, Gerling et al. 2006, Berger-Preiß, Koch et al. 2009) to 3 hours (Llewellyn, Brazier et al. 1996) depending on the different applications of products. Also the positions and the directions of the spray products with regard to the measurement equipment differed. Some studies were conducted with ventilation (Class and Kintrup 1991, Berger-Preiß, Koch et al. 2004, Berger-Preiß, Koch et al. 2006, Vernez, Bruzzi et al. 2006, Berger-Preiß, Koch et al. 2009) while for other studies no information on ventilation was provided. (Gold, Holclaw et al. 1984, Llewellyn, Brazier et al. 1996, Berger-Preiß, Boehncke et al. 2005)

Analytical Setup

Suspension analytics: Suspensions of the spray products were analyzed to assess the chemical composition of the sample. Thereby, the ingredients list could be verified and potentially harmful substances identified. One group analyzed the original suspension using GC/FID. (Class and Kintrup 1991) This analytical method focuses on the mass of the substances. The

applied measurement technique is well-established and appropriate for mass measurements. All other groups did not analyze the suspension.

Aerosol analytics: For human exposure to substances in conventional sprays the mass of the released substance, and hence the size distribution of the released droplets is of major importance. Aerosol size distribution has been monitored online, e.g. with a laser diffraction spectrometer. (Berger-Preiß, Koch et al. 2004, Berger-Preiß, Gerling et al. 2006) For offline analysis samples were collected on filter pads, (Llewellyn, Brazier et al. 1996, Berger-Preiß, Koch et al. 2004, Berger-Preiß, Gerling et al. 2006), on silica, (Class and Kintrup 1991) or by pumping air into a glass impinge bottle filled with a solution of ethylene glycol and water. (Gold, Holclaw et al. 1984) The filters or the silica gel were extracted prior to analysis, the solution could be analyzed directly. The organic solutions were analyzed by gas chromatography coupled with mass spectrometry (GC/MS) (Berger-Preiß, Koch et al. 2009) and other techniques similar to GC/MS, namely gas chromatography/flame ionization detector (GC/FID) or gas chromatography/electron capture detector (GC/ECD). (Class and Kintrup 1991, Llewellyn, Brazier et al. 1996)

In another study a personal aerosol exposure monitor (Koch, Dunkhorst et al. 1999) allowed the simultaneous sampling of three health-relevant size fractions described in the ASTM Standard D6062-07. (ASTM 2012) Measurements with a dust monitor and an impactor delivered the mass of substance per volume of air. (Vernez, Bruzzi et al. 2006)

Results und discussion

The reviewed studies report substance concentrations ranging from a few $\mu\text{g}/\text{m}^3$ to 60 000 $\mu\text{g}/\text{m}^3$. Since the spray duration differed, also the difference in the mass of released substance was pronounced. Normalization by the spray duration alone, however, does not allow comparison of the results, because the amount of mass generated during spraying also depends on the spray can (and here mainly the nozzle type) and the formulation of the product. In the reviewed studies no information on e.g. the nozzle type or its influence on the sprayed amount was given. Another complicating factor is that the spray direction and the position of the spray products with regard to the measurement equipment influence the concentration. These vary among the studies, and likewise the size of the room or chamber.

Further, under realistic conditions loss processes take place as documented for one extensive experiment (Berger-Preiß, Koch et al. 2009) in Table 2.2: For the same spray event different recoveries can be calculated for substances contained in the same spray.

Table 2.2: Comparison of aerosol data and amount of substance sprayed (S = substance).

Product	Amisia		Blattanex			Blattanex new		Paral		Contra Insect		
	S1	S2	S1	S2	S3	S1	S2	S1	S2	S1	S2	S3
Conc. suspension [g/100g]	0.04	0.06	0.04	0.2	1	0.15	0.15	0.25	1	0.5	0.15	n.a.
Sprayed amount [g]	23.8	23.8	11.4	11.4	11.4	11.4	11.4	19.8	19.8	9.5	9.5	9.5
Conc. aerosol [$\mu\text{g}/\text{m}^3$]	67.7	85.6	120.9	587.1	2122	145	147	345	1467	846	427	1167
chamber volume [m^3]	40	40	40	40	40	40	40	40	40	40	40	40
recovery of substance sprayed*	0.28	0.24	1.06	1.03	0.74	0.34	0.34	0.28	0.30	0.71	1.20	n.a.

* calculated by dividing the actual amount of substance sprayed with amount recovered after spraying

In spite of the many different experimental setups, we identified two approaches to calculate the inhalable dose of sprayed insecticides that on principle can be compared. (Class and Kintrup 1991, Berger-Preiß, Koch et al. 2009) The group of Berger-Preiß applied products in accordance with the manufacturer's instructions (10, 20 sec) and simulated a worst case scenario (2 min), respectively. The calculated inhalable dose for the worst case scenario is 5 to 8 times higher than for the manufacturer-recommended scenario (2-60 µg in contrast to 10-480 µg). (Berger-Preiß, Koch et al. 2009) Class and Kintrup also used a scenario similar to the manufacturer-recommended scenario of Berger-Preiß (10, 15, 20 sec). They found inhalable doses in the same size range (30-60 µg). (Berger-Preiß, Koch et al. 2009) Both groups used different products, with different ingredients and respective concentrations. They also used diverging experimental setups (ventilation, spray direction etc.), but similar in that they both used fully equipped model rooms that had about the same dimensions in size. Therefore, it might be possible to conclude that if insecticides are used that have similar ingredient concentrations as in the presented studies, the mass concentrations may be similar, if applied according to the manufacturer's recommendations.

Still, consumers not always follow the recommendations on the label so that for the assessment of human exposure to substances in sprays a realistic worst-case needs to be constructed as attempted by Berger-Preiß *et al*, (Berger-Preiß, Koch et al. 2009) and both consumer and bystander have to be considered. For worst case experiments, not only the spray duration needs to be extended beyond manufacturer's recommendations, but also the direction of spraying and the distance between can and instrumentation needs to represent realistic worst-case conditions. Additionally, the ventilation needs to be adapted to the analyzed spray: Some sprays are used outdoors hence ventilation is necessary during a chamber exper-

iment. Some sprays are used indoors, so that the ventilation needs to be reduced. Assessment of different spray durations for the same sample would enable extrapolation to other spray durations.

Table 2.3 summarizes the most important studies including parameters and results for all reviewed spray experiments with conventional sprays.

Table 2.3: Overview conventional spray experiments (n.a. = no information available).

		Berger-Preiss et al. (D)		Class & Kinttrup (D)		Llewellyn et al. (UK)		Gold et al. (USA)		Vernez et al. (CH)	
		insecticides		insecticides		insecticides		insecticides, pesticides		waterproofing sprays	
samples	medium	water	n.a.	x	n.a.	x	n.a.	x	n.a.	n.a.	n.a.
		organic	x	x	n.a.	x	n.a.	n.a.	n.a.	n.a.	x
	spray type	pump_spray	x	n.a.	n.a.	n.a.	n.a.	n.a.	n.a.	n.a.	n.a.
		propellant gas	x	n.a.	n.a.	x	n.a.	n.a.	n.a.	x	n.a.
		other	+ electro vaporizers, sprayers		+ electro evaporators		+ compression sprayer, smoke generators, bellow pumps, dusting		B&G handsprayer operated at 137.9 kPa pressure		n.a.
setup	instrumentation	suspension	n.a.	GC/FID (5890 series II, Hewlett Packard)	n.a.	n.a.	n.a.	n.a.	n.a.	n.a.	n.a.
		aerosol	online	personal aerosol exposure monitor Respicon (TM 3-F, Hund), laser diffraction spectrometer (HELOS 1269, Symapatec)		n.a.	n.a.	n.a.	n.a.	n.a.	Grimm dust monitor (1.102, Labortechnik GmbH), DataRAM (PdR-1000AN, MIE)
	offline		sampling on glass fibre filters → GC/ECD (5890 series II, Hewlett Packard), GC/MS (6890N, Agilent Technologies),		GC/ECD (5890 series II, Hewlett Packard)	GC/ECD (5890 series II, Hewlett Packard)	GF/A filter → GC/ECD	pump + impinging, exposure pads → GC	Andersen Impactor (1ACFM, Andersen 2000 Inc)	7.9 m ³	
	type of room	model rooms with area 16 m ² , volume 40 m ³ , each room was equipped with a cupboard, shelves, a sofa, a coffee table, a chair, a dining table, a window and a radiator		furnished room with wallpaper, carpet, bookshelves, a desk, a sofa, a wooden closet and some plants; floor space 20 m ² air volume 50 m ³	outdoor and indoor exposure	outdoor and indoor exposure	inside a house	n.a.	n.a.		
experiment	spray duration	(1) realistic scenario: 10 and 20 seconds (2) worst case scenario: 2 minutes		10, 15 or 20 sec electro evaporators: 4 and 12 h	few minutes for eradications of wasp nests; 2-3 h for larger spraying operations	25.5 min	each 5 sec a short spray pulse (0.5 sec) was emitted	5 m distance to instrumentation laminar flow	10 min		
	spray direction/position	in the middle of the room between the door and the window		in the center of the room, distance to sampling 2 m	realistic scenarios	spray can was moved around	5 m distance to instrumentation laminar flow	10 min			
	ventilation	no ventilation during measurement		open window, door	n.a.	air	n.a.	10 min			
results	measurement time	during spray operation and 2-3 minutes thereafter		during and after application	minimum 20 min were required; corresponds with treatment time	n.a.	10 min	10 min			
		exemplary insecticide « Amisia » d-Tetramethridin		25 to 4200 µg/m ³ depending on the compound and spray duration	n.d. - 77 µg/m ³ for ground spraying n.d. - 237 µg/m ³ for overhead spraying	21 µg/m ³	1.77 and 2.39 µg/m ³				
	measured concentration	spraying time [sec]	average inhalable exposure conc [µg/m ³]								
	20	67.7									
	120	231.2									

2.5 NOAA – containing sprays: experimental and analytical setup

Investigated sprays

mNOAA-containing sprays can be categorized according to their formulation, packaging and chemical composition. Nanoparticle behavior depends on the solvent, therefore water-based sprays (Shimada, Wang et al. 2009, Hagendorfer, Lorenz et al. 2010, Nørgaard, Wolkoff et al. 2010, Berlin, Dietrich et al. 2011, Lorenz, Hagendorfer et al. 2011, Nazarenko, Han et al. 2011, Oomen, Bennink et al. 2011, Quadros and Marr 2011) and organic solvent based sprays (Hagendorfer, Lorenz et al. 2010, Nørgaard, Wolkoff et al. 2010, Berlin, Dietrich et al. 2011, Lorenz, Hagendorfer et al. 2011, Oomen, Bennink et al. 2011, Bekker 2014) should be distinguished. Also the vessel type is of major importance: propellant gas sprays (Nørgaard, Jensen et al. 2009, Chen, Afshari et al. 2010, Hagendorfer, Lorenz et al. 2010, Liroy, Nazarenko et al. 2010, Nørgaard, Larsen et al. 2010, Nørgaard, Wolkoff et al. 2010, Berlin, Dietrich et al. 2011, Lorenz, Hagendorfer et al. 2011, Nazarenko, Han et al. 2011, Nørgaard, Janfelt et al. 2011, Oomen, Bennink et al. 2011, Bekker 2014) generate different droplet sizes than pump sprays, (Nørgaard, Jensen et al. 2009, Hagendorfer, Lorenz et al. 2010, Liroy, Nazarenko et al. 2010, Nørgaard, Larsen et al. 2010, Nørgaard, Wolkoff et al. 2010, Berlin, Dietrich et al. 2011, Lorenz, Hagendorfer et al. 2011, Nazarenko, Han et al. 2011, Nørgaard, Janfelt et al. 2011, Oomen, Bennink et al. 2011, Quadros and Marr 2011) thereby influencing substance availability for human exposure. In two studies experiments were reported that used nebulizers to generate a standardized mNOAA containing aerosol (Shimada, Wang et al. 2009, Nazarenko, Han et al. 2011) in order to study the influence of the vessel and nozzle on the generated aerosol.

Also, the chemical composition of the particles is important for later risk assessment. Nanoparticles present in the investigated sprays encompass metals and metal oxides like ZnO,

(Shimada, Wang et al. 2009, Hagendorfer, Lorenz et al. 2010, Berlin, Dietrich et al. 2011, Lorenz, Hagendorfer et al. 2011, Oomen, Bennink et al. 2011) Ag, (Hagendorfer, Lorenz et al. 2010, Berlin, Dietrich et al. 2011, Lorenz, Hagendorfer et al. 2011, Nazarenko, Han et al. 2011, Oomen, Bennink et al. 2011, Quadros and Marr 2011) Cu, (Nazarenko, Han et al. 2011) Ca, (Nazarenko, Han et al. 2011) Mg, (Nazarenko, Han et al. 2011) Zn, (Nazarenko, Han et al. 2011) SiO₂ (Berlin, Dietrich et al. 2011, Oomen, Bennink et al. 2011, Bekker 2014), MgO (Bekker 2014) and TiO₂ (Chen, Afshari et al. 2010, Berlin, Dietrich et al. 2011, Oomen, Bennink et al. 2011), but also nanoparticulate fullerenes (C₆₀), (Shimada, Wang et al. 2009) or silanes and siloxanes (not nanoparticulate in suspension) being used in sprays. (Nørgaard, Jensen et al. 2009, Nørgaard, Larsen et al. 2010, Nørgaard, Wolkoff et al. 2010, Nørgaard, Janfelt et al. 2011)

Many different mNOAAs in different media with different vessels were analyzed. All studies delivered different size distributions.

Experimental Setup

For spray experiments, most groups (Nørgaard, Jensen et al. 2009, Shimada, Wang et al. 2009, Hagendorfer, Lorenz et al. 2010, Nørgaard, Wolkoff et al. 2010, Lorenz, Hagendorfer et al. 2011, Nazarenko, Han et al. 2011, Nørgaard, Janfelt et al. 2011, Quadros and Marr 2011, Bekker 2014) proposed a small glove box setup as a controlled environment, which can represent near field exposure. One study (Berlin, Dietrich et al. 2011) was performed in a larger exposure chamber and two studies (Chen, Afshari et al. 2010, Bekker 2014) were conducted in real rooms.

As reported for the conventional sprays, also for mNOAA containing sprays the experimental conditions vary largely. The spray duration ranged from a few seconds of continuous spraying (Nørgaard, Jensen et al. 2009, Hagendorfer, Lorenz et al. 2010, Lorenz, Hagendorfer et al. 2011) to discontinuous spraying for several minutes. (Chen, Afshari et al. 2010, Nazarenko, Han et al. 2011, Quadros and Marr 2011, Bekker 2014) Variations have different reasons: For example a small exposure chamber allows for only few seconds of spraying; otherwise the chamber will be oversaturated with aerosol. A real room allows longer spray durations so that the manufacturer's instructions for product use can be followed without adaptation. Another reason is that as discussed before the exposure conditions need to be adapted to the respective application of the product.

For three studies the spray duration was not mentioned. (Shimada, Wang et al. 2009, Berlin, Dietrich et al. 2011, Oomen, Bennink et al. 2011) In one study it was shown that the generated number of particles increased linearly with the spray duration. (Lorenz, Hagendorfer et al. 2011) The spray direction and the position of the spray inside the chamber or room differed in all reviewed studies. One study also included experiments with spray can positions representing near-field and far-field scenarios. (Bekker 2014) Authors often mention that the background concentration is monitored, but only two studies report the particle background concentration (< 10 particles/cm³, respectively). (Berlin, Dietrich et al. 2011, Quadros and Marr 2011) In three studies, humidity and temperature were monitored. (Nørgaard, Jensen et al. 2009, Quadros and Marr 2011, Bekker 2014)

In most experiments not the particle size of the mNOAA was measured, but the size of the droplets generated by spraying. Consequently, these experiments yield an upper bound for the particle size, but not the exact size. In one study the droplets were dried prior to analysis

by using a thermo-desorber (Lorenz, Hagendorfer et al. 2011) so that the size of the dried particles could be measured. In many studies the term “particle size” is used for describing the size distribution of the aerosol. It should be kept in mind that if the aerosol is not dried prior to analysis the measured “particle” size distribution rather represents the droplets or the particles in the aerosol (in case that the solvent has already evaporated) or a mixture of both.

Analytical Setup

For the analysis of the suspension and the aerosols of mNOAA sprays different approaches were used. Both analyzing the suspension and the aerosols is important for risk assessment, since information on the change of the particles during spraying may help to extrapolate to other sprays. With suspension analytics the chemical composition of the sample, the original size and shape of the particles can be determined; with aerosol analytics the number concentration and size distribution of the released aerosol as well as the shape of the particles. Comparison of both suspension and aerosol analytics suggests how the size and concentration of the particles change during the spray process and thereby informs on the influence of the vessel type, vessel geometry and the propellant gas, respectively.

Suspension analytics: Particle size and morphology in the original suspension were mainly measured by batch analysis using dynamic light scattering (DLS) (Shimada, Wang et al. 2009, Chen, Afshari et al. 2010, Quadros and Marr 2011) and electron microscopy techniques like scanning electron microscopy (SEM) or transmission electron microscopy (TEM), usually in combination with energy dispersive x-ray spectrometry (EDX) (Hagendorfer, Lorenz et al. 2010, Lorenz, Hagendorfer et al. 2011, Nazarenko, Han et al. 2011, Quadros and Marr 2011, Bekker 2014) for specific single particle analysis, information on morphology and size distri-

bution (via image analysis) as well as chemical identity. All methods have their advantages and disadvantages. DLS is more sensitive for larger particles, which means that for polydisperse samples the size distribution is shifted to larger sizes. This technique is fast and cheap. By contrast, SEM and TEM are very time consuming and expensive, but they are the only techniques that can visualize particles. In combination with EDX also information about the chemical identity of the particles can be obtained. For chemical quantification of organic nanoparticle species mainly GC-MS was employed, (Nørgaard, Jensen et al. 2009, Nørgaard, Larsen et al. 2010, Nørgaard, Wolkoff et al. 2010, Nørgaard, Janfelt et al. 2011) whereas for the metallic nanoparticles a bulk analysis using plasma mass spectrometry (ICPMS) was used. (Ulrich and Hagendorfer 2009, Hagendorfer, Lorenz et al. 2010, Lorenz 2010, Lorenz, Hagendorfer et al. 2011, Quadros and Marr 2011) Those techniques are well established and fast. Additionally, asymmetric field flow fractionation in a multi-detector approach (A4F) in combination with UV/Vis, light scattering and ICPMS was tested as a novel integrative analytical tool to achieve information on size and chemistry simultaneously. (Berlin, Dietrich et al. 2011, Hagendorfer 2011, Hagendorfer, Kaegi et al. 2011, Hagendorfer, Kaegi et al. 2012) A4F collects a lot of information in one measurement, but it has also some big disadvantages like e.g. unspecific particle membrane interactions and retention time shifts. (Ulrich, Losert et al. 2012)

Aerosol analytics: For the nano-sized fraction of the generated spray aerosols, size distribution and particle number concentration were determined online by scanning mobility particle sizer (SMPS) or fast mobility particle sizer (FMPS). The larger sizes between 300 nm and 20 µm were investigated by an aerodynamic particle sampler (APS). One SMPS measurement takes 1.5 to 3 minutes depending on the type of instrument. This is much too long for deter-

mining the release in one spray event, because agglomeration alters the size distribution already during the measurement. With newer generation instruments a size range of 2.5-1000 nm can be scanned in 16 seconds, but only one study (Quadros and Marr 2011) reports using such a new generation instrument. FMPS is even faster (<10 seconds). A big disadvantage, however, is the lower size limit of 5.6 nm and the high costs of the instrument. Nørgaard *et al* (Nørgaard, Jensen et al. 2009) analyzed particulate emissions with an APS and FMPS, and in addition with a GC/MS and a mini MS, because they were interested not only in the metallic but also in the organic particles/components.

Four groups connected their exposure chamber to a sampler on which particles can be sampled on TEM grids. (Shimada, Wang et al. 2009, Hagendorfer, Lorenz et al. 2010, Lorenz, Hagendorfer et al. 2011, Quadros and Marr 2011, Bekker 2014) The grids were analyzed by TEM-EDX and particles counted for comparison with SMPS.

Results and discussion

All studies report a release of particles/droplets in the nm (Nørgaard, Jensen et al. 2009, Shimada, Wang et al. 2009, Chen, Afshari et al. 2010, Hagendorfer, Lorenz et al. 2010, Berlin, Dietrich et al. 2011, Lorenz, Hagendorfer et al. 2011, Nazarenko, Han et al. 2011, Oomen, Bennink et al. 2011, Quadros and Marr 2011, Bekker 2014) or μm size range (Nørgaard, Jensen et al. 2009, Oomen, Bennink et al. 2011) depending on several influencing factors. The following results and discussion will mainly focus on propellant sprays, since for pump sprays the generated droplets are so large that most of them immediately sediment and, thus, cannot be detected by the measurement devices for aerosols, but also become irrelevant for consumer exposure by inhalation.

Chamber and room experiments are based on different philosophies. The idea behind chamber experiments is to achieve highly standardized conditions, while room experiments attempt to achieve highly realistic conditions. The chambers used in the reviewed studies were of different sizes. For a smaller chamber like the one described by Lorenz *et al* (Lorenz, Hagendorfer et al. 2011) with a volume of 0.33 m³ the relative humidity will increase very fast and the concentration of mNOAAs in the air will become homogeneous throughout the box after a short time. This setup can represent the near-field breathing zone of a consumer when using on-person products like an antiperspirant or an anti-itch spray. The spatial distribution of the concentrations inside a real room, however, cannot be investigated with such a small chamber. When a consumer is moving inside the room after applying the spray his/her exposure to mNOAA will vary. This scenario can better be represented in real room experiments.

Real room experiments, however, have the disadvantage that they are usually conducted with ambient air, so that the particle background concentration is not standardized. While this setup is more relevant for assessing realistic consumer exposure, it is not so helpful for understanding the behavior of the nanoparticles released from the products and the latter is crucial for the generalization of results and extrapolation to other consumer sprays. Experiments carried out under the same conditions (spray duration, direction, humidity etc.) within a small chamber, a big chamber and a real room could identify if and how near-field results from a small chamber can be transformed to predict realistic worst-case exposure conditions.

We tried to normalize the particle number concentration of all experiments to a defined spray duration or rather to a defined spray amount, as it was done by Lorenz *et al*. (Lorenz 2010) As all other studies measured the particle number concentration released from the cans just for one defined spray duration an extrapolation was not possible in those cases. Presumably, an

extrapolation can only be used for a spray with the same chemical formulation and spray can, because the particle number is dependent on the spray nozzle, the original nanoparticle concentration (in the suspension), the formulation of the spray and in the case of propellant gas vessels on the filling level of the propellant.

Nevertheless two groups calculated the amount of particles released per one single application. (Nørgaard, Jensen et al. 2009, Hagendorfer, Lorenz et al. 2010) The two obtained results fit quite well (10^{10} and ranging from $3 \cdot 10^8$ to $2 \cdot 10^{10}$ particles per application), when considering that spray amount and spray ingredients differed. Both studies had no air exchange during spraying and measuring. Furthermore related instruments were used to determine the particle number concentration (SMPS and FMPS). The chamber volumes were similar (0.33 m^3 (Hagendorfer, Lorenz et al. 2010) and 0.66 m^3 (Nørgaard, Jensen et al. 2009)) and also the spray direction and distance were similar in that in both setups spraying was directed towards the measurement device (distance of 80 cm and 35 cm, respectively).

For mNOAA-containing sprays also temperature and humidity have an influence on the droplet size and also on the final particle/agglomerate size. With an increase of the humidity, aerosol droplets will become larger which shifts the final particle size distribution. (Seipenbusch, Binder et al. 2008) In 2010 a DIN EN ISO norm (ISO 2010) set acceptable ranges for temperature and humidity when characterizing mNOAAs in exposure chambers: the temperature should be $22 \pm 3 \text{ }^\circ\text{C}$ and humidity between 30-70%. Two studies reported a relative humidity $< 10\%$, (Quadros and Marr 2011, Bekker 2014) another study a relative humidity of $23 \pm 2\%$ and a temperature of $25 \pm 2 \text{ }^\circ\text{C}$. (Nørgaard, Jensen et al. 2009) All other groups apparently did not monitor these climate variables.

Another influencing factor that was not discussed for any study is the tubing material, which is important because once nanoparticles reach the wall of the tubing they will stick to the walls; thereby fewer particles will be detected. This process can be reduced by using conductive tubing (Jankovic, Hall et al. 2010) instead of non-conductive tubing (e.g. Tygon), in which electrostatic forces do not attract the nanoparticles.

Not always were nanoparticles detected in the suspension of products that generated nanoparticles in the aerosol: In some products the particles in the suspension were in the μm size range (Lorenz, Hagendorfer et al. 2011, Nazarenko, Han et al. 2011, Quadros and Marr 2011) or the element was present in ionic form. (Quadros and Marr 2011)

Despite the variety of setups, we identified some general findings in the reviewed studies. First, all studies report nanoparticle release only when propellant gas spray cans are used. Studies that analyzed pump sprays conclude that no single particles but agglomerated are released and that the particle number released is much lower than from propellant gas sprays. (Hagendorfer, Lorenz et al. 2010, Quadros and Marr 2011) When the solvent evaporates particles cluster to form agglomerates. But most of the initial droplets released from pump sprays are too large to stay in the air for long. Second, a change from the initial particle size and concentration in the suspension to the final particle size distribution and number concentration in the generated aerosol was observed by many groups. (Shimada, Wang et al. 2009, Hagendorfer, Lorenz et al. 2010, Quadros and Marr 2011) Some groups relate this phenomenon to the dispenser type, having shown that the same suspension yields different results for particle concentration and particle size when sprayed with an aerosol generator rather than the commercial spray can. (Nazarenko, Han et al. 2011, Quadros and Marr 2011) This may also hold true for different commercial spray cans where the geometry of the noz-

zle, the filling level of the propellant and presumably also the size of the vessel itself may have a strong influence on the final particle size and concentration. Notably, two publications that analyzed products of the same type, one containing mNOAA and one not, found nano-sized particles also for the non-nano products. (Lorenz, Hagendorfer et al. 2011) From these results we conclude that it is very important to analyze the size not only of the wet droplets, but also of the dried particles. This conclusion was already drawn by Chen *et al.* (Chen, Afshari et al. 2010) One of the presented studies assessed the influence of the distance from the aerosol source to the instrumentation (Bekker 2014) and reported that for the near field scenario a higher number of small nanoparticles was obtained than for the far field scenario. This information is of huge importance for human exposure modeling.

By merging all of these important results a good basis for a standardized protocol can be obtained. The crucial points therefore are to distinguish between wet and dried particles, to standardize the spray duration and the spray distance, and to investigate the spraying device (vessel type, nozzle etc).

Table 2.4 gives an overview over the most important parameters and results for all reviewed experiments with mNOAA-containing sprays.

Table 2.4: Overview of inorganic spray experiments (n.a. = no information available).

		<u>Hagendorfer et al., Lorenz et al. (CH)</u>	<u>Nørgaard et al. (DK)</u>	<u>Nazarenko et al., Liroy et al. (USA)</u>	<u>Quadros & Marr (USA)</u>	<u>Chen et al. (USA)</u>	<u>Shimada et al. (JAP)</u>	<u>Winterhalter et al. (D)</u>	<u>RIVM (NL)</u>	<u>Bekker et al. (NL)</u>	
samples	mNOAA type	Ag, ZnO	Silane, Siloxane, VOC	Ag, Cu, Ca, Mg, Zn	Ag	TiO ₂	NiO, C ₆₀	TiO ₂ , SiO ₂ , Ag	TiO ₂ , ZnO, Ag	SiO ₂	
	medium spray type	water	x	x	x	x		x	x	x	
		organic	x	x	x				x	x	x
		pump Spray	x	x	x	x			x	x	
		propellant	x	x	x				x	x	x
other	uniform vessels	n.a.	2 types of nebulizers	n.a.	n.a.	n.a.	nebulizer	n.a.	n.a.	n.a.	
instrumentation	suspension	ICPMS (Agilent 7500ce), TEM (FEI Tecnai F30)	n.a.	Photon Correlation Spectroscopy (Brookhaven ZetaPALS 90 Plus)	DLS (Malvern Zetasizer), ICPMS (Thermo Electron X-Series), TEM (FEI Philips EM420), UVVis (Varian Cary 5000)	n.a.	DLS (Otsuka Electronics FPAR-1000), HPLC (Agilent 1100)	A4F – MALS, UVVis (Postnova Analytics)	n.a.	FEG-SEM/EDX	
		SMPS (TSI 3034), Electrostatic Sampler	GC, GC/MS (Perkin Elmer Turbomass), APS (TSI 3321), FMPS (TSI 3091), mini MS (Mini10), CPC (Grimm 5.403)	SMPS (TSI 3081 DMA+3786 CPC), APS (TSI 3321)	SMPS (TSI 3936NL), CPC (TSI 3025A), OPC (TSI Aerotrak), DC (EcoChem DC 2000), Thermophoretic sampler	Data RAM (Thermo Electron DR-4000), GRIMM (1.108), APS (TSI 3321), SMPS (TSI 3080) LDS Analyzer (Malvern)	SMPS (MSP Corp 1000XP WPS), Electrostatic Sampler	OPC (Grimm 1.108) CPC (TSI 3025) SMPS (Grimm 5.400), Portable particle counter (PPC (TSI 3007))	n.a.	SMPS (TSI 3080), APS (TSI 3321), ELPI (Dekati), Nanotracer (Aerasense, Philips), LQ1-DC (Matter Engineering)	
	aerosol	Online									
		Offline	TEM (FEI Tecnai F30)	(mass concentration)	TEM (JEOL 2010F)	Cascade Impactor (SKC, Sioutas), ICPMS (Thermo Electron X-Series), TEM (FEI Philips EM420)	SEM (Hitachi S-4800)	FE-SEM (Hitachi, S-5200), TEM (Carl Zeiss SMT EM922)	n.a.	HR-SEM (Carl Zeiss LEO 1550), TEM (Philips CM300ST), XPS (Physical Electronics QuanteraSX)	TEM (FEI Tecnai F30), FEG-SEM/EDX
	type	chamber	0.33 m ³	0.66 m ³	0.73 m ³	0.52 m ³	n.a.	0.52 m ³	2.5 m ³	n.a.	n.a.
	real room	n.a.	n.a.	n.a.	n.a.	9-ft ceiling room	n.a.	n.a.	n.a.	n.a.	
	total spray duration	1-5 sec continuous	25 sec continuous	3 min discontinuous	30 min discontinuous	2.5 min discontinuous	n.a.	3 times 1 second	n.a.	3 times sequentially for 3 sec with 3 sec intervals	
	spray direction/position	80 cm from source	20 cm behind the nozzle	spray cone towards back wall	n.a.	"near spray activity"	n.a.	90, 140, 190 cm (90 degree)	directly on TEM grids	towards a back wall (70 x 70 cm ²)	
ventilation		vent, vacuum	two fans	n.a.	n.a.	n.a.	n.a.	n.a.	n.a.	off	
	aerosol	18, 300 nm	nm – μm range	30 – 400 nm	20 nm – 10 μm	75 nm	50-100 nm	6 – 110 nm	nm – μm range	50 – 200 nm	
	suspension	8 nm – some μm	n.a.	< 5 nm – 5 μm	nm – μm range	n.a.	n.a.	no particles; 10 – 110 nm	n.a.	n.a.	
measured particle number [# / m ³]		7.8*10 ⁵ – 1.9*10 ⁶	2.8*10 ⁸ – 2.1*10 ¹⁰	10 ² – 10 ³	7.3*10 ⁶ – 5.6*10 ⁷	1.6*10 ⁵ resp. 1.2*10 ⁵	NiO 10 ⁵ C ₆₀ 10 ⁴	277 - 180438	n.a.	n.a.	

Chapter 3

3 Investigation of appropriate analytical concepts for nanoparticle analysis in suspensions

3.1 Overview over hyphenated techniques for nanoparticle analysis

So far a lot of different methods for nanoparticle analysis in suspensions are available. There are, on the one hand, common techniques like sequential filtration or centrifugation (often called bulk analysis), which are good developed methods to obtain information about the size of the particles. Nevertheless, they are time consuming, the cut off (size) is limited and sample losses are very high (as particles get in direct contact with e.g. filters). An also well-known and good developed method is dynamic light scattering (DLS). The particle size and the polydispersity index (PDI) of a suspension can be determined within a few minutes. However, the method is not ideal for polydisperse samples, as the mean particle size is overestimated. Furthermore, the instrument cannot distinguish between different particle types/chemistry. Electron microscopy (scanning (SEM) or transmission (TEM)) is an imaging method, also well established and the only technique, which can provide information about the morphology and the size of particles. In addition, when using an energy-dispersive X-ray detector, information about the chemistry can be obtained. Nevertheless, it is very time consuming and data interpretation is not very representative, as only a very small part of the sample is analyzed.

On the other hand there are two new, promising hyphenated techniques. The first new technique, called single particle inductively coupled plasma mass spectrometry (spICPMS) seems to be very promising, as the size distribution of a suspension can be determined with a common ICPMS within a few seconds. However, it is not well established and only one single element can be measured in one run. In addition the size is not directly measured, but calcu-

lated. The last hyphenated technique is called asymmetric flow field flow fractionation (A4F), Coupled to several detectors like UV Vis, light scattering or ICPMS., different information can be obtained during one measurement (size, chemistry, coating, etc.). Nevertheless, also this method has disadvantages, which are the unpredictable particle losses and particle-membrane interactions. During the next chapter this method and especially the particle-membrane interactions will be handled in detail.

Table 3.1 gives an overview over often used techniques, their advantages and disadvantages.

Investigation of analytical concepts for nanoparticle analysis in suspensions

Table 3.1: Advantages and disadvantages of hyphenated techniques for nanoparticle suspension analytics.

Method	Information	Advantage	Disadvantage
DLS	particle size, PDI	very fast	not for polydisperse samples, no differentiation of particle types
EM EDX	morphology, particle size distribution, chemical information	several informations only methode for morphology	time consuming sample preparation data interpretation
A4F + Detectors	size, mass, chemical information, coating	fast, several informations	particle - membrane interactions quite expensive
spICPMS	size distribution	very fast	single element; not well established
Bulkanalysis	size classes	good developed methods	time consuming; cut off limited; sample losses

3.2 Evaluation of membrane surface characteristics on particle-membrane interaction in field-flow-fractionation analysis

Field flow fractionation and especially the sub-technique of asymmetric flow field flow fractionation (A4F) is a promising method in the field of nanoparticle characterization. It has already been implemented for size separation and characterization of natural- and engineered nanoparticles (Hassellöv, Readman et al. 2008, Baalousha, Stolpe et al. 2011, Kammer, Legros et al. 2011). Due to the possibility of coupling different detectors such as light scattering, UV/Vis, Fluorescence, differential refractive index or mass spectrometers in series, online analysis of several physicochemical parameters can be obtained simultaneously. (Kammer, Baborowski et al. 2005, Dubascoux, Le Hecho et al. 2010, Hagendorfer, Kaegi et al. 2011, Hagendorfer, Kaegi et al. 2012) Furthermore, A4F features a wide dynamic size separation range, μL sample volumes and comparable analysis times to conventional HPLC separations which make it interesting as routine analysis tool for nanoparticle characterization.

The main disadvantage of A4F is that almost all current systems use ultrafiltration membranes at the accumulation wall of the separation channel. This can lead to unpredictable particle loss due to particle-membrane interactions. Particle loss can be observed particularly during the focus step and upon high cross flow rates, as in these two cases particles are strongly pushed to the surface of the membrane. Based on the principle of A4F the cross flow drives particles towards the bottom of the channel and diffusion as contrarious force drives them back into the channel. Smaller particles, having a higher Brownian motion are able to diffuse higher into the channel than bigger particles. Due to a laminar flow perpendicular to the cross flow in the channel particles will be eluted in an order from smaller to larger size. This mechanism will no longer be undisturbed, when particles interact with the membrane. As

a consequence the change of the membrane surface during the first few injections and the unspecific interactions upon membrane materials with different particle types lead to retention time shifts and poor recovery rates during separation.

Whilst the phenomena of retention time shifts (impeding precise calculation of particle size from the FFF theory) has already been overcome using size specific detectors or nanoparticle reference materials matched to the investigated sample, recovery issues are still the main drawback of A4F. With unpredictable recoveries, quantification of nanoparticles cannot be performed reliably and this degrades the A4F technique to a very sophisticated but rather qualitative tool, albeit one of the most specific nanoparticle analysis tools next to electron microscopy. To display the full potential of this technique, the membrane-particle interactions have to be understood and, if possible, overcome.

Some previous studies analyzed membrane materials and it was found that polyethylenesulfone (PES) and polysulfone sulfonate (PSS) membranes are negatively charged and that the intensity of the charge can be changed with composition of the liquid media. (Causserand, Nyström et al. 1994, Nyström, Pihlajamäki et al. 1994) The streaming potential is directly dependent on the ionic strength, the pH and membrane cut-off. (Ricq, Pierre et al. 1997) In respect to A4F accumulation wall membranes, the influence of the carrier fluid composition on recovery in A4F when using a 30 kDa regenerated cellulose (RC) membrane was studied. (Schachermeyer, Ashby et al. 2012) Results show that larger particles suffer higher attractive forces and are stronger influenced by variations of the carrier solution composition. In another study it was found that the ionic strength of the carrier solution and the sample load influences the particle retention behavior. (Neubauer, V.d. Kammer et al. 2011) For the A4F setup an optimum retention behavior for a carrier solution with high ionic strength and a minimum

injected load of nanoparticles was found. In a recent published study an additional influence on the retention behavior of nanoparticles was presented. The retention time was different for metallic nanoparticles relative to lower bulk density particles. Differences in the attractive van der Waals forces between nanoparticles and membrane surface were assumed to be the reason for that. For Au nanoparticle losses due to adhesion to the membrane surface was reported. (Poda, Bednar et al. 2011) Hartmann *et al* first introduced the concept of repulsive forces between the particle sample and the membrane surface. (Hartmann and Williams 2002) Based on these assumptions Schmidt *et al* analyzed the membrane surface of a used A4F membrane. (Schmidt, Loeschner et al. 2011) Therefore the surface of a PES membrane was investigated after six injections with Au nanoparticles using scanning electron microscopy (SEM). SEM images showed Au nanoparticles sticking on the surface of the membrane, which is a direct proof for attractive forces between particles and the membrane surface. In a study performed by our group, also for Au nanoparticles, different recovery rates were observed after several injections. (Hagendorfer, Kaegi et al. 2011) When comparing different membrane types to study materials dependence, it was found that recovery rates increases for all membrane types after several injections. However, the recovery was strongly dependent on the membrane material itself. It is therefore suggested that the charge and the hydrophobicity of the membrane surface influences adsorption. With repeated injections the absorbed particles on the membrane surface increase the surface charge and yields to better recovery due to increased repulsion. Consequently Ulrich *et al* (Ulrich, Losert et al. 2012) proposed the ζ -potential to be the main reason for the unspecific particle-membrane interactions. First studies when analyzing TiO_2 nanoparticles showed that the pH and composition of the carrier liquid substantially influences the ζ -potential of different membranes, thereby having a direct impact on recovery. (Bendixen, Losert et al. 2014) This leads to the assumption

Investigation of analytical concepts for nanoparticle analysis in suspensions

that with careful optimization of the carrier liquid, particle loss in the separation channel can be overcome, minimized or at least reproducible to tackle reliable quantification with an A4F multidetector setup. This motivated us to investigate the behavior of A4F membranes upon different separation conditions to identify mechanisms leading to unspecific particle-membrane interactions and possibly find a strategy to overcome recovery issues.

3.3 Experimental Section

Approach

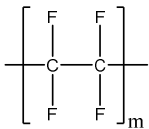
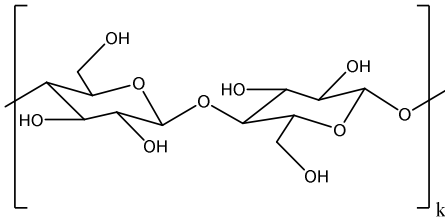
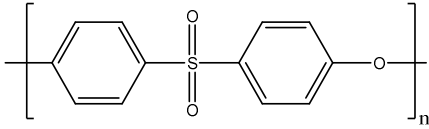
To evaluate the influence of the ζ -potential, morphology and hydrophobicity of the membrane and particle system on A4F separations, a series of experiments were conducted using different membrane/carrier solution combinations keeping the particle system constant (30 nm polystyrene (PS) nanoparticles for analysis of interactions and 80 nm PS nanoparticles to detect absorbed particles for SEM imaging). Separations were performed with different combinations of carrier/membrane/particle systems determining particle recovery as a direct measure for membrane/particle interactions.

Chemicals: Suprapur or pro analysis quality of nitric acid (65 % w/w), 2-propanol, sodium hydroxide, sodium hexametaphosphate, sodium azide, sodium dodecyl sulfate (SDS) (either Merck GmbH or Sigma Aldrich Chemie GmbH) were used. Triton X was employed in electrophoresis grade from Fisher Chemical (Thermo Fisher Scientific). A Milipore, Mili-Q A-10 water unit (Milipore AG) was used for the production of 18 M Ω cm deionised water (DI-water). The carrier solutions for the A4F system were degassed in an ultrasonic bath prior to analysis. The standards were always freshly prepared before measurements diluting with carrier solution directly in 2 mL HPLC (PE-LD) vials. Polystyrene nanosphere size standards were purchased from Duke Scientific Corporation (Thermo Scientific Inc., Fremont, USA).

Membrane Materials: Membrane materials were selected which were identified to be most commonly used for A4F separation; regenerated cellulose (RC) with cutoffs of 30 kDa (Wyatt Technology Europe GmbH, Germany), polyethersulfone (PES) with a cutoff of 10 kDa (Wyatt

Technology Europe GmbH, Germany) and polyvinylidene difluoride (PVDF) with a cutoff of 30 kDa (GE Healthcare, Switzerland). Table 3.2 illustrates the chemical structures of the different materials.

Table 3.2: Chemical structure of used membrane materials.

Membrane	Full name	Chemical structure
PVDF	polyvinylidene difluoride	
RC	regenerated cellulose	
PES	polyethersulfone	

Instrumentation

A4F setup: The A4F system is composed of a separation channel and a flow control (Eclipse3, Wyatt Technology Europe, Germany) connected to a metal-free HPLC system (DGU-20A3 degasser, LC-10Ai pump, SIL-20AC autosampler, CBM-20A control unit) from Shimadzu Europe (Germany). The A4F system was coupled to an UV/Vis diode array detector (SPD-M20A, Shimadzu GmbH, Germany). The separation channel had the dimension of 145 mm in length and 50 mm in width with a spacer height of 350 μm . Data from the light scattering detector

were processed with the ASTRA software (Wyatt, Version 6.0) and UV/Vis data using the LC solution software (Shimadzu, Version 1.22 SP1).

A4F separation program: The separation program consists of 5 consecutive steps. A detector flow of 1.0 mL/min, a focus flow of 2.0 mL/min and an injection flow 0.2 mL/min is applied to the system. After a short pre-separation step and a focus and inject step the sample was focused and over a time range of 20 minutes the flow was reduced from 2.0 mL/min to 0.1 mL/min to guarantee a complete separation. During 3 following minutes the flow is decreased from 0.1 mL/min to 0.0 mL/min.

Batch dynamic light scattering (DLS) and ζ -potential: For DLS and ζ -potential measurements of the nanoparticles a Malvern Zetasizer NanoZS (Malvern Instruments Ltd., Germany) was used. All samples were equilibrated in temperature for 5 minutes to 20°C in the batch cell before analysis.

Membrane ζ -potential: The streaming zeta potentials of membranes (sheets of 2 cm in diameter) for the A4F have been analyzed using a flow-through zeta potential analyzer Müttek (TM) System SZP-06 (BTG Instruments GmbH, Germany). ζ -potential measurements were performed with DI water, DI water + NaOH, DI water + HNO₃ (influence of the pH) and DI water + SDS, Na₆P₆O₁₈, Triton X-100 or NaN₃. Membranes as well as chemicals were chosen due to their numerous applications in other publications (Dulog and Schauer 1996, Contado and Pagnoni 2008, Bolea, Jiménez-Lamana et al. 2011, Hagendorfer, Kaegi et al. 2011, Gigault and Hackley 2013).

The suspensions are suck through the membrane until both electrodes, beyond and above the membrane are completely covered with suspension. The measurements were repeated ten times.

Conductivity and pH were additionally determined using a MultiLine P3 (WTW, Germany) apparatus including a TetraCon® 925 conductivity probe and a SenTix® 940 pH electrode (both WTW, Germany).

SEM and AFM measurements: For surface imaging carbon coated membranes (MED 020 Coating system, BAL-TEC) were analyzed using a high resolution SEM (Hitachi, 5kV). Roughness and surface topography measurements were conducted on an AFM instrument from NanoScan AG.

Contact-angle measurements: The dynamic sessile drop method was used to determine the advancing and receding contact angles of DI water on the tested surfaces with a DataPhysics OCA-20 contact angle analyzer (DataPhysics Instruments GmbH, Filderstadt, Germany). The measurements were performed at 20 °C and at a relative humidity of 65 %. To determine the advancing contact angle, a 10 µL droplet was placed on the specimen's surface. The contact angle was determined 30 seconds after the droplet was placed on the surface.

3.4 Results and Discussion

Membrane ζ -potential

Homogeneity of the membrane material: RC 30 kDa membranes from different producers show different ζ -potentials (Figure 3.1b). The membrane which is named with Wyatt is distributed by the company, but produced by another company, which is not mentioned on the label of the membrane.

All of the tested materials show differences in their ζ -potential distribution over the length of a membrane in the range of 11% (Figure 3.1a). Although the variations are in a low range they are still higher than the measurement uncertainty defined by the instrumental setup ($\pm 9\%$) and thus significant. It can be assumed that small differences in the surface structure (impurities from the production process or different surface roughness) result in slightly different ζ -potentials. From our observations obtained from different measurements the inhomogeneity's have no measurable influence on the particle elution or recovery.

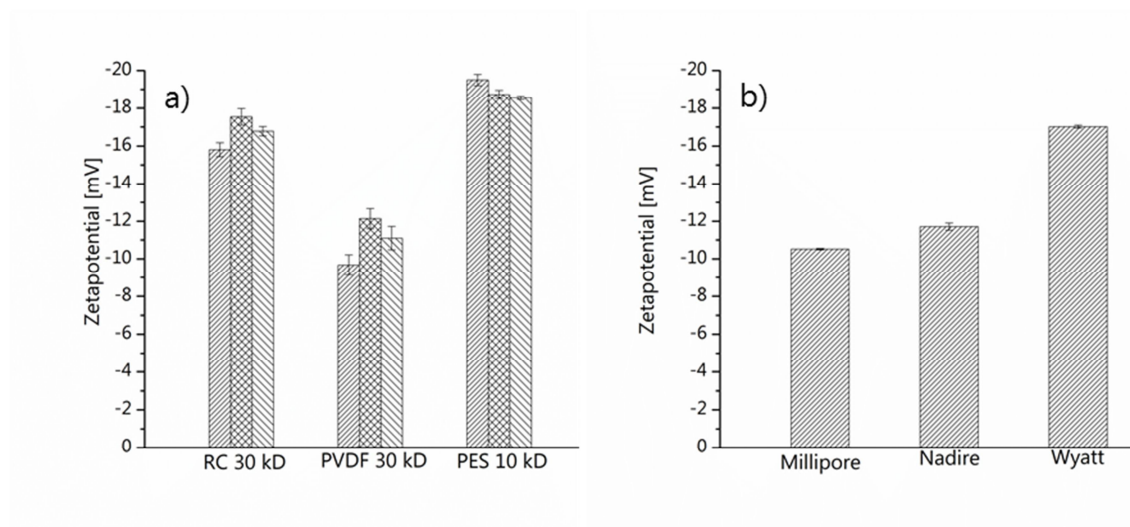


Figure 3.1: a) ζ -potential distribution over the length of a membrane at 3 different positions (RC, PVDF, PES); a) ζ -potential of a RC 30 kDa membrane from different producers.

Particle size of PS suspended in different media: Before the influence of different surfactants and salts on the ζ -potential of 30 nm PS particles was studied, the initial particle size in the different media was analyzed using DLS. PS particles were suspended in DI water, NaN_3 , Triton, SDS and $\text{Na}_6\text{P}_6\text{O}_{18}$. All of the suspensions have a medium particle size of 36.5 ± 0.7 nm. Consequently for all further experiments the initial particle size of PS in suspension is the same.

Effects of pH, surfactants and salts: The ζ -potential of 30 nm polystyrene (PS) nanoparticles suspended in different solutions is presented in Figure 3.2a. The nanoparticles have a negative surface charge of -20.7 ± 1.4 mV. A change of pH to higher values (from 7 to 10), using sodium hydroxide increases the surface charge to -106.4 ± 7.3 mV. Upon use of surfactants SDS only slightly increases the surface charge (-25.1 ± 2.1 mV) whereas Triton X-100 significantly raises values to -51.4 ± 0.3 mV. Addition of salts influences the surface charge similarly to the membranes. With NaN_3 (-17.0 ± 2.6 mV) a decrease and with hexametaphosphate an increase to highest obtained values, for addition of salts (-57.6 ± 1.0 mV) was determined. The ζ -potential dependence of the membrane material on pH is depicted in Figure 3.2b. All membrane materials have a negative surface charge but the influence of the pH does vary significantly. For all membranes a similar trend can be observed. As expected the PVDF membrane shows the least influence on surface charge (-9 to -14 mV) with changing pH, due to the absence of polarizable functional groups. The RC and PES membrane show almost similar behavior, with a surface charge ranging from below -10 mV up to -25 mV.

Figure 3.2c reveals the influence of surfactants on the ζ -potential of the investigated membrane materials. In contrast to the pH, the influence is drastically different for particular

membranes. SDS remarkably increases the PVDF membrane ζ -potential to -275 mV. In contrast, Triton does not show any effect on the PVDF membrane but increases the ζ -potential of RC and PES significantly. For both membranes values higher than -100 mV (RC -115 mV; PES -110 mV) using Triton were obtained. These effects might be contributed to the different membrane material and surfactant chemistry. In case of SDS with PVDF and RC membranes selective adsorption of the surfactant hydrophobic "tail" on the membrane is likely. Attributed to the charged hydrophilic surfactants functional "head" group and its orientation towards the membrane surface in an aqueous environment, an increase of membrane surface charge can be achieved. With increasing "chemical similarity" of the membrane material and the surfactant "tail" itself, this effect is more pronounced. The results for Triton are surprising taking into account that Triton itself is a non-ionic surfactant and theoretically should have no influence on the ζ -potential. After repetition of measurements 5 times obtaining the same results we concluded that a measurement error can be excluded. We assume that Triton is not contributing to the zeta potential increase itself by absorbing on the surface, but seems to "clean" the membrane surface from absorbed chemicals functioning as detergent and thus leads to an increase in electrostatic forces. The exact mechanism is definitely of interest but was not further studied exceeding the scope of this work. (Madaeni and Mansourpanah 2004)

The effect of commonly used salts for A4F separation is presented in Figure 3.2d. As expected the surface charge of membranes is reduced with addition of NaN_3 due to compression of the electrostatic double layer leading to a decrease of the ζ -potential. Upon addition of sodium hexametaphosphate, a salt used for separation of oxide nanoparticles (e.g TiO_2), a contrary effect on the membrane surface charge was observed. The polar and strongly negatively charged salt increased the ζ -potential of all except the PES membrane. It can be assumed that in this case the sulfone groups inhibit adsorption of the hexametaphosphate molecule

and thus the same effect upon addition of NaN_3 can be observed. For the other membranes the formation of a strong negative surface charge can only be explained with adsorption of the hexametaphosphate on the membrane surface.

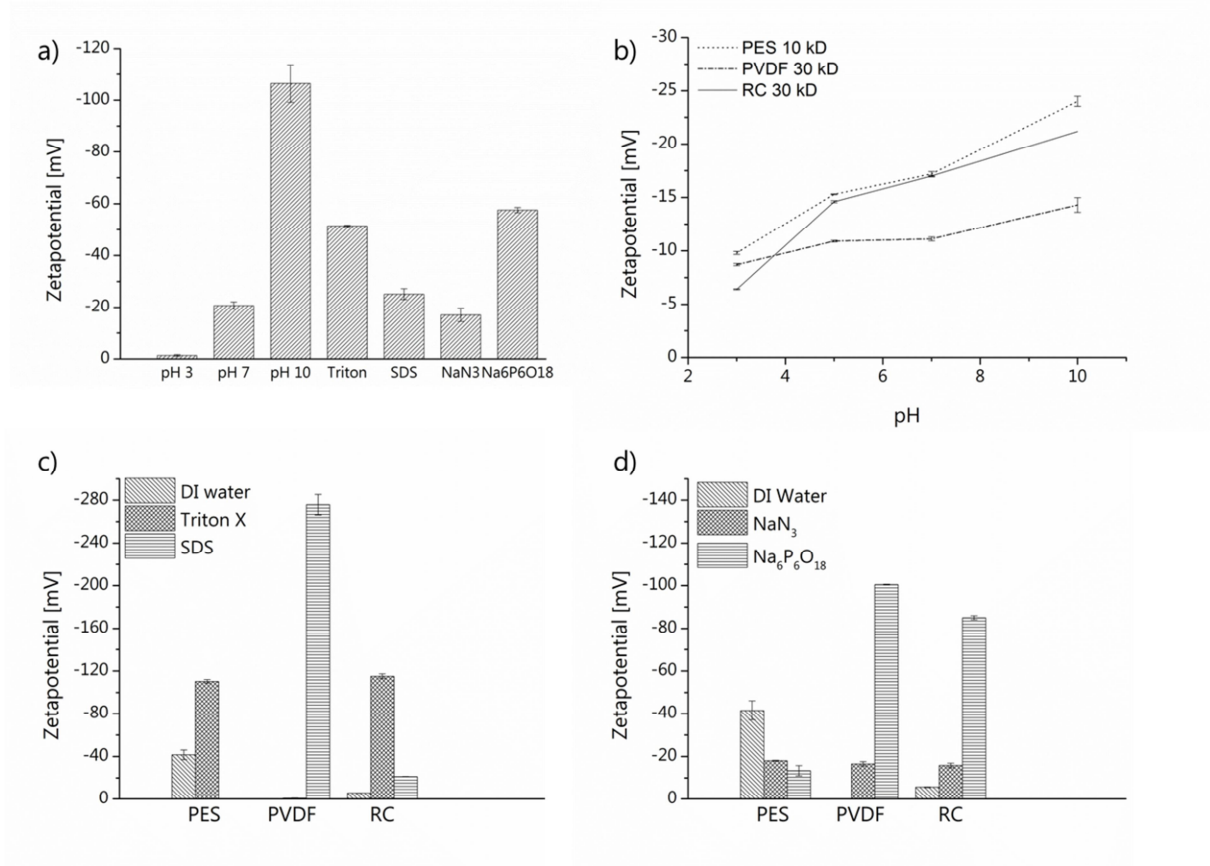


Figure 3.2: a) ζ -potential of 30 nm polystyrene nanoparticles suspended in different solutions and b) the effect of pH, c) surfactants and d) salts on the ζ -potential of the different membrane materials (no bar = potential close to 0).

Membrane morphology

AFM images: To elucidate morphology for particle recovery, the surface roughness and morphology of different membranes were determined. New membranes and old, used membranes were analyzed. In Figure 3.3 AFM images of all 3 membranes are presented.

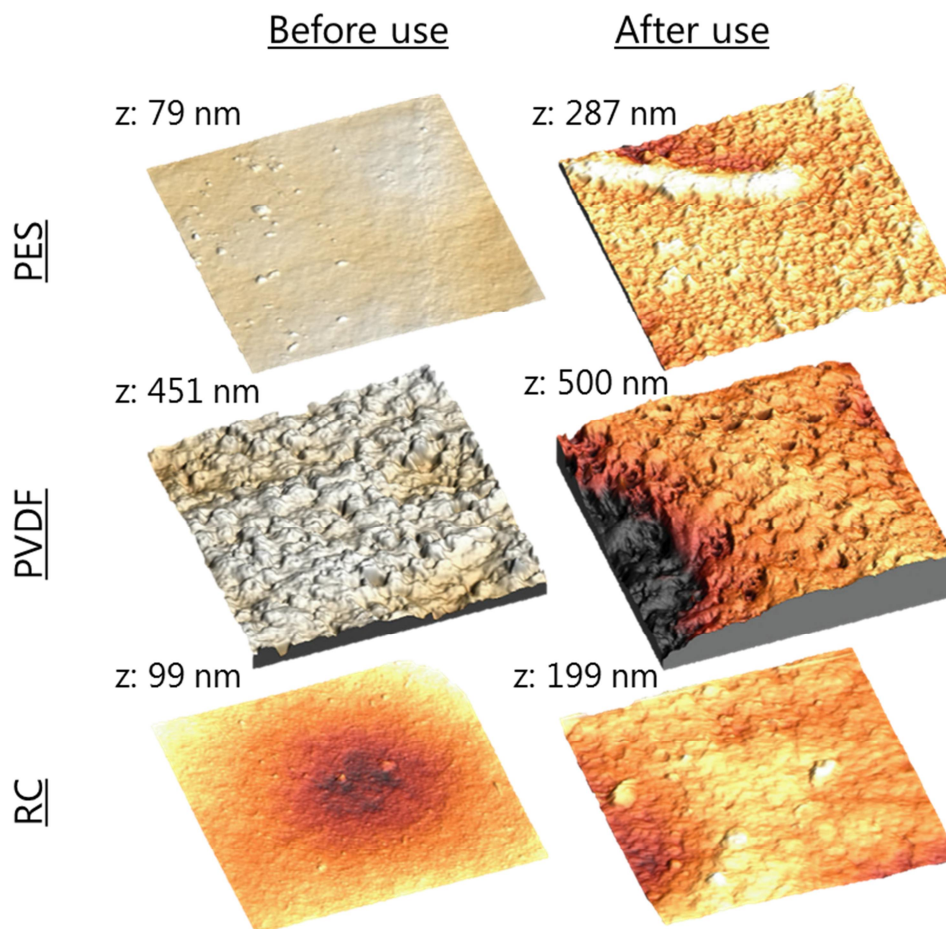


Figure 3.3: 3D AFM images of A4F membranes before and after use ($x= 5.0 \mu\text{m}$; $y= 5.0 \mu\text{m}$).

All membranes show a surface roughness in the nm range before use. PES exhibit the smoothest surface with a roughness (roughness = maximum peak height) of 79 ± 8 nm, whereby PVDF has the highest roughness with 451 ± 17 nm, followed by RC, which is with 99 ± 5 nm much smoother. After use for A4F separations (nine injections) an increase in sur-

face roughness for all membranes is observed. In the case of RC the roughness is 2 times, and for PES almost 4 times higher. Just for PVDF the roughness does not change significantly. This increase in roughness can be caused by two factors. One is the absorption of particles on the membrane. When particles will stick on the membrane the surface would no longer be smooth, but rough. The second reason can be a damage of the membrane. As a quite high pressure is applied on the membrane within the A4F channel (depending on the flow rate and time) it is supposable that the membrane gets damaged, especially in the focus area.

SEM images: More information can be obtained from SEM top view images (Figure 3.4).

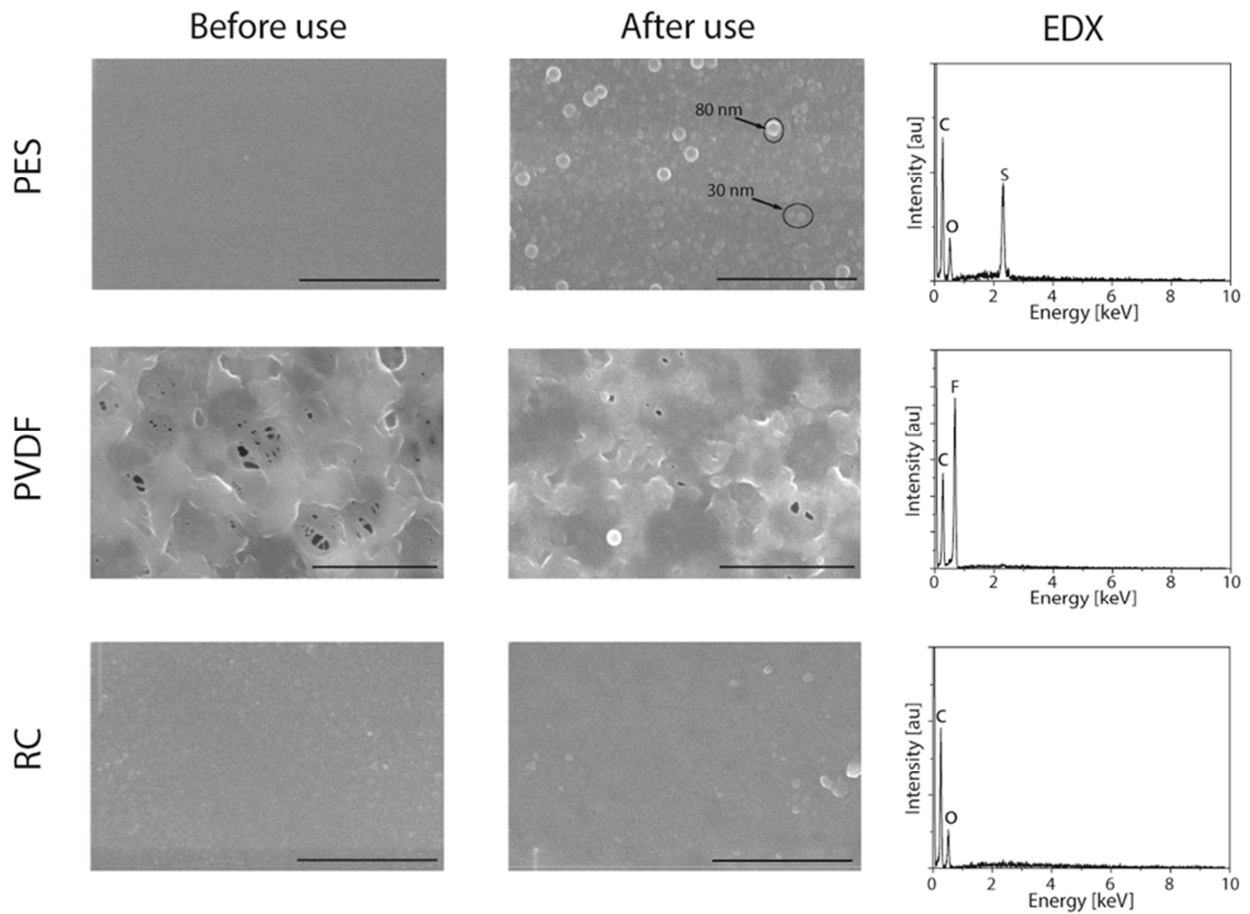


Figure 3.4: SEM images and EDX profiles of A4F membranes before and after use (scale bar = 1 μm). Absorbed polystyrene particles (30 nm and 80 nm) on the used NF and PES membrane are highlighted (80 nm polystyrene particles were injected after the studies with 30 nm particles to obtain a measure for particle absorption irrespective possible poor SEM resolution for imaged membrane materials).

PES and RC membranes show to have very smooth surfaces with no big cavities or pores. Surprisingly the PVDF membrane shows pores and cavities in the nm to μm size range, where nanoparticles can easily be trapped or pass through. After use, particles can be observed on the surface of all membranes (all images were recorded on 1x2 cm^2 species from the area of the focus point). The amount of particles differs strongly depending on the material of the membrane. PES membrane exhibits a substantial absorption of particles where on the RC and

PVDF membrane just a few particles can be found. Due to the big cavities found on the PVDF membrane, particles will pass through these cavities. The potential of absorption and the pores explain, next to the stability upon mechanical forces during A4F separation, the difference in roughness after use.

Membrane hydrophobicity

The membrane hydrophobicity is determined by measuring the contact angle of a water droplet to the membrane surface. Experiments show high angles for PVDF and PES (66.9 ± 1.7 and 60.5 ± 3.2) and low angles for RC (15.07 ± 0.9). This translates to RC membranes being hydrophilic whereas PVDF and PES have a hydrophobic character.

Influence on separation and recovery

To evaluate the influence of the investigated parameters for every measurement the recovery (corresponding UV/Vis peak area to the peak area of a pre-hand performed flow injection) and the retention time shift were compared. In Figure 3.5 a fractrogram (UV/Vis @ 280nm) for the separation of a 30 nm PS nanoparticle sample using the PVDF membrane and different carriers is depicted. To demonstrate the influence of repulsive forces on separation performance conditions with lowest (DI Water at pH=7; ζ -potential membrane/particle = 0.0/-20.7 mV) and highest (SDS ζ -potential membrane/particle = -275.8/-25.1) repulsive forces between particles and membrane are studied.

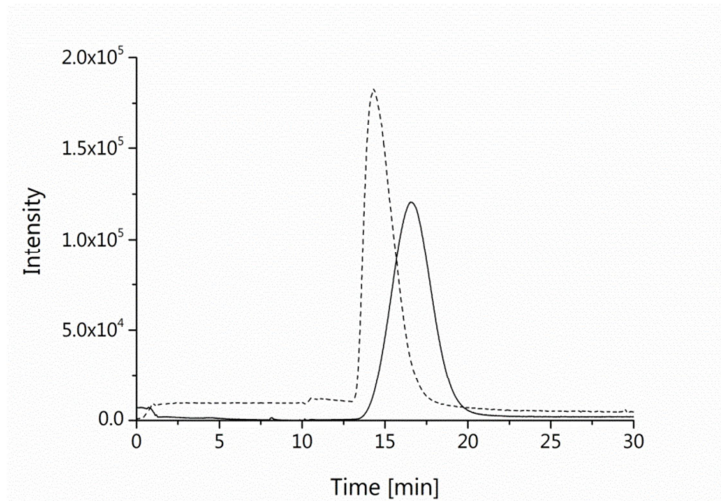


Figure 3.5: UV signal of 30 nm PS nanoparticles with a PVDF membrane and SDS (dotted line) and DI water (continuous line).

This was also performed for other particle/membrane combination as reported in Table 3.3.

In general stronger repulsive forces between the membrane and particles result in better recoveries and lower retention times. At the same cross flow values particles are repelled more from the membrane surface with higher surface charge (under the assumption they have the same charge sign) and thus fewer particles are absorbed on the membrane surface. This should result in higher recoveries when compared to lower charged membrane surfaces. Furthermore particles rejected from the membrane are constrained to faster flow profiles in the separation channel and thus are eluted earlier. For the PES and RC membrane the general situation (as discussed above) holds true. In terms of retention times this is also the case for the PVDF membrane. Surprisingly, the recovery for the PVDF membrane is not going along with the proposed mechanism. Although the PVDF membrane shows a more than two times higher surface charge than the RC and PES membrane, recoveries are about a factor of 3-4 lower.

When correlating results from ζ -potential measurements and morphology of the membranes to data obtained from A4F measurements, it can be seen that the poor recovery of the PVDF membrane underlies the μm size pores and cavities. In this case recovery is dominated by the morphology and does not show a dependency on the ζ -potential of the membrane/particle system at all as also expressed for same recovery rates of $13\pm 1\%$ for a ζ -potential membrane/particle of $-0.0/-20.7\text{ mV}$ and $14\pm 1\%$ for a ζ -potential membrane/particle of $-275.8/-25.1\text{ mV}$. For the RC membrane, with highest recoveries upon all tested membranes, the membrane morphology does not change substantially during separations and thus only has an inferior influence. In this case particle recovery can be maximized by adjusting the electrostatic repulsion, but still a particle loss of 40% or higher can be observed. PES membranes behave again contrarily, where poor recovery cannot be explained due to the ζ -potential or the morphology of the membrane. Consequently for PES the recovery is clearly influenced by other factors beside the electrostatic repulsion and morphology. Our results let conclude that also the hydrophobicity of the membrane surface plays a major role. Increasing van-der-Waals forces (expressed in the Hamaker constant) between the membrane surface and particles may lead to a higher tendency of absorption and consequently a lower recovery. As PS particles are also hydrophobic an interaction of the particles with the PES membrane is likely. This is in good agreement to the SEM top view images, where a high load of particles on the PES surface can be observed which is not the case for the hydrophilic RC membrane.

Investigation of analytical concepts for nanoparticle analysis in suspensions

Table 3.3: Retention time shifts and intensity differences for PS particles separated in A4F with different membranes and different carrier solutions.

Membrane	30 kDa RC		10 kDa PES		30 kDa PVDF		NF	
	Carrier							
	Triton	DI	Triton	Na ₆ P ₆ O ₁₈	SDS	DI	Na ₆ P ₆ O ₁₈	Triton
Ret.time maximum [min]	11.9	14.1	12.6	no signal	13.9	16.8	10.7	15.2
Recovery [%]	61±2	9±1	54±2	0	14±1	13±1	15±1	23±5
Δ ζ-Potential [mV]	-63.4	-15	-58.9	-44.2	-250.1	-20.7	-84.6	-51.4

Chapter 4

4 Investigation of appropriate analytical concepts for nanoparticle analysis in aerosols

4.1 Introduction

Nanoparticle-containing sprays are categorized as critical consumer products due to their direct exposure path via lungs and a potential enhanced toxicity of nanoparticles. Recent studies proposed the first analytical concepts for simulated exposure experiments and a first approach for risk assessment, but these studies lack from systematic evaluation (see Chapter 1). For this reason one aim is the optimization and validation of analytical concepts for proper quantification and the proposition of guidelines for appropriate analytical simulation experiments as basis for a reliable risk assessment of exposure to nanoparticle containing consumer spray products.

Therefore the behavior of nanoparticles during the spray application needs to be studied and understood. It is known from the work of Hagendorfer and Lorenz (Hagendorfer, Lorenz et al. 2010, Lorenz, Hagendorfer et al. 2011) that droplet size, and with it the final size of the nanoparticles and its agglomerates, are strongly dependent on the type of spray vessel. Other factors like the solvent type are also proposed to have a strong effect on type and behavior of nanoparticles in the aerosol. Particle size distribution and particle number concentration is also affected by the position of the spray inside the spray chamber and the spray direction.

4.2 Classification of nano sprays

4.2.1 General categorization

To generate a realistic worst-case scenario nanoparticle containing sprays need to be categorized concerning their use. Figure 4.1 illustrates the four major classes of sprays and the distribution percentage, determined for sprays which were analyzed within this work. From 27 bought products (stores and online), four are cleaning sprays, five are cosmetic sprays, three are plant-strengthening sprays and the rest are impregnation sprays.

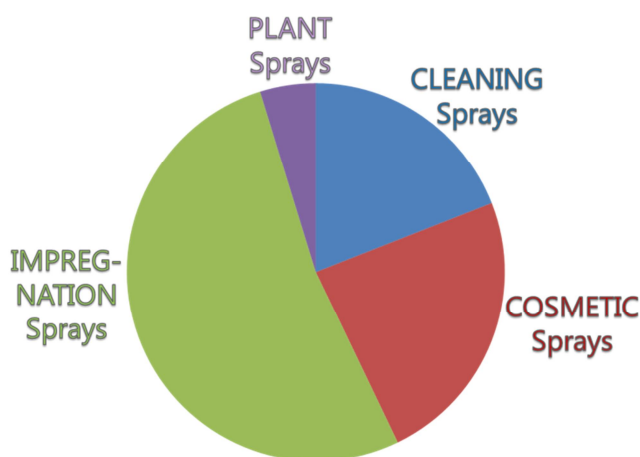


Figure 4.1: Categorization of nanoparticle containing spray products.

Impregnation sprays represent the biggest class of nano sprays. The majority of the impregnation sprays vessels are propellant gas vessels. The second largest group is cosmetic sprays, which use both propellant gas and pump spray vessels. In both, the cleaning sprays and plant-strengthening sprays, all are delivered in pump spray vessels.

4.2.2 Application

The application varies most between cosmetic sprays and the other three groups. While the application direction is towards the consumer (faced) in most of the applications of cosmetic sprays, the direction for all other sprays is away from the consumer (advert). In addition, the distance from the consumer to the released aerosol is less than that for the other three spray types, as cosmetic sprays are mostly applied with bent arms (in the direction of the consumer), while the others with outstretched arms, away in the direction from the consumer. However, the application duration is much longer for impregnation, cleaning, and plant-strengthening sprays than for cosmetic sprays. Whereas cosmetic sprays are applied for a few seconds, the application duration of the other sprays can range from a few seconds up to 1 minute.

The following studies should clarify the influence of the spray duration, spray direction, and spray distance.

4.3 Experimental Section

Approach: All experiments were carried out with a standardized aqueous spray solution: a 50 ppm, 50 nm silver nanoparticle suspension in a standardized propellant gas or pump spray dispenser. The chamber design is described already in a previous study (Hagendorfer, Lorenz et al. 2010). With a volume of 0.33 m³ it represents the near breathing zone of a consumer. The chamber was connected to a SMPS and an electrophoretic TEM grid sampler via conductive tubing. Spray vessels were weighed before and after each spray event to determine the released mass. Experiments were carried out to study the influence of the tubing material and length, the linearity of spray experiments, and the influence of different positions of the spray inside the chamber. Temperature and humidity were monitored throughout the whole experiment.

Chemicals: Aqueous 50 nm silver nanoparticles were purchased from NanoSys (NanoSysy GmbH, Switzerland). A Milipore Mili-Q A-10 water unit (Milipore AG, Germany) was used for the production of 18 MΩ cm deionised water (DI-water).

Instrumentation: The generated spray aerosol was investigated for particle size distribution and particle number concentration using a scanning mobility particle sizer 3014 (TSI Inc, USA). Aerosol was dried using a low-flow thermodenuder (Fierz, Vernooij et al. 2007). Temperature and humidity were monitored using a Voltcraft DL-141TH Datalogger (Conrad Electronics AG, Switzerland).

Investigation of appropriate analytical concepts for nanoparticle analysis in aerosols

Aerosol cans: A propellant-portable spray device with gas unit was purchased from Preval (Haubold Technik, Germany). Pump spray dispensers were merchandised from VWR International (VWR International, USA).

Tubing: Tygon tubing was purchased from VWR International (VWR International, USA); electrically conducting tubes were purchased from Adpol (Adpol Advanced Polymers Ltd, UK).

4.4 Results

Humidity and temperature

During all experiments the temperature and the relative humidity inside the spray chamber is monitored. Figure 4.2 illustrates both parameters monitored during a 900 second spray experiment for propellant gas sprays and pump sprays.

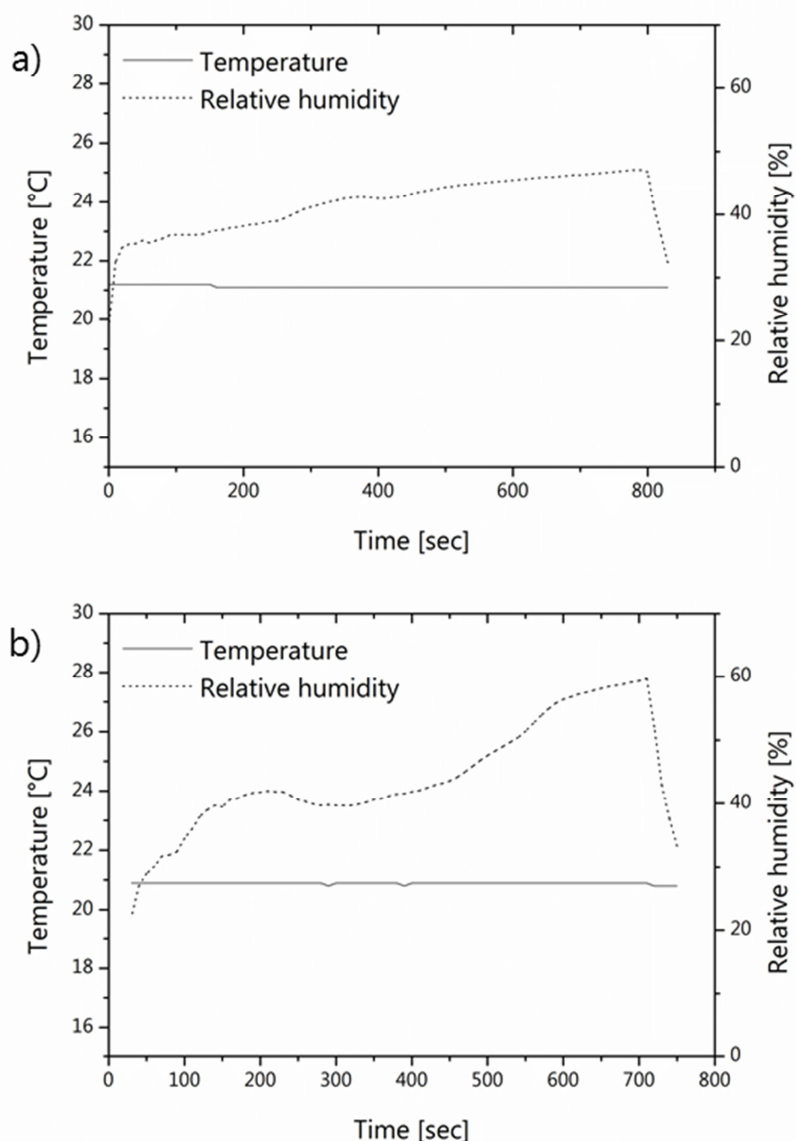


Figure 4.2: Relative humidity and temperature inside the spray chamber during one experiment; a) propellant gas spray; b) pump spray.

In both experiments, the temperature is constant during the measurement. The relative humidity increases at the moment the spray is engaged. The initial relative humidity inside the chamber differs, as also the relative humidity in the lab differs. In case of the propellant gas spray, the humidity increases from 22% to 47%. In case of the pump spray, the humidity increases from 15% to 60%. As the pump spray releases much bigger droplets than the propellant gas spray, the humidity reaches higher values during the experiments. The values are in agreement with a 2010 ISO/DIN (ISO 2010) where an acceptable humidity range from 30% to 70% for nanoparticle chamber experiments is given.

Tubing material

In a first step, the influence of the tubing material was studied. All connections from the spray chamber to the instrument were made of tygon tubing in one trial/experiment and made of an electrically conductive material in the other trial/experiment. Figure 4.3 demonstrate the difference in particle number concentration for both tubing materials over different spray durations.

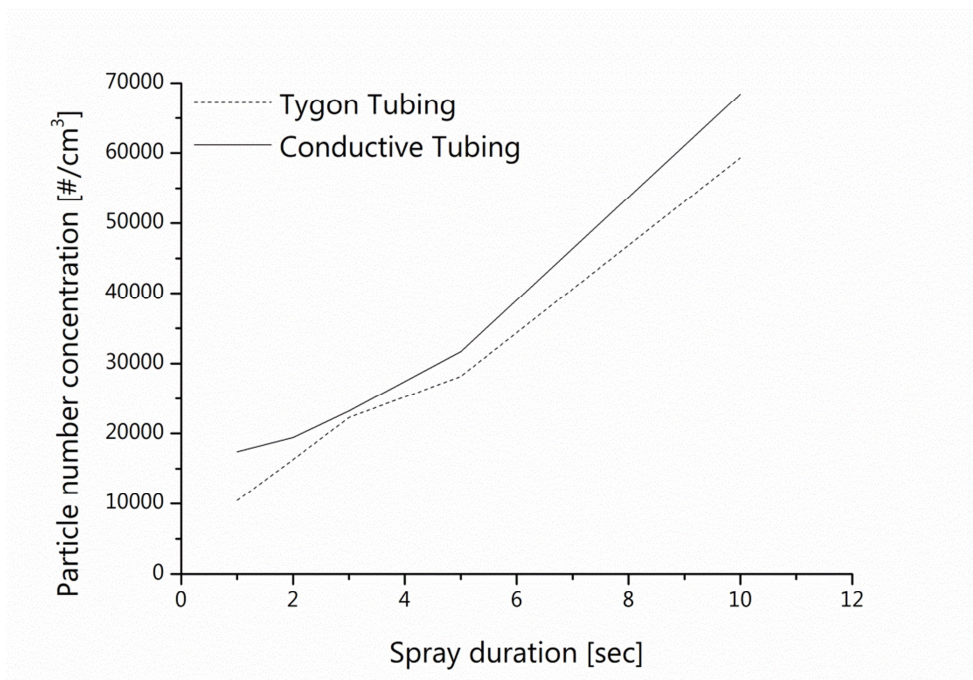


Figure 4.3: Particle number concentration dependent on different spray durations and different tubing materials.

With conductive tubing the particle number concentration is always higher than the particle number concentrations compared to tygon tubing. This can mainly be attributed to the fact that charged particles stick on the walls of the tygon tubing. This is not the case if conductive tubing material is used. Consequently, all further experiments were carried out with conductive tubing.

Linearity of spray experiments

In a second step, the linearity of spray chamber experiments was tested. In Figure 4.4, the particle number concentration was plotted against amount of sprayed dispersion for propellant gas sprays and pump sprays.

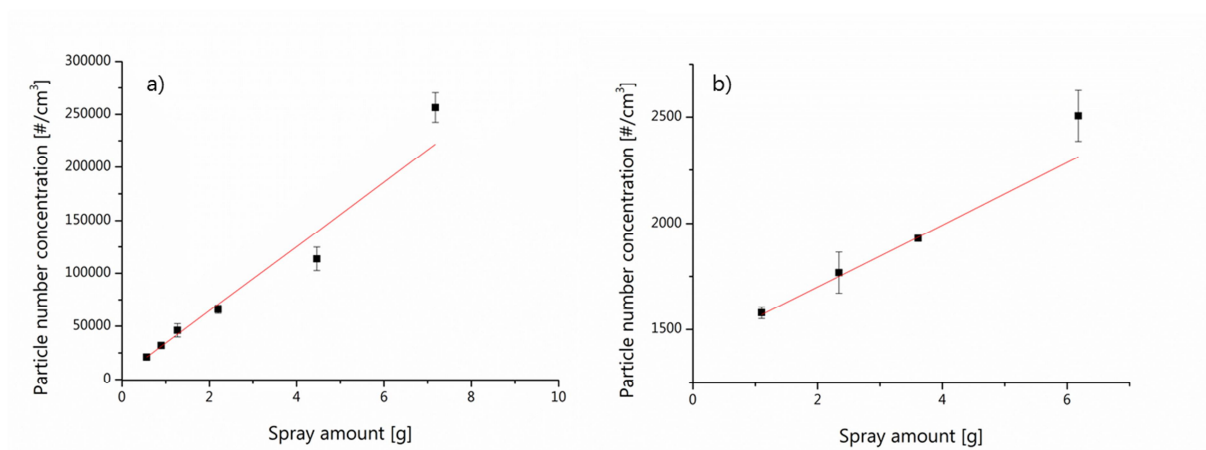


Figure 4.4: Linearity of spray experiments; a) propellant gas spray, b) pump spray (red line = linear extrapolation).

A clear linear increase in the particle number concentration can be observed. As a consequence, an extrapolation from low spray amounts to high spray amounts is possible. For a higher spray amount a saturation can be observed.

Spatial distribution

In a third step, the concentration and the particle sizes were measured at different positions inside the spray chamber in order to characterize spray behavior and change of the particle size distribution (PSD) at different positions and study if simulation of a worst case scenario for different spray situations is possible with this setup. Therefore the silver nanoparticle solution was sprayed at different positions to the SMPS as shown in Figure 4.5.

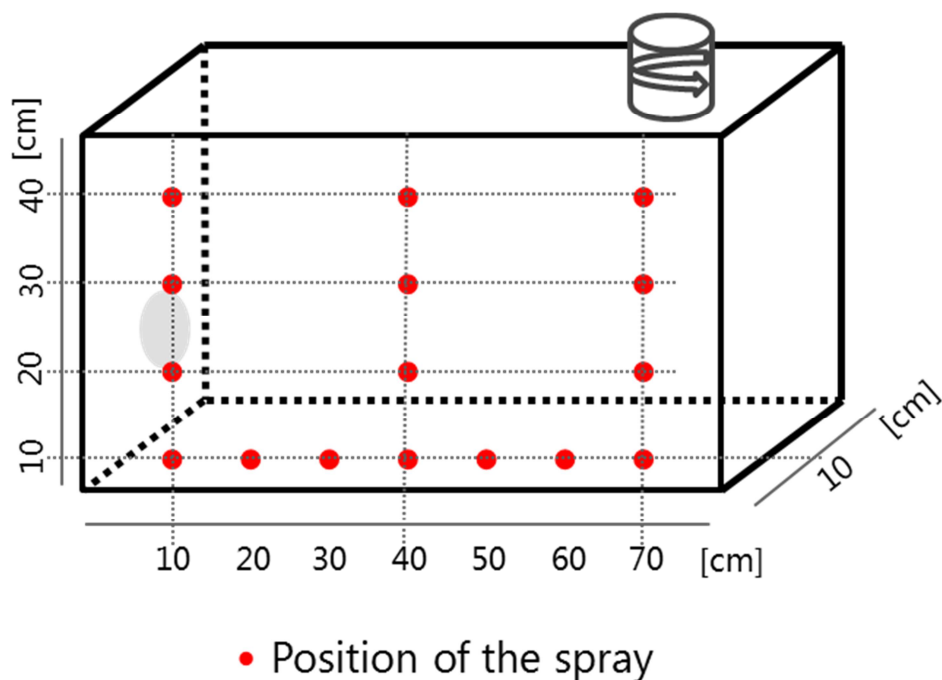


Figure 4.5: Experimental setup for space-resolved concentration and particle size measurements.

The different spray positions represent different types of applications. A short distance to the instrumentation is characteristic for cosmetic sprays and a long distance for impregnation, cleaning, and plant strengthening sprays.

Propellant gas spray: Figure 4.6a shows the particle number concentration for faced spray experiments after 180 seconds (left), 360 seconds (middle) and 540 seconds (right) as obtained from a propellant gas dispenser filled with Ag NP suspension and 3 seconds of spraying. “Faced” means that the spray nozzle is directed towards the instrumentation. In, Figure 4.6b the particle number concentration of the same spray is displayed but the spray can is turned 180° in an “advert” position.

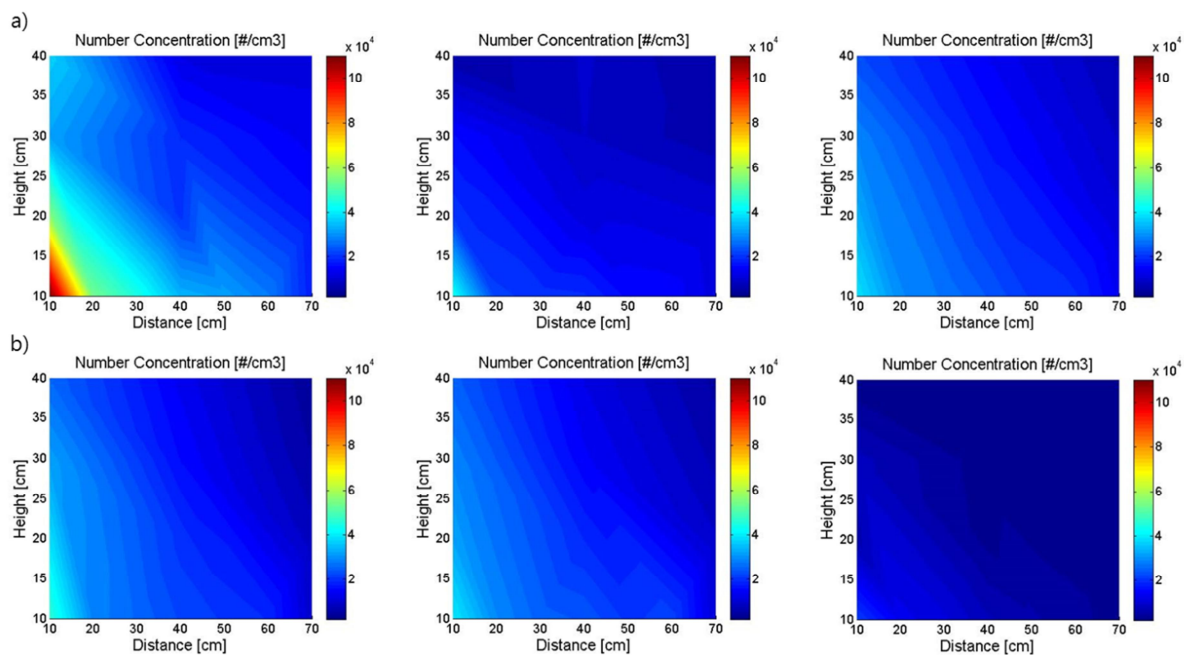


Figure 4.6: a) number concentration measurements of faced spray experiments; b) number concentration measurements of advert spray experiments. Both for propellant gas sprays.

It can be observed that the particle number concentration for a faced, near inhalation zone (20 cm distance) is around 5 times higher than the one of an advert, remote inhalation zone. Moreover, the particle number concentration for a faced spray setup is higher during the first three minutes than the one for an advert setup. After three minutes, the number concentration is more or less constant and uniformly distributed.

During these measurements the particle size was also monitored. In Figure 4.7 the particle size distribution is plotted over the size of the spray chamber.

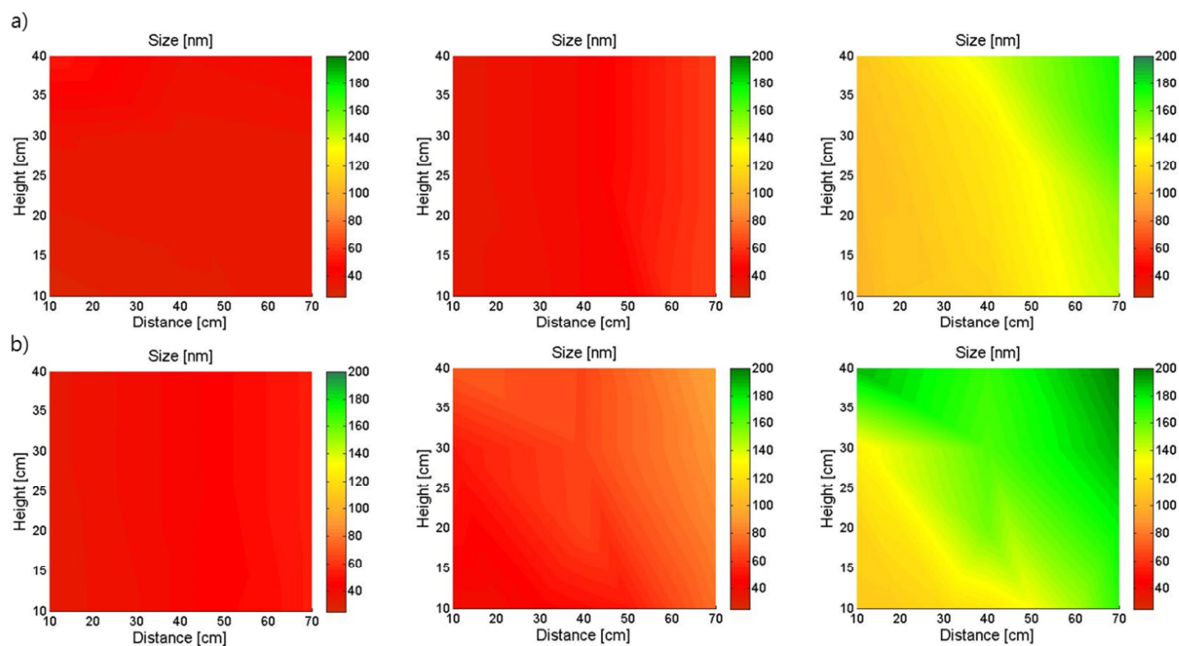


Figure 4.7: a) particle size measurements of faced spray experiments; b) particle size measurements of advert spray experiments; Both for propellant gas sprays.

For both setups (faced and advert) the particle size range during the first 3 minutes was in the range of 50-60 nm. For an advert spray direction, the particles detected after 6 and 9 minutes were larger than the ones of the faced setup. After 9 minutes, the particle sizes in both cases were over 100 nm. An aggregation occurred in both cases. Both experiments confirm that sprays which are applied in the near inhalation zone in a faced direction are the most critical ones. For this reason, a faced position with a distance of 30 cm from the vessel to the instrument was defined as a worst-case scenario for analysis of real consumer spray products. Based on the results obtained from the linearity experiments, a spray duration of 3 seconds was chosen to simulate a worst-case scenario for the used spray chamber design.

Pump spray: The same experiments as described above were also conducted with pump spray dispensers. Three pump strokes were applied and Figure 4.8 illustrates the correspond-

ing results for the propellant gas sprays and the particle number distribution for a pump spray applied at different positions inside the spray chamber.

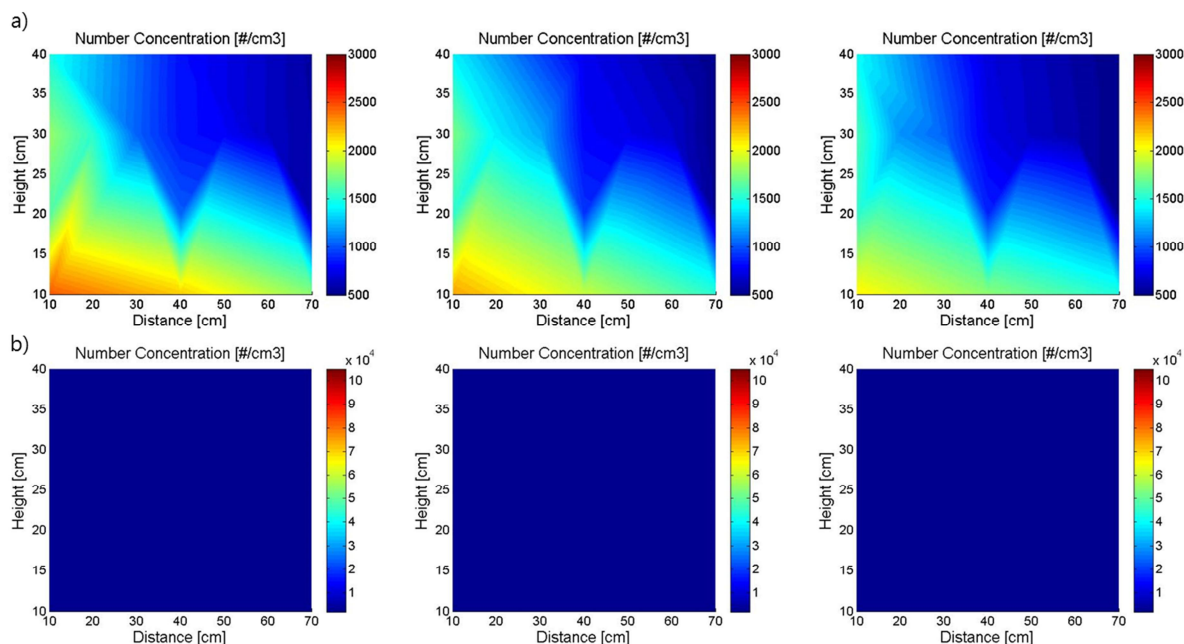


Figure 4.8: a) number concentration measurements of faced spray experiments; b) number concentration measurements of advert spray experiments; Both for pump sprays.

In general, the same effect can be observed as for propellant gas sprays: the number concentration for advert spray experiments is lower/less than the one for faced spray experiments. Nevertheless, when comparing the absolute numbers of particle number concentrations with the concentrations obtained from propellant gas sprays, the concentration for pump sprays is lower by a factor of 40.

The same holds true for the particle size distribution. Again, particles released in an advert spray scenario are bigger/larger than the ones released in a faced spray scenario. However, faced or advert, particles released from pump sprays are bigger/larger than the ones released by propellant gas sprays (Figure 4.9).

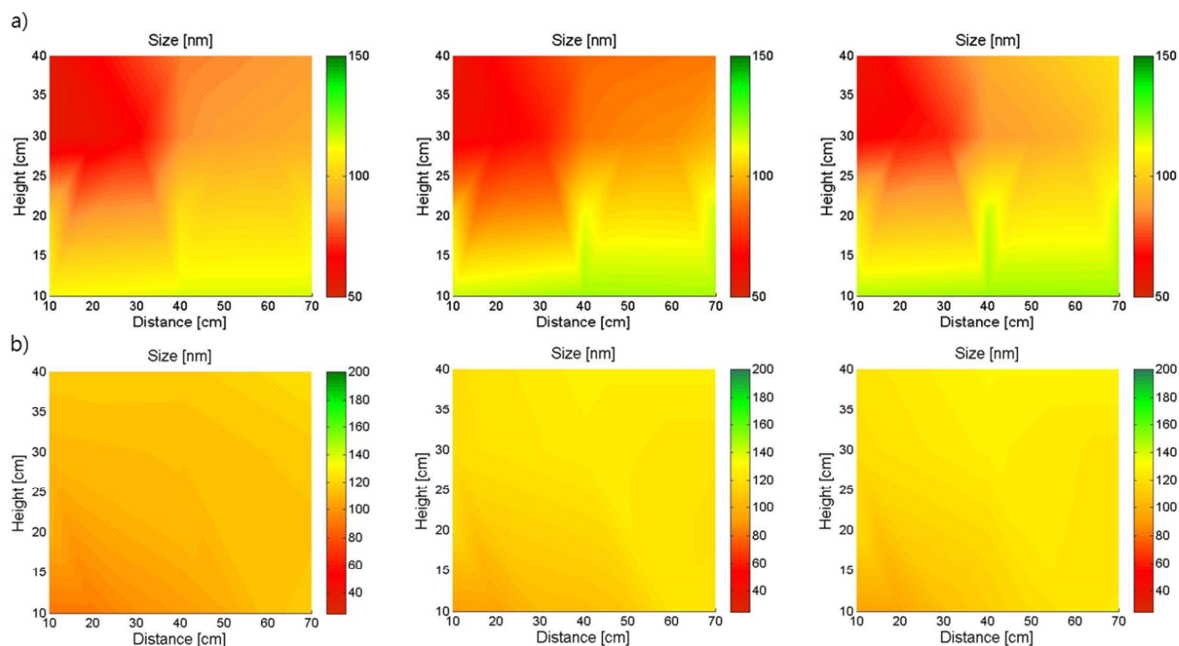


Figure 4.9: a) particle size measurements of faced spray experiments; b) particle size measurements of advert spray experiments; Both for pump sprays.

Both phenomena can be explained from the initial droplet size generated by the spray vessels. Because of the higher pressure inside the propellant gas sprays, the suspension is better dispersed in the aerosol as in the case of a pump spray. Consequently, for the aerosol spray smaller droplets carrying fewer particles are generated. When the solvent evaporates, smaller particle aggregates are formed. Concerning particle number concentration, finely dispersed droplets also go along with a slower deposition induced by sedimentation of such.

Influence of the background

To determine the influence of the background on the particle size distribution and the particle number concentration two different experiments were performed: one with a particle-reduced background and one with a high particle background. In the first situation, the spray chamber was evacuated until particle concentration levels reached 200 particles/cm³ inside the chamber. In the second setup, the chamber was vented with fresh lab air and closed

again before the spray experiment was conducted (particle concentration 8000 particles/cm³). Experiments were again performed with propellant gas sprays and pump sprays.

Propellant gas spray: Figure 4.10 illustrates the particle number concentration plotted over the particle size distribution for a propellant gas spray.

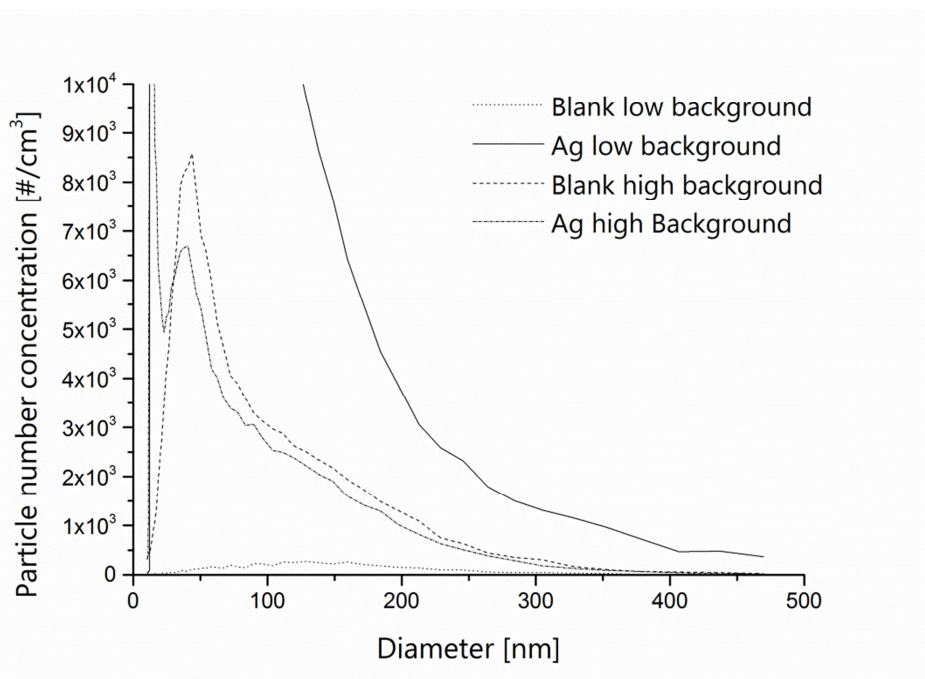


Figure 4.10: Particle size distribution with low and high particle background for a propellant gas spray.

The peak maximum for the low background + Ag curve lies at 290000 particles/cm³ and 13 nm in size. The maximum for high background + Ag lies at 126000 particles/cm³ and 13 nm in size. A second peak can be observed at 38 nm, which corresponds with the peak maximum of the high background curve. Consequently, the particle number concentration was reduced by a factor of 2.3 and a shift in size could be observed when suspending a higher particle background to the system. As primary particles are already present in the air, droplets released from the spray can stick to them, agglomerate, and sediment much faster.

Pump spray: For pump spray vessels, the particle size distribution looks a little bit different (Figure 4.11).

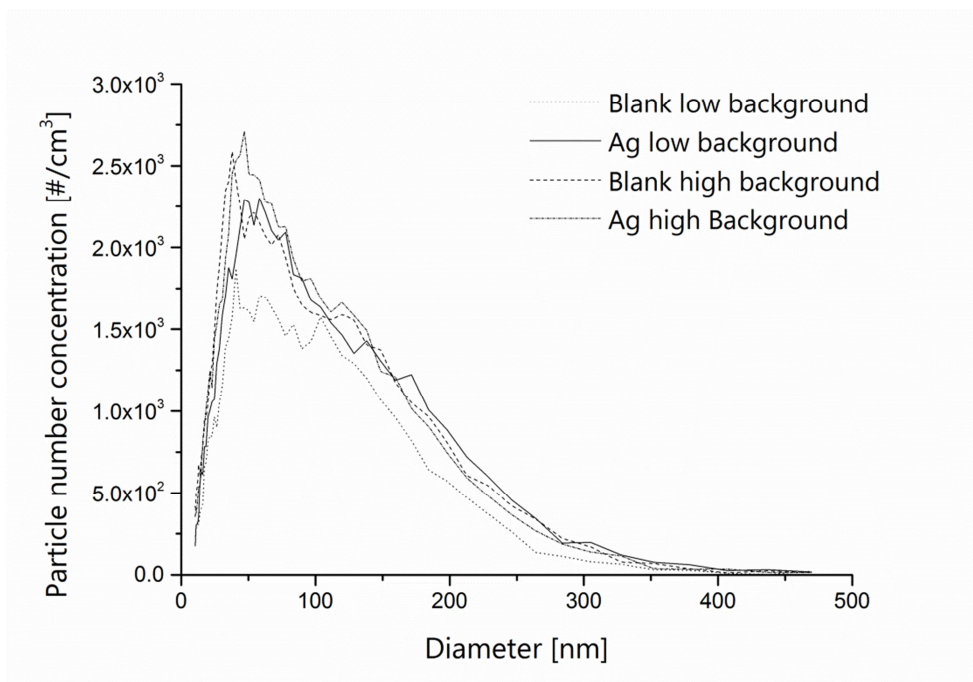


Figure 4.11: Particle size distribution with low and high particle background for a pump spray.

As a pump spray dispenser does not release as many particles as a propellant gas dispenser, there is no remarkable difference between the single curves. It could be observed that the curve for the low background + Ag was below the one of high background + Ag, but a shift in size could not clearly be observed.

Dried vs. wet particles

Almost all of the publications so far dealt with droplets instead of particles; meaning the aerosol was not dried before it was analyzed. Therefore, wet droplets as well as dried particles were analyzed. To accomplish the drying, a thermodenuder operated between the spray chamber and the SMPS.

Propellant gas spray: Figure 4.12 displays wet droplet and dried particle size distribution. It can clearly be observed that particle number concentration was higher for wet droplets. Particle size distribution for dried particles shifted to larger particles. At the peak maximum of the dried particle curve, a peak in the curve of the wet droplets can also be observed. When measuring wet droplets, two peaks can be observed, one at the maximum of the dried particle curve and one at smaller particle sizes. An explanation for the first peak in the wet droplets curve can be that some droplets do not even contain particles, as they are very small, meaning this peak is just generated by water/solvent and not by particles.

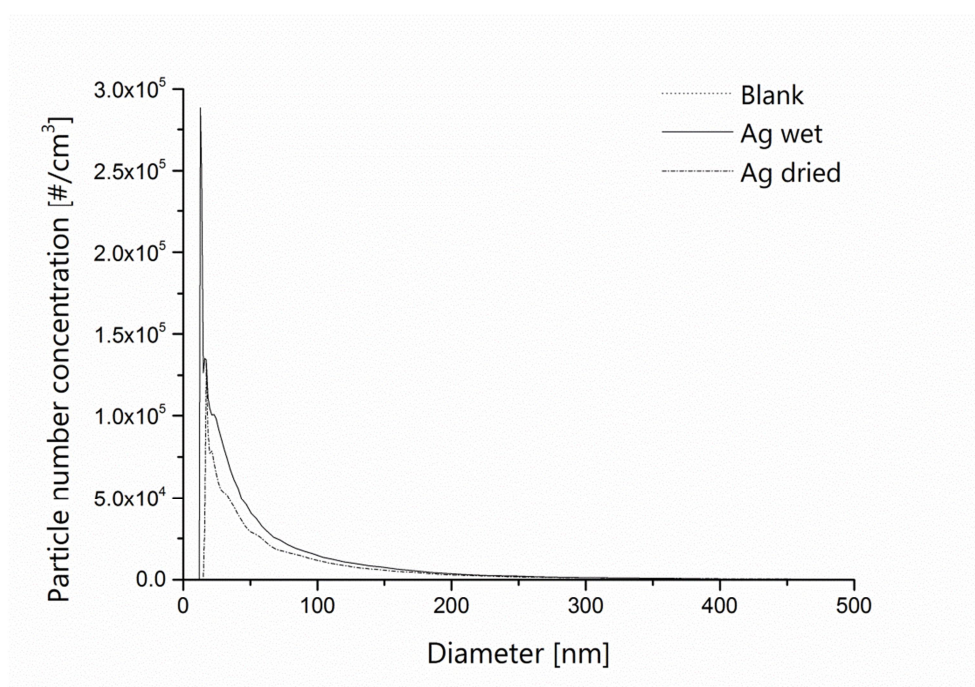


Figure 4.12: Particle size distribution of wet droplets and dried particles for a propellant gas spray.

Pump spray: The same experiments were conducted with pump spray dispensers. Figure 4.13 illustrate the size distribution for wet droplets and dried particles.

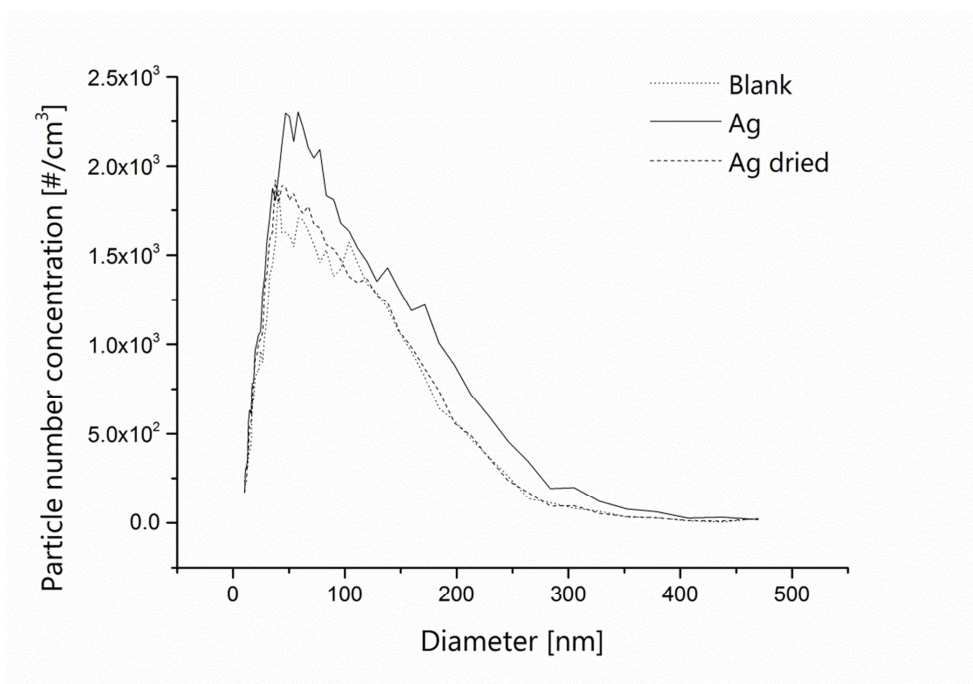


Figure 4.13: Particle size distribution of wet droplets and dried particles for a pump spray.

Again, the number concentration was higher for wet droplets than for dried particles, but the difference was much less than in the case of propellant gas sprays. One reason for this phenomenon might be the fact that, due to the large droplet size, a lot of droplets do not reach the thermodenuder as they sediment before they reach the drier. Therefore, the 100 times higher number concentration obtained from propellant gas sprays can be explained.

A shift in size could be observed for the pump sprays. As initial droplets were very large, they already contained a lot of particles. By drying, big agglomerates were generated in almost the same size as the initial droplets.

Chapter 5

5 Real consumer spray process assessment

5.1 Introduction

The number of nanoparticle containing consumer products increased over the last 10 years from a few to several hundreds and their number is expected to further increase in the future. (Woodrow_Wilson 2008) Market surveys identified silver, (Chen and Schluesener 2008, Benn, Cavanagh et al. 2010, Kaegi, Sinnet et al. 2010) zinc oxide, (Graf, Chaney et al. 2013) titanium dioxide, (Skocaj, Filipic et al. 2011) carbon and silica (Zhu, Zhao et al. 2010) as the species that are most frequently used as nanoparticles in consumer products like textiles, food and food storage, cosmetics (*e.g.* sprays), household chemicals (*e.g.* paints, sprays) or sports equipment. (Hall, Tozer et al. 2007, Brzeziński, Malinowska et al. 2012, Lorenz, Windler et al. 2012, Xue, Chen et al. 2012, Al-Kattan, Wichser et al. 2013, von Goetz, Fabricius et al. 2013)

Sprays that contain nanoparticles were identified as the most critical class of consumer products due to their direct exposure pathway via lungs, which implies an enhanced health risk. (Sung, Ji et al. 2008, Nørgaard, Larsen et al. 2010, Krug and Wick 2011, Schneider, Brouwer et al. 2011) During the last years first studies on nanoparticle containing sprays and associated nanoparticle exposure were published. (Nørgaard, Jensen et al. 2009, Chen, Afshari et al. 2010, Hagendorfer, Lorenz et al. 2010, Berlin, Dietrich et al. 2011, Lorenz, Hagendorfer et al. 2011, Oomen, Bennink et al. 2011, Quadros and Marr 2011) In some of these studies the original spray suspensions were investigated. (Hagendorfer, Lorenz et al. 2010, Lorenz, Hagendorfer et al. 2011) Information was collected about the following four important properties: particle size, chemical composition (of the particles and the whole suspension), particle number concentration and shape. However, thus far no analytical technique is available that

informs about all these parameters at the same time. Particle shape, size and chemistry can be determined offline via electron microscopy (SEM/TEM), which is very time consuming and costly. Size can also be determined online via dynamic light scattering (DLS), which, however, is not very precise for polydisperse samples, as the larger particles are overestimated and measured particle size is always larger than it really is. Bulk analysis of the chemical composition and concentration can be done by inductively coupled plasma mass spectrometry (ICPMS) after the digestion of a sample, which is very time consuming and requires a high level of sample preparation.

New promising techniques for suspension analytics investigate at least two or three of the desired four parameters. Via single particle inductively coupled mass spectrometry (spICPMS) particle size and number concentration can be measured, if the elemental composition is known and spherical particles can be assumed. This technique is extremely fast (a few seconds) and can be performed with most of the conventional ICPMS instruments. Second, asymmetric flow field flow fractionation (A4F) can provide information on the particle size distribution, coating of the particles and, when coupled to ICPMS, also on the chemistry and the concentration. (Berlin, Dietrich et al. 2011)

For the analysis of the nano-sized particle fraction generated by sprays, analytical techniques need to be used that are different from the techniques used for the suspension. To date the following techniques have been used for nanoparticle analysis in aerosols: Particle size distribution (PSD) and number concentration have been measured online by scanning mobility particle sizer (SMPS) (Hagendorfer, Lorenz et al. 2010, Berlin, Dietrich et al. 2011, Lorenz, Hagendorfer et al. 2011, Quadros and Marr 2011) or fast mobility particle sizer (FMPS) for

particles in the size range of 10 – 500 nm.^{20-22, 24, 26} However, with SMPS or FMPS it is not trivial to differentiate between droplets and solid particles, and in many studies only droplet sizes have been determined. Size and shape of particles have been identified offline by prior sampling on TEM grids and analysis by TEM, (Hagendorfer, Lorenz et al. 2010, Lorenz, Hagendorfer et al. 2011, Quadros and Marr 2011, Bekker 2014) and the aerodynamic diameter of larger particles between 300 nm and 20 µm online by aerodynamic particle sizer (APS). (Nørgaard, Jensen et al. 2009) The chemical identity of particles was determined by EDX coupled to TEM or SEM. Currently no technique is available that provides information on all properties simultaneously. Instead, properties of a sample have to be determined with online and offline techniques at the same time, which means that the sampled aliquot may differ between techniques. For example, particle size distribution and number concentration can be measured online and time resolved, whereas shape and chemistry need to be identified offline with TEM-EDX after sampling on a TEM grid over a longer period of time.

In this work a new promising coupling technique, SMPS-ICPMS, was used to analyze the aerosol of six commercially available sprays concerning particle size distribution, number concentration and elemental composition. Simultaneously, these properties were determined by other established methods in order to assess the performance of the new coupling technique. Furthermore, spICPMS was applied for characterizing the suspensions and compared to conventional methods, like dynamic light scattering (DLS) and scanning electron microscopy (SEM).

A standardized spray setup was employed that simulates worst-case consumer exposure. To meet worst-case conditions particle number concentration and the particle size distribution

of pump and propellant gas sprays were monitored at a defined position inside a spray chamber. This position had been identified to be the worst case for most spray applications. For good comparability among the experiments, the duration and direction of spraying had been predefined.

5.2 Experimental section

Experimental setup

Selection of products: The aim was that the selection be most representative of the range of consumer spray products with nanoparticles on the market. The first criterion was that the manufacturer should have labeled the product with “nano”. Second, since the composition of the aerosol depends on the spraying device and the formulation, we considered different vessel types, different solvents and different intended uses. (Losert, von Goetz et al. 2014) Thus, a broad spectrum of sprays was covered that included cosmetic sprays as well as impregnation sprays, and different types of nanoparticles (NP).

The six different spray products, which were selected for this study, are listed in Table 5.1.

Table 5.1: Selected consumer sprays.

	Vessel type	Solvent	Application	Target medium	NP type
Spray I	Pump	water	Cosmetic Spray	Skin	Ag
Spray II	Pump	water	Impregnation Spray	Glass	n.m.
Spray III	Propellant	water	Impregnation Spray	Glass, Ceramic	n.m.
Spray IV	Propellant	alcohols	Impregnation Spray	Textiles	n.m.
Spray V	Propellant	silicones (I)	Antiperspirant	Skin	Ag
Spray VI	Propellant	alcohols	Sunblock	Leather, Textiles	n.m.

n.m. = NP type not mentioned on the label; but labeled as a “nano product”

Standardization of exposure experiments: Spray experiments were conducted in a spray chamber with a volume of 0.33 m³, representing the near breathing zone of a consumer. Spray vessels were always positioned at a distance of 30 cm to the outlet of the chamber, based on the results obtained in chapter 4. The average arm length of a Swiss resident was calculated to be 57 cm average length. (Bammes 2001, FORS 2007, Rühli, Henneberg et al. 2008, Statistisches_Bundesamt 2009) As some sprays are applied with outstretched arms and others with bent arms, the chosen distance of 30 cm should represent a reasonable worst-case scenario.

Spraying was directed towards the outlet. The spray duration was always the same for each spray. Propellant gas sprays were sprayed for 3 seconds; 3 pump strokes were applied for pump spray dispensers.

The six nanoparticle-containing consumer spray products were analyzed for their chemical composition and particle size distribution. The suspension was analyzed by ICPMS, spICPMS, DLS and SEM. The aerosol was released by spraying inside a modified glove box setup with integrated analytical devices. (Hagendorfer, Lorenz et al. 2010) Based on the considerations by Losert *et al* (Losert, von Goetz et al. 2014) the spray direction, spray duration and the distance of the vessel to the measurement device were precisely defined for the spraying procedure.

Before each experiment the background of the chamber was measured and after each experiment the chamber was flushed with fresh air. The next experiment was performed when the background was again at the same level as at the beginning of the preceding experiment. Throughout the measurements the relative humidity and the temperature were monitored.

Humidity did not exceed 50% and 60% for propellant gas sprays and pump sprays, respectively. During the experiment an almost constant temperature of 21°C was measured.

Experimental setup: The spray chamber was connected to a modified SMPS coupled to a commercial ICPMS (Agilent Technologies, Waldbronn, Germany) to determine online the size distribution and size-resolved elemental composition. The SMPS, consisting of a differential mobility analyzer (DMA) followed by a condensation particle counter (CPC), first selected one particle size fraction from the heterogeneous aerosol and then determined the number concentration of particles contained in this fraction by condensation driven particle growth and subsequent optical detection. By varying the selected size fraction, a particular particle size ratio was scanned during 120 s and the instrument was ready for the next scan another 60 s later. The ICPMS ionized the particles and detected the mass to charge ratio. Thus, the elemental composition of the particles of each size class could be identified. A detailed explanation of this technique is given by Hess *et al.* (Hess, Tarik et al. 2014)

The shapes of the particles were determined by applying electron microscopy: a TEM sampler was connected to the spray chamber to collect samples for this offline analysis technique. Also a non-modified reference SMPS was connected to the spray chamber to validate the results obtained by the coupled instrument. A rotating disk dilutor (RDD) was positioned at the inlet of each SMPS instrument and served as sample introduction interface and heated dilution unit (see Figure 5.1). The RDD's were heated to 80°C, so that the solvent droplets were evaporated and only the solid particles could enter the measuring instrumentation. Conductive tubing was used for all connections from the spray chamber to the instruments and also within the instruments to minimize electrostatic particle losses at the tubing walls.

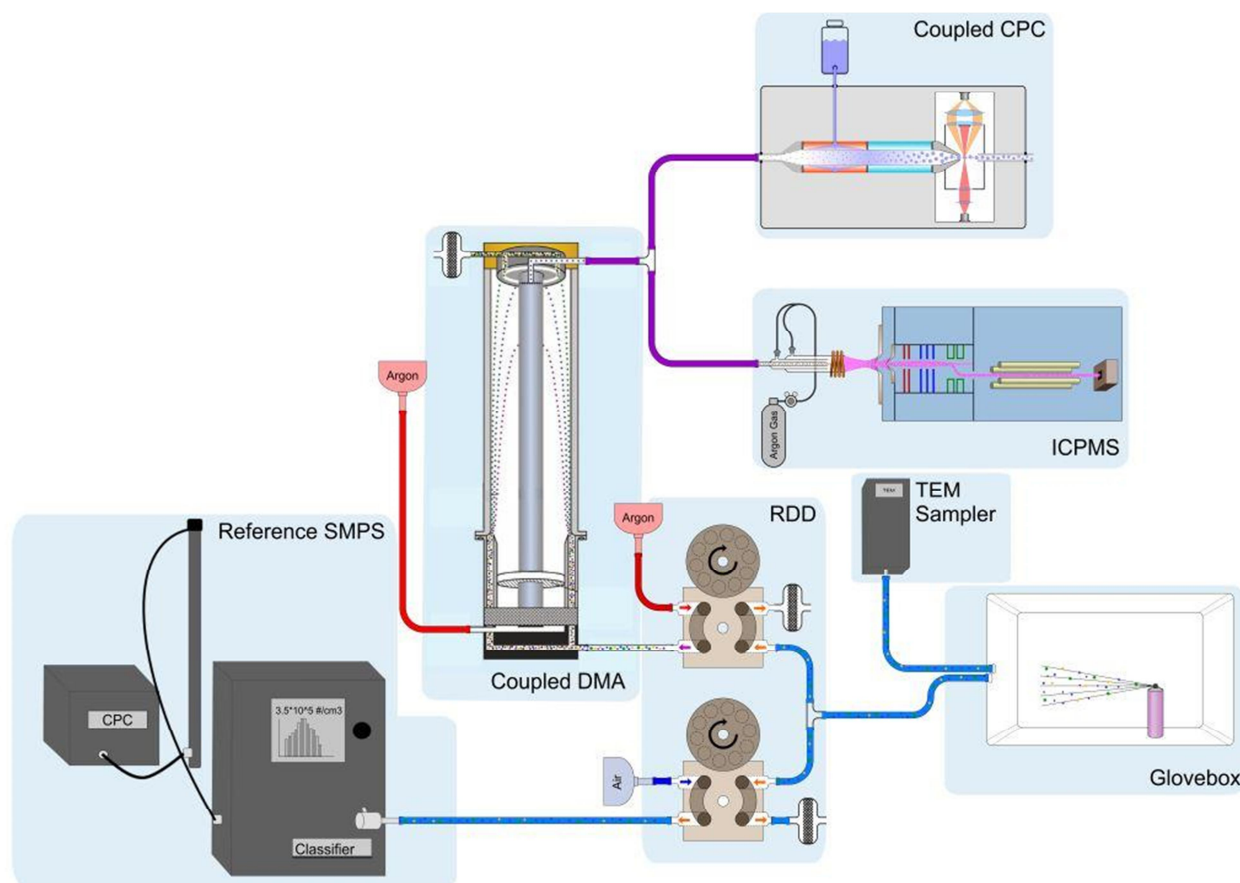


Figure 5.1: Experimental setup for aerosol analysis; right to left: Glovebox connected to the TEM sampler and two RDD's, one leading to the reference SMPS and the other to the coupled DMA on the other hand. After the DMA the stream is split between CPC and ICPMS.

Chemicals: Nitric acid (65% w/w) and hydrochloric acid (30% w/w) were purchased in suprapure quality and hydrogen peroxide (31% w/w) in pro analysis quality from Merck (Merck GmbH, Darmstadt, Germany). ICPMS multi-element standard Merck VI (110580, Merck GmbH, Darmstadt, Germany) and single element standards of 1g/L Au, P, Pt, S, Si, Sn, Ti (Specpur, Alfa Aesar GmbH & Co KG, Karlsruhe, Germany) were freshly diluted with deionised (DI) water before each measurement. For the production of the deionized (DI) water (18 MΩ

cm) a Milipore, Mili-Q A-10 water unit (Milipore AG) was used. The single element and multi element standards were always freshly diluted before each measurement.

Suspension analysis: For the suspension analysis, the spray cans were cooled with liquid nitrogen for 15 minutes. Then they were opened and left over night to let the organic solvent and the expanding propellant evaporate. The next day one part of the suspension was digested by microwave digestion for subsequent total elemental analysis and another part was diluted for nanoparticle analysis. The digestion method was adapted to each spray product depending on its labeled composition and observations during the digestion process. For the digestion of product I, 6 mL nitric acid and 2 mL hydrochloric acid were added to an aliquot of 200 μ L. For products II and IV, 2 mL nitric acid and 6 mL hydrochloric acid were added to an aliquot of 200 μ L. For products III, V and VI 3 mL nitric acid and 1 mL hydrogen peroxide were added to an aliquot of 50 μ L. After microwave digestion (220°C, 30 min) a clear solution was obtained. The digests were transferred to PE vessels and filled up with DI water to 50 mL. Suspension ICPMS analysis was carried out on an Agilent 8800 ICPMS (Agilent Technologies, Waldbronn, Germany) using an external calibration adjusted against Scandium, Germanium and Rhodium as internal standards. The instrument was equipped with two quadrupole analyzers (MS/MS) and a collision/reaction cell. The limit of detection (LOD) was calculated as three times the standard deviation of the background signal.

The diluted, non-digested samples were analyzed via batch dynamic light scattering (DLS). Measurements were carried out on a Malvern Zetasizer NanoZS (Malvern Instruments Ltd., Germany). Before analysis, all samples were warmed in the batch cell to 25°C (1 min).

For SEM analysis the suspensions were centrifuged on "FORMVAR carbon coated mesh 200 copper TEM grids" (SPI#3420C, SPI Inc., West Chester, PA, USA). Imaging was done on a Nova NanoSEM 230 (FEI Corporate, Hillsboro, USA). Particles were counted using image analysis software (ImageJ, National Institutes of Health, US).

Single particle ICPMS measurements were carried out on the same Agilent 8800 ICPMS as the suspension analysis. A dwell time of 5 ms and a flow rate of 0.24 mL/min were applied.

Aerosol Analysis: A commercially available Poly(methyl methacrylate) PMMA glove box (Meca Plex, Grenchen, Switzerland) with dimensions of 94 x 55 x 67 cm was modified as described by Hagendorfer *et al.* (Hagendorfer, Lorenz et al. 2010) The basic SMPS instrumentation used for the coupling to ICPMS included a differential mobility analyzer (DMA) 3081 (TSI, GmbH, Aachen, Germany) and a condensation particle counter (CPC) 3010 (TSI, GmbH, Aachen, Germany). The aerosol flow rate directed to the CPC was accurately defined with 0.3 L/min. (Hess, Tarik et al. 2014) A radioactive source (Kr 85 aerosol neutralizer 3077A (TSI, GmbH, Aachen, Germany)) was installed at the inlet of the DMA to generate a known charge equilibrium state of the particles. In addition to the coupled SMPS a reference instrument was used to determine the particle size distribution and particle number concentration. The instrument contained an electrostatic classifier 3080L (TSI GmbH, Aachen, Germany) and an ultrafine condensation particle counter (UCPC) 3776 (TSI GmbH, Aachen, Germany). The modified coupled SMPS was able to scan a particle size range from 7.5 to 156 nm, the reference instrumentation from 7 to 300 nm.

The same Agilent 8800 ICPMS was used for the SMPS-ICPMS coupling. The sampling introduction system was removed. The DMA was operated with 1.0 l/min sample flow, being split at the DMA outlet, and a 0.7 l/min fraction was directed to the ICP torch.

Aerosol samples were collected on TEM grids using a portable nanoparticle detector, which sampled on standard TEM grids by electrostatic precipitation (Partector TEM sampler, Naneos particle solutions GmbH, Windisch, Switzerland). TEM Images were acquired on a JEOL 2200 microscope operated at 200 kV.

5.3 Results

Suspension

Total chemical analysis: Total elemental analysis was carried out with a diluted digestion of spray suspensions. Figure 5.2 shows the concentration of metals determined after digestion and total elemental analysis of the spray suspensions. Suspension I contained next to silver (18.1 µg/L) and zinc (52.6 µg/L) no further metals in higher concentrations. In suspension II tin was found in the highest concentration of all investigated elements (395 µg/L). Suspension III contained a high concentration of zinc (224 µg/L) and tin (9.5 µg/L). In suspension IV tin (413 µg/L) and zinc (52.8 µg/L) were found. Suspension V contained the highest concentration of metals: In addition to a high concentration of aluminum (185'300 µg/L), also iron (392 µg/L), titanium (27.9 µg/L) and silver (27.2 µg/L) were present. Suspension VI contained a high concentration of zinc (73'000 µg/L).

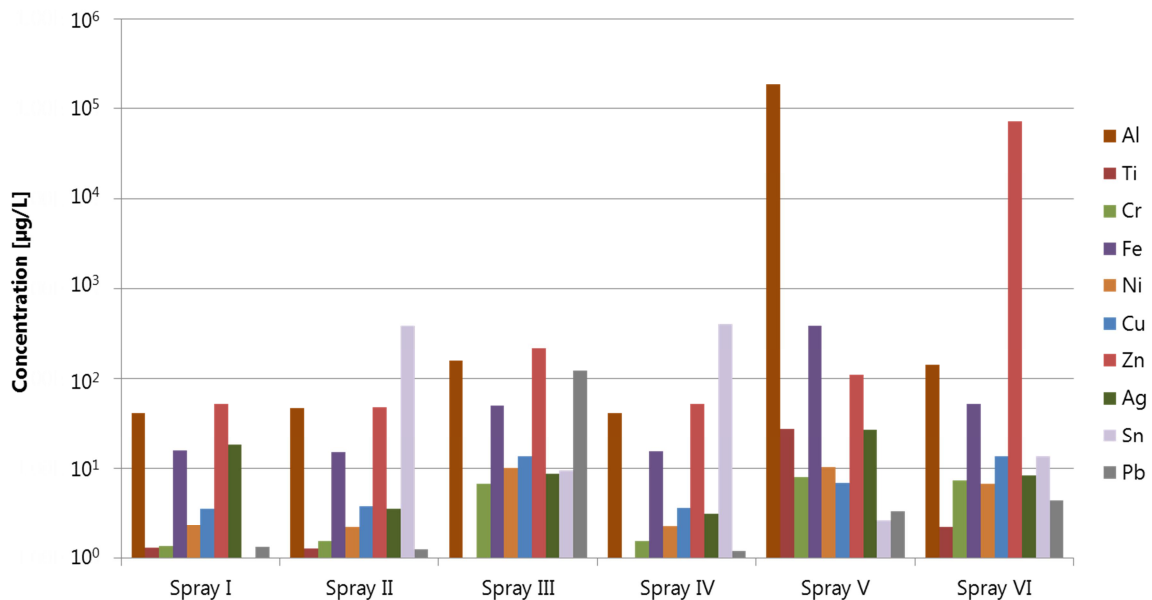


Figure 5.2: Metal concentrations in the investigated commercial spray suspensions.

Particle analysis: Dynamic Light Scattering (DLS) measurements showed that in suspension I particles of the size 320 ± 39 nm were present. In suspension II particles of 555 ± 120 nm were found. For suspension III the size of the particles was outside the effective range, which was between 0.3 nm up to $10 \mu\text{m}$. (Malvern 2004) Suspension IV contained particles of 373 ± 73 nm. For suspension V, DLS analysis was not possible since the residue resisted to dilution after evaporation of the organic solvent. For suspension VI the size of the particles was outside the effective range.

spICPMS detected Ag particles of 303 ± 12 nm for suspension I, and tin particles of 263 ± 10 nm and 244 ± 37 nm for suspensions II and IV, respectively. For suspension III no particles in the nano range were detected. Consequently either dissolved tin and zinc ions or very big agglomerates were present in suspension III. The same can be supposed for suspension VI.

SEM images of particles/agglomerates in the original spray suspensions (see Figure 5.3) show huge agglomerates of particles in the μm size range for all tested suspensions. For suspension I (Figure 5.3a) a three-dimensional agglomerate with the dimensions $6 \mu\text{m} \times 3 \mu\text{m}$ was observed consisting of single particles of 369 ± 87 nm. Also for suspensions IV and VI similarly structured agglomerates were found (Figure 5.3d and e). The agglomerate in suspension IV had the dimensions $6.8 \mu\text{m} \times 4.3 \mu\text{m}$, single particles were 205 ± 31 nm. The agglomerate of suspension VI was $26 \mu\text{m} \times 24 \mu\text{m}$; the single particles were as large as 1700 ± 250 nm. Particles found in suspension II and III (Figure 5.3b and c) were also agglomerated, but the height of agglomerates is not as high as for the other three suspensions. Primary particles found in suspension II were 600 ± 143 nm; primary particles in suspension III were 1000 ± 400 nm. EDX analysis (see Figure 5.3) agrees well with bulk ICPMS results, with the exception of sus-

pension I (no silver was found with EDX). In all of the analyzed samples aluminum was detected with EDX.

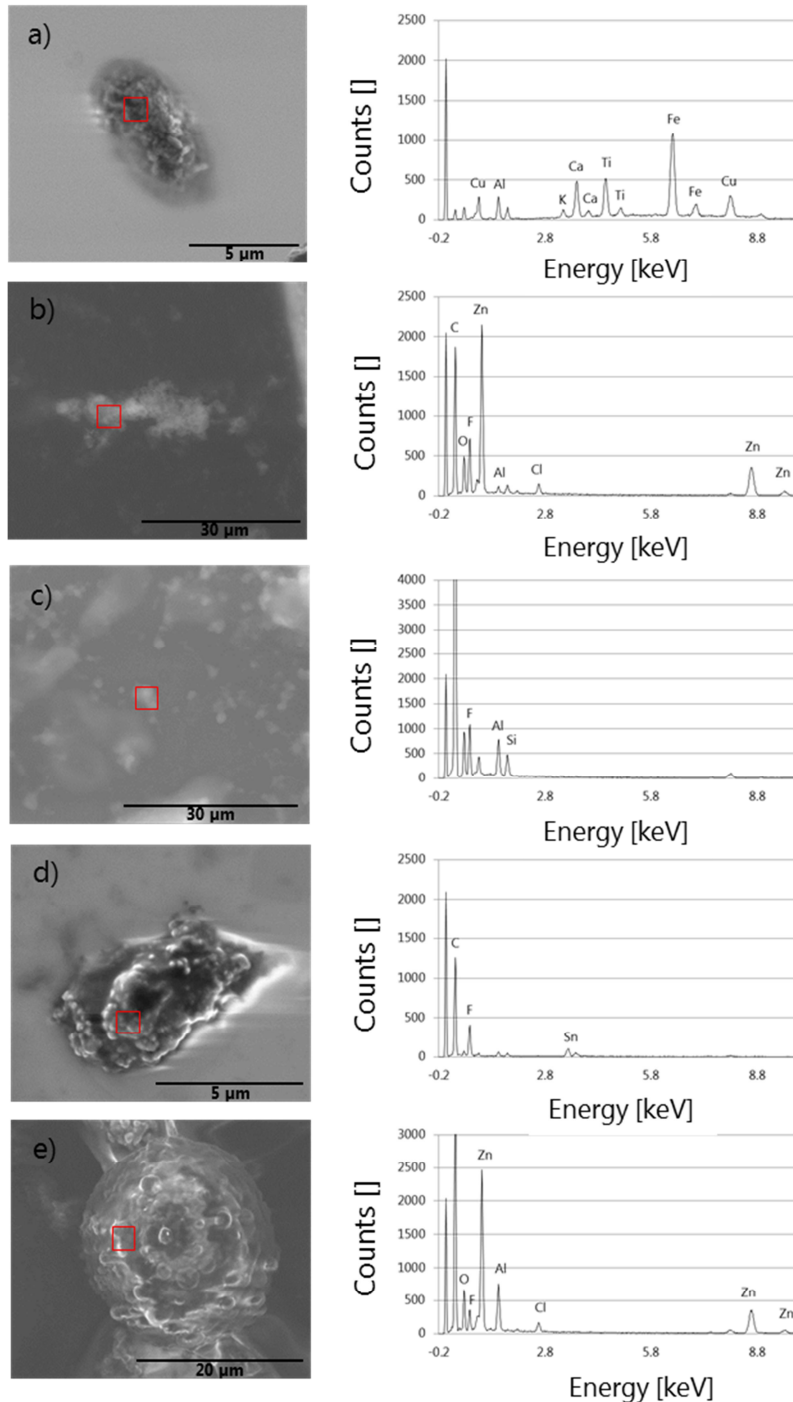


Figure 5.3: SEM/EDX images of nanoparticles present in the spray suspensions (a= spray I, b= spray II, c= spray III, d= Spray IV, e= spray VI).

Aerosol

Validation of SMPS data: With an SMPS being hyphenated to ICPMS (SMPS-ICPMS) and an additional, non-modified reference SMPS, particle concentrations above the measured particle background signal were measured for all tested sprays apart from sample I. Generally, both instruments agreed well (see Table 5.2), but the particle sizes measured by the reference SMPS were slightly larger than the sizes measured by the coupled instrument, because the instruments have different delay times due to different tubing lengths (the delay time describes the time a particle needs to travel from the outlet of the DMA to the inlet of the CPC Figure 5.1). The particle number concentrations in most cases agreed well for the coupled SMPS, if compared to the reference SMPS.

Real consumer spray process assessment

Table 5.2: Average particle number concentrations and particle sizes of the aerosol of all six products obtained from the two SMPS instruments.

	reference SMPS	coupled SMPS		
	particle number concentration at mean diameter in dN/dlog dP representation [#/cm ³]	particle size [nm]	particle number concentration [#/cm ³]	particle size [nm]
Spray I	no signal	no signal	no signal	no signal
Spray II	$5.2 \cdot 10^5 \pm 1.8 \cdot 10^4$	95 ± 5	$5.8 \cdot 10^5 \pm 8.2 \cdot 10^3$	85 ± 3
Spray III	$2.1 \cdot 10^5 \pm 8.2 \cdot 10^3$	25 ± 0	$2.8 \cdot 10^5 \pm 3.8 \cdot 10^3$	24 ± 1
Spray IV	$5.2 \cdot 10^5 \pm 5.0 \cdot 10^3$	85 ± 1	$6.4 \cdot 10^5 \pm 3.5 \cdot 10^3$	85 ± 0
Spray V	$1.5 \cdot 10^5 \pm 4.6 \cdot 10^4$	24 ± 1	$5.0 \cdot 10^5 \pm 9.4 \cdot 10^3$	24 ± 1
Spray VI	$4.5 \cdot 10^5 \pm 1.4 \cdot 10^4$	22 ± 1	$4.8 \cdot 10^5 \pm 3.0 \cdot 10^4$	19 ± 1

SMPS-ICPMS: Based on the results from the conventional suspension measurements with ICPMS, sample specific elements were selected for SMPS-ICPMS aerosol analysis. Since for the coupled device the scanning time of the SMPS needs to match the acquisition time of the ICPMS, (Hess, Tarik et al. 2014) only 5 metals could be measured simultaneously and the ICPMS was adjusted to the masses of the metals found in the suspensions.

No increased particle concentrations, in comparison to the background level, were recorded by SMPS after spraying of spray I, which was one of two pump sprays. The particles found in

the second pump spray, spray II, had the highest mean diameter of all investigated products. Nevertheless, we could observe a release of nanoparticles also from pump spray dispersers. Among propellant sprays, the mean particle diameter in spray IV was about 3.5 times higher than those in the other three sprays. The originally number weighted particle size distribution (PSD) determined by SMPS was transformed into a volume-weighted curve, in order to be comparable to the mass-related ICPMS data. As an approximation, spherical particles were assumed for this data conversion.

Figure 5.4 a-c illustrates on the left the volume-weighted PSD, and the size resolved ICPMS signal intensity, and on the right the number-weighted PSD, determined by the hyphenated SMPS-ICPMS instrumentation. SMPS data are represented as grey dashed lines, scaled at the left, ICPMS intensities as straight black curves, scaled at the right.

Since the ^{118}Sn ICPMS curve agrees very well with the PSD determined by SMPS (see Figure 5.4 a and b) SMPS-ICPMS demonstrated that the particles found in sprays II and IV were mainly consisting of tin. On the left the volume-weighted PSD is plotted and on the right the number-weighted PSD.

Figure 5.4 c illustrates the average SMPS signal of spray VI and the zinc ICPMS signal of the same spray. The SMPS signal of spray VI and the zinc ICPMS show a similar trend for the volume-weighted PSD: an increase in the zinc concentration can be observed for sizes above 80 nm. Around this size (70-90 nm) the curves of the number-based SMPS and the corresponding ICPMS signal fit quite well. This observation hazards the guess that particles present in sample VI consist of zinc but also of another element, which could not be identified by the coupled device.

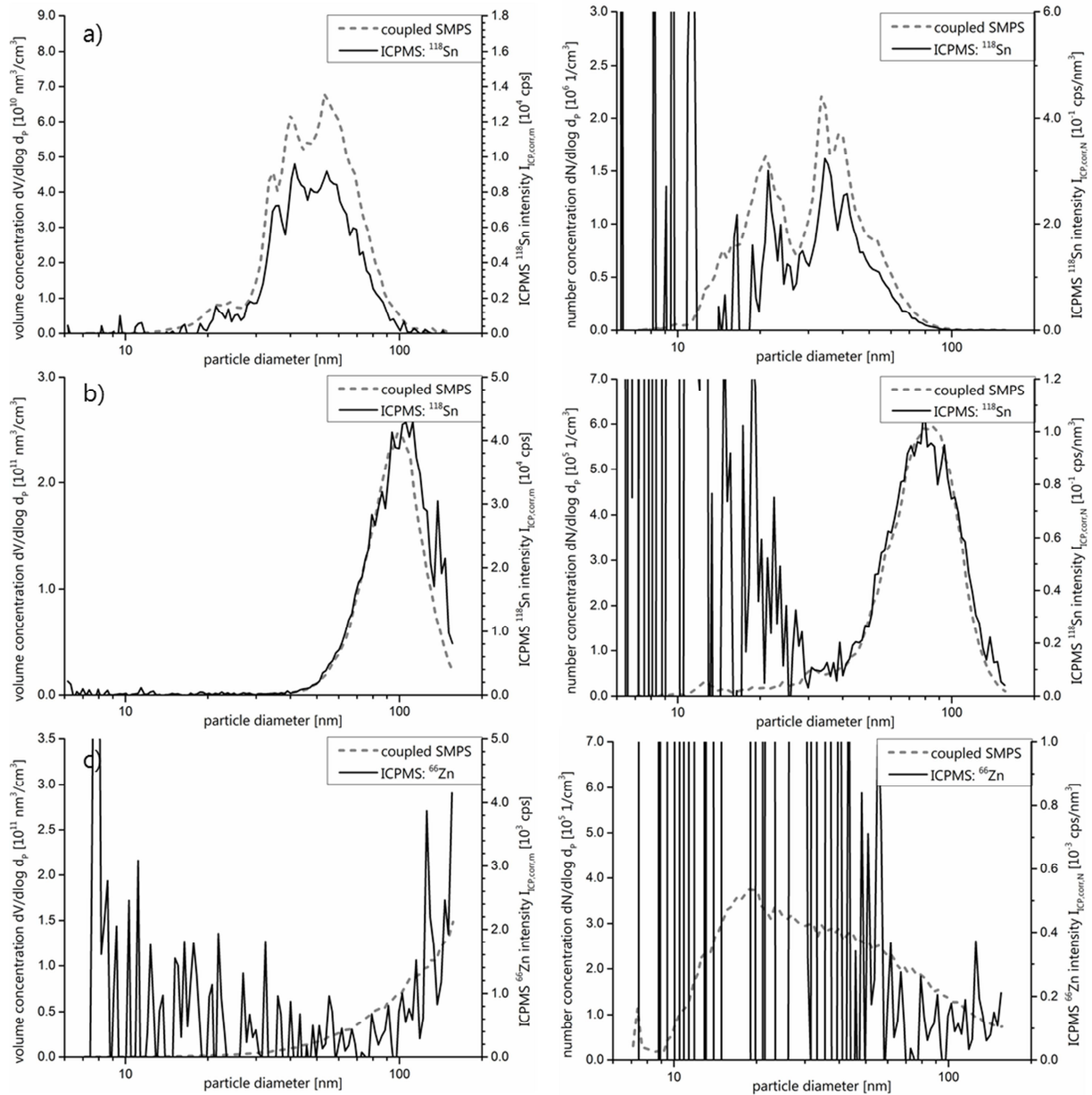


Figure 5.4: SMPS-ICPMS results for a) spray II, b) spray IV and c) spray VI; left: volume-weighted PSD, right: number-weighted PSD.

Also for sprays III and V SMPS signals were found, which could not completely be matched to an ICPMS signal (see Figure 5.5).

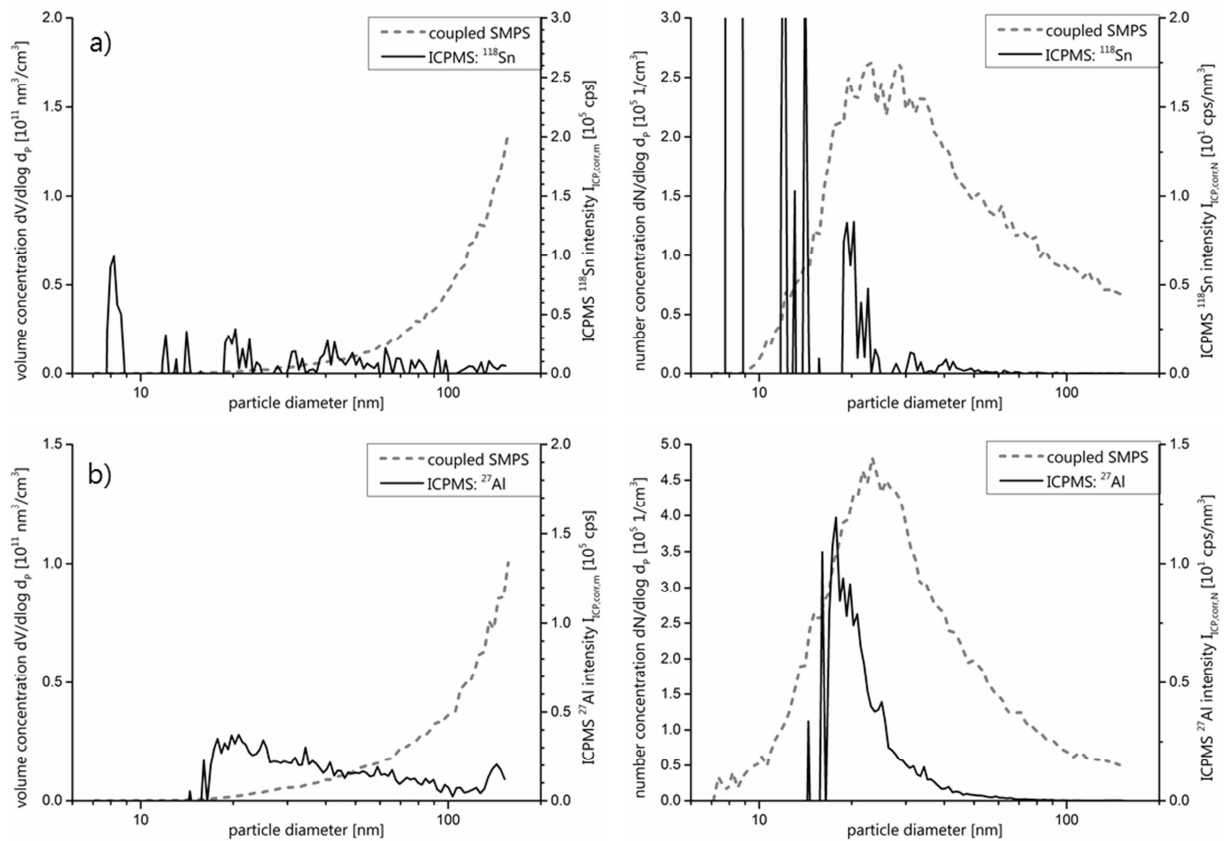


Figure 5.5: Volume-weighted (left) and number-weighted (right) SMPS-ICPMS signals a= spray III, b= spray V.

SMPS signal does not fit to the corresponding ICPMS signal.

Therefore, the TEM-EDX measurements were consulted to identify the chemical identity of the aerosol. Spray I did not evoke an SMPS and corresponding ICPMS signal, but with bulk ICPMS Ag was found in the suspension. Therefore, with EDX it was further investigated, whether Ag in particular form was present in the aerosol (see below). Other investigated elements, which are listed in Table 5.3, gave no ICPMS signal.

Table 5.3: Elements which were additional analyzed with SMPS-ICPMS, but gave no ICPMS signal.

Sample	Elements preselected for ICPMS, which gave no signal				
Spray I	¹⁰⁷ Ag (no gas)	²⁸ Si			
Spray II	²⁷ Al (He)	⁶⁵ Zn (He)	⁵⁶ Fe (He)	²⁸ Si (He)	
Spray III	²⁷ Al (He)	⁶⁵ Zn (He)	²⁸ Si (He)		
Spray IV	²⁷ Al(He)	⁶⁵ Zn (He)	⁵⁹ Ni (He)	⁵² Cr (He)	
Spray V	²⁷ Al (He)	⁵² Cr (He)	⁵⁶ Fe (He)	⁵⁹ Ni (He)	¹⁰⁷ Ag (no gas)
Spray VI	²⁷ Al (He)	⁵² Cr (He)			

Comparison of online measurements with TEM: TEM images of nanoparticles released from the different sprays are displayed in Figure 5.6. (red squares = area of EDX)

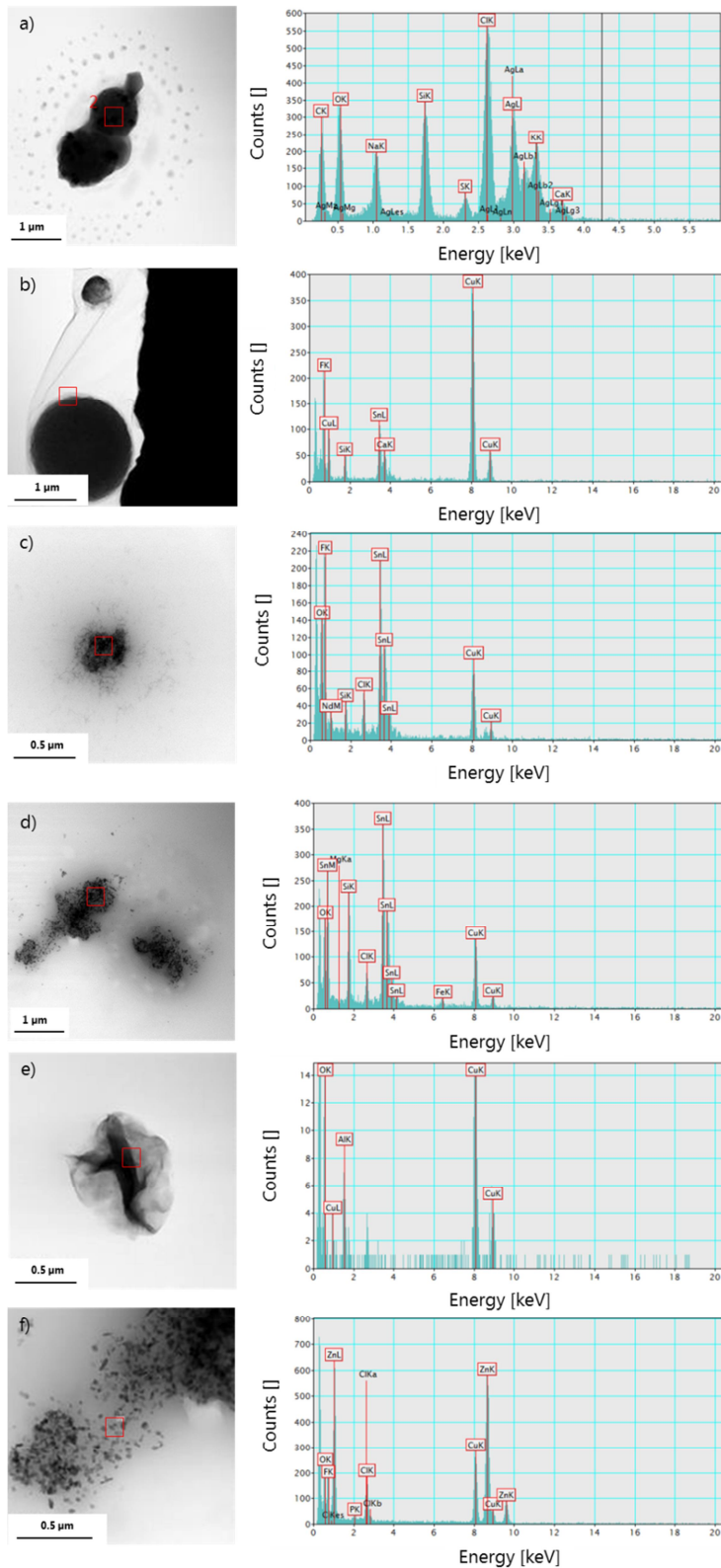


Figure 5.6: TEM/EDX images of nanoparticles collected from the aerosol (a= spray I, b= spray II, c= spray III, d= Spray IV, e= spray V, f= spray VI).

No nanometer sized particles had been detected in the aerosol of spray I by SMPS. This was confirmed by TEM analysis, but a 1.35 μm agglomerate was detected, consisting of primary particles with a size of about 30 nm. Smaller particles were observed, which are arranged in a ring-shaped area surrounding the big particle. These smaller particles did not contain metals, but organic compounds (see EDX results Figure 5.6).

The primary particles inside the agglomerate were identified as silver particles. Summing up, there were primary silver particles in the nm size range. These were agglomerating very fast and the resulting structures were above the SMPS-ICPMS measuring range, and/or the primary particles were shielded by organic compounds and therewith not ionized and detected in ICPMS. No single particles were found from spray II, but two agglomerates of 0.5 and 1.5 μm diameters, respectively, were observed by TEM, with primary nanoparticles of around 30 nm building these big agglomerates. SMPS, however, produced a signal between 80 and 90 nm. Most probably this finding indicates a shortcoming of TEM analysis, being an offline technique, which requires aerosol sampling over a longer period of time. For most of the analyzed products, 3-6 spray experiments were necessary to deposit enough particles on the TEM-grids, especially long sampling times were needed for collecting pump spray aerosol particles. During the time on the grid, the primary particles from spray II may have agglomerated. (Hagendorfer, Lorenz et al. 2010, Lorenz, Hagendorfer et al. 2011) Furthermore, the TEM images show that the bigger agglomerate from spray II was consisting of a tin core and a light shell around the core, which mostly consisted of fluorine. For sprays III, IV and VI, primary particles with mean diameters of 25, 85 and 20 nm (in the number-weighted PSD), respectively, were found by SMPS. This result could be verified by TEM (Figure 5.6): All TEM images show primary particles, but agglomeration was observed as well. Via EDX the composition of

the particles was analyzed. Nanoparticles detected in spray III and IV contained tin and fluorine. Particles present in spray VI contained also zinc. For spray V no particles in the nm size range were detected by TEM: the PSD determined by SMPS and the size-resolved ICPMS intensities recorded in terms of the SMPS-ICPMS online measurements did not match. The particles mainly contain aluminum (determined by EDX).

Summary of suspension and aerosol measurements: For all investigated products particle sizes changed due to spraying. With the exception of spray V, all aerosols contained primary particles smaller than 50 nm (Table 5.4) even though particles in the suspensions had been larger.

Table 5.4: Characteristics of the investigated spray products (suspensions and aerosols) as determined with different analytical methods. (agg. = agglomerate); for SMPS results the number PSD was used to determine the mean size.

	Suspension					Aerosol				
	Identity		Particle size [nm]			Identity		Particle Size [nm]		
	ICPMS	EDX	DLS	spICPMS	SEM	ICPMS	EDX	SMPS (cpl)	TEM	SMPS (cpl)
Spray I	Ag	Al, Ca, K	320 ± 40	305 ± 12	agg	Ag	Ag, Cl	---	1350±270	---
Spray II	Sn, Zn	Al, Zn, F	555 ± 120	265 ± 10	agg	Sn	Sn, F	85±3	1060±590	5.5*10 ⁵ ± 4.0*10 ⁴
Spray III	Zn, Sn	Al, Si, F	agg	agg	agg	Sn	Sn, F	24±1	330±20	2.4*10 ⁵ ± 1.2*10 ⁴
Spray IV	Sn, Zn	Al, Sn, F	373 ± 73	245 ± 37	agg	Sn	Sn, F	85±0	124±25	5.6*10 ⁵ ± 4.5*10 ⁴
Spray V	Al	n.m.	n.m.	n.m.	n.m.	---	Al	24±1	---	3.7*10 ⁵ ± 1.0*10 ⁴
Spray VI	Zn	Al, Zn, F	agg	agg	agg	Zn	Zn, F	19±1	25 ± 4	4.7*10 ⁵ ± 1.5*10 ⁴

5.4 Discussion

Standardized setup for spray experiments

By using a standardized spray setup good reproducibility was achieved. Although a larger number of sprays with different applications were tested, results could easily be compared, marking an improvement over previous studies. (Berger-Preiß, Boehncke et al. 2005, Nørgaard, Jensen et al. 2009)

Suspension Analysis

Elemental composition: Product I was labeled with a content of 50 mg/L silver, but only 18 µg/L Ag were found with ICPMS analysis of the diluted and digested suspension. As product I is an aqueous cosmetic spray to be applied on the skin, presumably no acid had been added to the formulation and without acid silver is not stabilized. Hence, the contained Ag may actually have been adsorbed to the vessel walls, so that it was not detectable in the suspension.

In suspensions II, III and IV, tin was found. Tin is typical for impregnation sprays, since they often contain organotin compounds, which are used as accelerators (for faster hardening of the other ingredients). (BgVV 2000) The high aluminum concentration in product V can be explained by the fact that this was an antiperspirant spray. These sprays usually contain high amounts of aluminum to prevent perspiration. According to the product label, the aluminum had been added to the product in the form of aluminum chlorohydrate, which had the highest concentration of all product ingredients, apart from the solvents (in Europe ingredients with a concentration > 1% are listed on the product label in descending order relative to their

concentration). The same suspension also contained small concentrations of iron and titanium, which were not labeled, but those elements can be part of so-called alums, being chemical compounds with the formula $AM(SO_4)_2 \cdot 12H_2O$, where A is a cation and M is a metal like iron or titanium. Alums have antiperspirant and antibacterial effects. For those compounds no labeling is required, because their concentration is below 1%.

Particle sizes: Sizes obtained with different methods fit well. Particle diameters determined by spICPMS were smaller than those determined by DLS and SEM, which can be explained by matrix effects: As all samples were simply diluted for spICPMS analysis and the matrix was not removed, probably interferences with the matrix occurred, causing higher background and therewith lower net signal intensity, and finally resulting in smaller calculated particle sizes. Additionally, spray II and IV contain high amounts of fluorine, which covers the metal nanoparticles. As fluorine cannot be ionized in the plasma and subsequently be detected by ICPMS, the calculated particle size is smaller than that obtained from methods that are able to detect fluorine. For spray III and VI no particles were found with DLS and spICPMS, whereas SEM allowed observing agglomerates of 1.0 and 1.7 μm . Possibly the respective particles got dissolved during the sample preparation for spICPMS and for DLS measurements.

Particle composition: Silver was found by ICPMS analysis of suspension I, but not via SEM-EDX of the particles, which were sampled from the suspension. This is presumably due to the lower detection limit of the ICPMS, compared to SEM-EDX.

Aerosol measurements

The slight discrepancy between particle number concentrations obtained by coupled SMPS and reference SMPS can be explained with the use of two different rotating disc diluters (RDD). The sampling line included a flow splitter, and each RDD was absorbing about 1 l/min raw aerosol. In the RDD, heated to 80°C, a defined amount of raw aerosol was added to 1.0 l/min dilution air in the case of the conventional SMPS, resulting in a dilution factor of 28 (reference RDD) or with argon in the case of SMPS-ICPMS, resulting in a dilution factor of 18 (coupled RDD). The difference of the resulting dilution factors was caused by geometrical differences of the disks of the two RDD devices. (Hueglin, Scherrer et al. 1997)

SMPS-ICPMS and conventional SMPS curves correlate very well for both, volume weighted and number weighted diagrams. The number-weighted distributions appear to be shifted a little bit towards smaller particles compared to the volume-weighted curves, since small particles contribute more to the number concentration and larger particles contribute more to the mass and volume concentration. This is also the reason for the high intensity of the number related ICPMS signal for particles below 15 nm. As mass concentration and thereby ICPMS signal intensity scales with the third power of the particle diameter, ICPMS intensity is much higher for very small particle sizes.

Comparison of suspension and aerosol

For some products the metals found in the suspension were not detected in the SMPS-ICPMS aerosol measurements, but with TEM-EDX. Fluorine can generally not be detected by ICPMS, because its first ionization energy is higher than that of argon so that it cannot be ionized with argon plasma. For aluminum, which was not detected in the aerosol of spray V, the ICPMS has a relatively low intensity, due to the use of a collision cell to eliminate mass-based interferences. In spray VI nanoparticles consisting of zinc were detected with TEM-EDX. With the SMPS-ICPMS coupling this finding was confirmed. Nevertheless, larger particles found by SMPS could not be correlated to the ICPMS zinc signal. As discovered by EDX, at larger sizes the zinc particles were imbedded in fluorine, which apparently “shielded” them from the ICPMS.

Particle sizes found in the released aerosol were always smaller compared to particle sizes in the suspensions. This means that during spraying the agglomerates decrease in size or are fully broken to release the primary particles. This result was confirmed by different analytical methods. Spray IV and VI showed the biggest agglomerates in suspension, which broke up into the nanoparticles found in the aerosol. In the TEM these agglomerates looked like raspberries with single particles on the surface, which may be a structure that is easily cleaved during the spray process.

For three products (Spray I, II and III) large agglomerates containing small primary particles were detected by TEM. The SMPS could not detect these agglomerates as their sizes were exceeding the SMPS measuring range.

After spraying, the aluminum, which had been detected in all six suspensions by SEM-EDX, was only detected in the aerosol of spray V via TEM-EDX. With the SMPS-ICPMS instrumentation, an increase of the aluminum background signal was observed after spraying spray III, IV, V, and VI, remaining stable on this elevated level during several minutes. So far we have no explanation for the observation of aluminum. As we observed no corresponding SMPS signal, it is not likely that the ICPMS signal was caused by Al nanoparticles in or above (bigger particles would not stay in the aerosol phase) the size range scanned by SMPS. A mass interference is not supposed, as Al was measured in the collision mode of the ICPMS. One possible reason could be that this signal was caused by particles smaller 3 nm, but it is expected that these would have been detected with TEM.

With TEM we found that some of the primary particles were not spherical. This phenomenon was already observed by Bekker *et al.* (Bekker 2014) But it should be kept in mind that the online methods assume always spherical particles for the size calculation, making calculations simpler. For non-spherical particles the dynamic shape factor has to be determined, before size could be calculated. (Scheuch and Heyder 1990)

Chapter 6

6 Conclusion and Outlook

The following conclusions and outlook are based on results presented and discussed within the chapter 2-5.

The experimental setup for measuring release of substances from conventional spray products cannot directly be used for mNOAA containing sprays as the measurement methodology and the analytical instrumentation are different. For conventional products the mass is in the analytical focus. For mNOAAs the mass is of less interest, because nanoparticles show high activity even if their contribution to mass is very small. For example, a 4 nm CdS nanoparticle contains approximately 1500 atoms, of which about a third is present on the surface and determines the activity of the nanoparticle (which is connected with potential health risks), (Krystek, Ulrich et al. 2011) whereas the actual mass contribution of the particle is only $3.59 \cdot 10^{-22}$ kg. Therefore, the assessment of exposure via mass concentrations only is not suitable for mNOAA. Accordingly, in almost all reviewed studies the particle size and number were measured, instead of the mass.

Nevertheless, huge differences in the experimental setups of the reviewed studies lead to different results. This was observed for both conventional and mNOAA-containing sprays. Normalization was not possible, because crucial information on the spraying can was not available. The spraying can influences the spray by the nozzle type and the propellant gas. The spray nozzle can vary by the number and diameter of the outlets. The higher the number of outlets the more droplets can be generated. The smaller the outlets the smaller the size of the droplets will be. The size and number of droplets in turn determine the time course and degree of agglomeration. In addition, also the residual content of propellant gas in the can

needs to be taken into account. For a given spraying duration, freshly opened bottles will emit more droplets and particles than older bottles that contain less propellant. Therefore, the bottle needs to be weighed before and after the experiment, so that instead of the spraying duration the sprayed amount can be used for calculations.

Even more helpful for exposure assessment and comparison of different types of spray mixtures, spray cans or nanoparticles would be a standardized protocol for spray experiments, which could be tested in an interlaboratory comparison. The ideal setup would assess different spray types, like cleaning sprays, impregnation sprays and cosmetic sprays. Different sizes of chambers would be helpful to see if results from a small chamber can be extrapolated to results obtained in a larger chamber or even a real room. Experiments should simulate realistic conditions as well as realistic worst-case conditions.

But even without an agreed standard protocol some standardization could be achieved if studies would follow the already existing guidelines (e.g. standardization of temperature and relative humidity). Of the reviewed studies none is taking into account existing norms and regulations e.g. concerning aerosol investigation. The OECD guidelines for inhalation toxicity (OECD 2009, OECD 2009, OECD 2009) and the ISO/TR norm for workplace atmospheres (ISO/TR 2007) were published in 2009 and 2007. (Nørgaard, Jensen et al. 2009, Shimada, Wang et al. 2009) Some papers were published after the implementation of these norms and could have considered them. (Chen, Afshari et al. 2010, Hagendorfer, Lorenz et al. 2010, Berlin, Dietrich et al. 2011, Lorenz, Hagendorfer et al. 2011, Nazarenko, Han et al. 2011, Oomen, Bennink et al. 2011, Quadros and Marr 2011, Bekker 2014) Some of the norms, however, are for workplace exposure (ISO/TR 2007, ASTM 2010, DIN 2012, DIN 2012) and not for

consumer exposure. Still, for the sake of standardizing human exposure experiments they could easily be adapted for consumer exposure by adjusting the use scenario. Others like the "ASTM D4336-054: Standard test method for determination of the output per strokes of a mechanical pump dispenser", (ASTM 2010) are helpful for data evaluation. "DIN EN ISO 10808:2010: Nanotechnologies – Characterization of nanoparticles in inhalation exposure chambers for inhalation toxicity testing" (ISO 2010) describes inhalation exposure studies, defines humidity and temperature ranges inside the exposure chamber and recommends instruments, which can be used for particle number and size measurements. For further studies on nanoparticle release from consumer sprays it is advisable to take this norm into account.

In summary, three general aspects emerge from this review that may help to make results of exposure studies comparable and, thus, help in the extrapolation to other spray products:

1) Adequate techniques

For understanding the fate of particles during the spray process and also to estimate the associated risk some basic information on the suspension and the aerosol needs to be generated. For both states the particle size distribution, the shape of the particles and the chemical composition, and for the aerosol in addition the particle number concentration need to be determined. It is well known that size is a crucial factor for mNOAA toxicity. Therefore, not only the droplet size should be measured, but the size of the particles inside the droplet that finally will be transferred into the lungs. Analytical concepts for the online measurement of particle identity need to be developed and validated. Up to now information about the chemical identity can only be obtained by offline electron microscopy. Furthermore, for nanoparticle analytics, either in suspension or in the aerosol, a combination of several tech-

niques is needed to obtain information on particle size, shape and identity. This coupling of different instruments needs careful consideration as to the sequence and positioning of different measurements.

2) Improvement of reporting

For the use in exposure or risk assessment studies need to provide more information on the experimental setting and the spray cans that have been used. This holds true for both conventional and mNOAA-containing sprays. In addition, for mNOAA information about the particle background, temperature and humidity is crucial, since these parameters have a strong influence on the particle number and size.

3) Standardized experimental setup

The experimental setup should either follow guidelines or be described in detail including the position of the spray can inside the chamber and the direction of the spraying. Also, the exact size and dimension of the chamber should be reported. Generation of a standard protocol for spray experiments would be a good option for allowing reliable comparison of spray mixtures, cans and ingredients. In the absence of such an agreed protocol using existing guidance from related fields (aerosol analysis, workplace exposure assessment) may already result in more comparable experimental results.

From all the results obtained, a standardized setup for investigation of spray scenarios was established (see Figure 6.1).

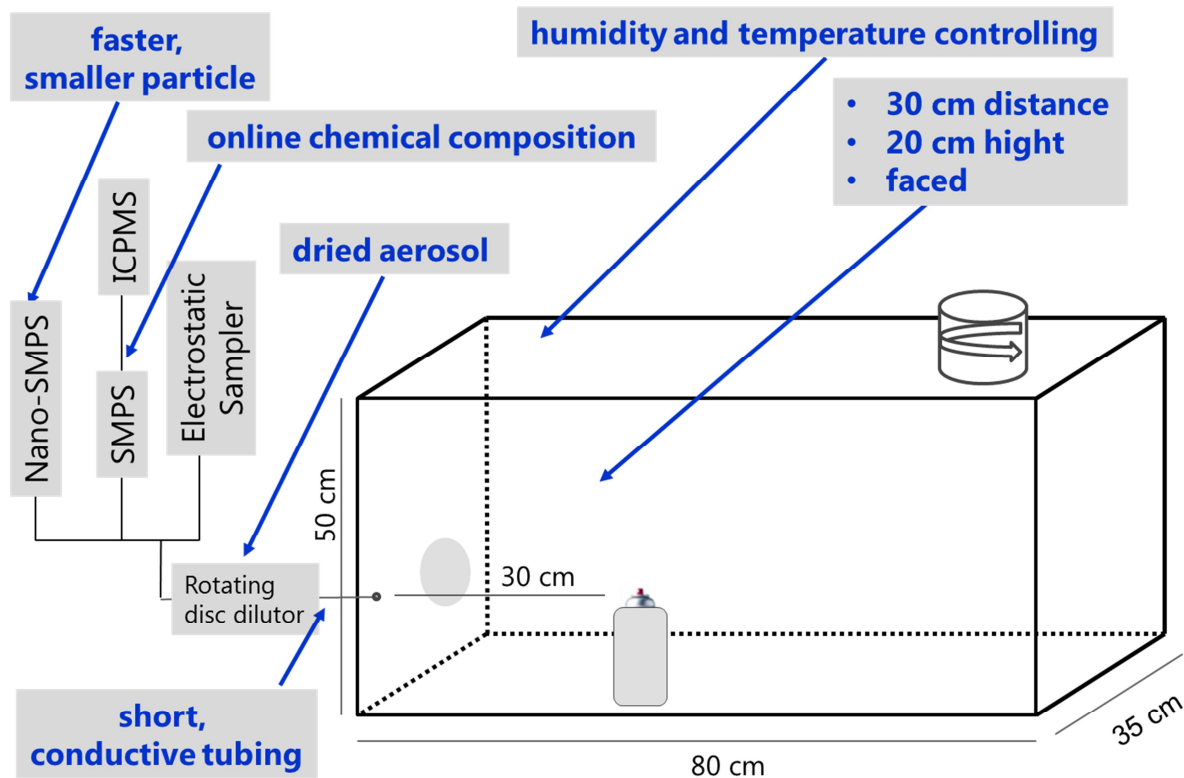


Figure 6.1: Standardized spray chamber setup for aerosol analysis.

Conductive tubing is used to minimize particle losses due to electrostatic deposition on the tubing walls. Humidity and temperature is controlled throughout the experiments going along with the DIN EN ISO Norm 10808:2010. (ISO 2010) The vessel is stationed in a distance of 30 cm and a height of 15 cm to simulate a worst-case scenario. The distance is chosen based on a medium arm length of a European citizen. As some sprays are applied with outstretched and some with bent arms, the medium of both lengths is recommended as a practical. The direction of the spray is towards the instrumentation. An electrostatic sampler is connected to the chamber for offline analysis via TEM. Online analysis is conducted with a nano SMPS and an SMPS coupled to an ICPMS. A rotating disc dilutor dries the particles before they enter the instruments.

Using this setup, six different commercial available spray products were analyzed. New methods were tested for both media: spICPMS for suspension analysis and SMPS-ICPMS coupling for aerosol analysis. Despite the fact that also in future experiments a combination of several methods will be necessary, since there is no perfect single method, spICPMS can be highly recommended for suspension analysis, because it is a fast method and delivers reproducible results, compared to conventional methods like TEM and DLS.

A4F analysis was not used for suspension analysis based on the results obtained from the particle-membrane interaction studies. The results obtained for ζ -potential dependence, morphology and hydrophobicity of membranes and particles upon different chemical environments plays an important role for particle analysis with A4F. For all membranes a different retention behavior upon increase of the ζ -potential can be observed, with decreased retention times above higher electrostatic particle membrane repulsion. This behavior matches well the theory proposed in literature. (Schachermeyer, Ashby et al. 2012, Ulrich, Losert et al. 2012, Bendixen, Losert et al. 2014) For PVDF membrane the assumption of better recovery adjusting the ζ -potential did not hold true at all, although it shows an even larger charge. Another influencing factor in membrane-particle interaction seems to be the roughness and morphology of the membrane surface and its degradation during use. For the PVDF membrane, irrespective of the ζ -potential matching, the recovery was not enhanced. In this case the dominating effect influencing the recovery was clearly found to be nm to μm size pore holes and the roughness of the membrane itself. A third and important influencing factor is the hydrophilic/hydrophobic character of the membrane material corresponding to the investigated nanoparticles material itself. Hydrophobic PS particles strongly interact with hydro-

phobic membrane materials resulting in low recoveries, although showing high repulsion forces from charge stabilization.

Nevertheless, future work should still focus on mechanisms additionally driving particle-membrane interactions. Because in this study we purposely limited the degrees of freedom for the particle chemistry a broader picture investigating other particle systems would increase the understanding of particle-membrane interactions. In this respect the behavior of different particle systems (humics, metallic, metal oxide, and organic nanoparticles) with different stabilization mechanisms (charge and steric stabilization) are also of interest. Moreover, further experiments with Triton must clarify how a non-ionic surfactant can influence the ζ -potential. Furthermore, as deduced from this study, evaluation of metal oxide membrane materials for A4F (if applicable and compatible) could be of high interest.

For aerosol analysis, SMPS-ICPMS coupling is a very promising technique. Compared to conventional methods it is very fast and delivers the most important information during one online measurement. A drawback, however, is the low detection efficiency of ICPMS for elements with high ionization energy, which is problematic e.g. for sprays containing fluorine. With the new online coupling method also small primary aerosol particles can be monitored online and their chemistry can be identified, without the generation of artificial agglomerates due to sampling on a TEM grid. Thus, our project is the first to characterize online nanosized aerosols regarding particle size and corresponding composition. (Nørgaard, Jensen et al. 2009, Lorenz, Hagedorfer et al. 2011, Quadros and Marr 2011, Bekker 2014) The shape of the particles still can only be determined using offline techniques like electron microscopy, and TEM-EDX should support the method.

In general a release of nanoparticles was observed for all sprays apart from spray I. Hence, not only propellant gas, but also pump sprays can release nanoparticles. Therefore, the assumption of Hagendorfer *et al.* (Hagendorfer, Lorenz *et al.* 2010) and Lorenz *et al.* (Lorenz, Hagendorfer *et al.* 2011) that only propellant gas sprays can release nanoparticles has to be revisited.

The final size and the agglomeration state of the released particles seem to depend on different factors like the solvent and the formulation. Metals found in the suspensions are the main component of the nanoparticles in the released aerosol. Some particles, especially the ones released from impregnation sprays, had a metal core covered by a fluorine-carbon shell. This was already observed by Lorenz *et al.* (Lorenz, Hagendorfer *et al.* 2011) During the spray process the size of the initial particles that were present in the suspension decreased: Particles/Agglomerates present in the suspensions were about 10 times larger than the ones released after application of the sprays. Consequently, also sprays, which are not labeled as nano, may release particles in the nanometer size range. This confirms the results published by Bekker *et al.* (Bekker 2014)

Summary

Within this PhD thesis, a standardized spray setup was developed to analyze nanoparticle containing sprays. Based on a detailed literature review, lacks in the systematic characterization of nanoparticle containing spray products were detected. Measurement results, obtained with this standardized spray setup are now comparable Thus, reliable data for risk assessment can be generated, what was not the case in former studies.

In addition, nanoparticle suspension analysis with A4F was optimized. Reasons for particle-membrane interactions in A4F were elucidated. This was the first systematic study in the field of A4F research. With our results, the quality (recovery and retention time shifts) of measurements can be maximized.

In a last step, optimized aerosol and suspension analysis was applied for real consumer product analysis. This is the first study, where a lot of different analytical methods were tested and critically compared. Additionally, a new developed method for aerosol analysis was applied: SMPS-ICPMS. This is the first analytical technique, which enables an online characterization of particle size and particle chemistry/composition.

Within this work, data was generated, which can be the basis for a reliable and extensive consumer exposure risk assessment.

Chapter 7

7 Appendix

7.1 Critical aspects of sample handling for direct nanoparticle analysis and analytical challenges using asymmetric field flow fractionation in a multi-detector approach

7.1.1 Introduction

The interest in engineered nanomaterials (ENM) increased constantly during the past decade. Nanomaterials exhibit rich physical and chemical phenomena, and their fascinating and unusual properties have opened up a myriad of applications in industry, medicine and many other fields *and several* products based on nanotechnology have already been introduced to the market. (Krystek, Ulrich et al. 2011) This is also visible in the increasing number of patents and publication related to nanotechnology. (Dang, Zhang et al. 2010, Grieneisen and Zhang 2011) Several studies have shown that products containing ENM can release particles, some of them in the nano-range. (Hagendorfer, Lorenz et al. 2010, Kaegi, Sinnet et al. 2010, Gottschalk and Nowack 2011, Lorenz, Windler et al. 2012, Windler, Lorenz et al. 2012, Bekker 2014) Hence, powerful, and sensitive analysing techniques are required to characterize nano-objects such as engineered nanoparticles (ENPs) originating from ENM synthesis or application studies and for the investigation of safety aspects related to nanotechnology. Size information and chemical composition probably belong to the mostly demanded parameters, but also surface functionality and shape are quite important as they significantly influence the behaviour of ENPs. Several well established analytical techniques are available, among which electron microscopy and light scattering are predominately applied for size determination. (Hagendorfer, Kaegi et al. 2011) Typical techniques and their application range are, summarized e.g. in the review article of Hassellöv *et al.* (Hassellöv, Readman et al. 2008) For chemical

characterization of nanoparticles, plasma spectrometry is one of the most powerful techniques. Krystek *et al* (Krystek, Ulrich *et al.* 2011) recently reviewed the application of plasma spectrometry for the analysis of ENPs in suspensions and consumer products. The applicability of straight forward analytical methods such as sequential filtration or centrifugation, but also latest, more sophisticated analytical trends are discussed.

Techniques which allow direct online analysis of ENPs, by obtaining several parameters (e.g. size and chemical information) simultaneously, are preferred and therefore of growing interest in analytical research. Direct single particle mode analysis with inductively coupled plasma mass spectrometry (spICPMS) (Degueldre, Favarger *et al.* 2006, Tuoriniemi and Hasselov 2010, Laborda, Jimenez-Lamana *et al.* 2011, Mitrano, Leshner *et al.* 2012, Loeschner, Navratilova *et al.* 2013) as well as the coupling of asymmetric flow field flow fractionation with inductively coupled plasma mass spectrometry (A4F-ICPMS) (Von der Kammer, Babrowski *et al.* 2004, Poda, Bednar *et al.* 2011, Hagendorfer, Kaegi *et al.* 2012) are currently the two mainly discussed innovation trends for nanoparticle analysis in literature.

However, nanoparticle analysis in general can be challenging. Beside storage conditions (e.g. temperature or UV light), handling and sample preparation of ENPs might be critical. Changes in the chemical environment (e.g. dilution, or addition of surfactants) occurring during sample preparation or analysis can result in significant changes of the samples. Nanoparticle stability and agglomeration behaviour strongly depends on the particle type and structure, the chemical composition as well as the coating or functionalization. For example silver or gold nanoparticles can be synthesized in a bottom-up or top-down approach with a large number of different coatings/functionalization. These coatings or functionalization can range from inorganic components like sodium bicarbonate as capping agent, or covalently bonded

SiO₂ to organic coatings like citrate, polyvinylpyrrolidone (PVP) or polysaccharide. Composites are also possible. The bonding mechanisms between the coating / functionalization agents and the particle cores are yet not fully understood. However, they can be mainly divided into covalent and non-covalent. While non-covalently bound coatings/functionalization are more likely to desorb and detach from the surface for example upon dilution, covalently bound coatings can provide better stabilization for a broad range of conditions. Irrespective of the bonding mechanism between coating/functionalization agent and particle core, two types of stabilization mechanisms are distinguished, charge and steric stabilization. Figure 7.1 displays examples for possible structures of various silver nanoparticles with examples for possible coatings / functionalization.

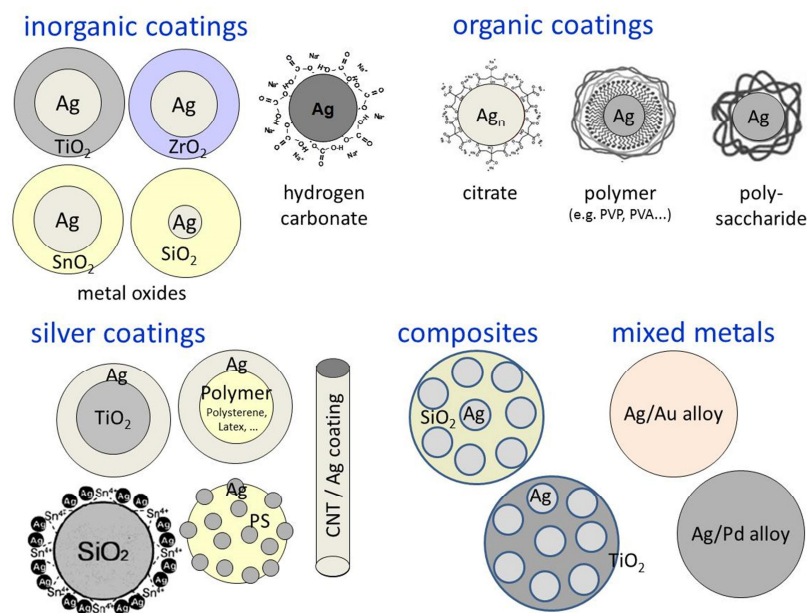


Figure 7.1: Possible silver nanoparticle structures with different coatings/functionalization as well as composite materials.

Steric stabilizations for nanoparticles are often assumed to be relatively unsusceptible against changes in the chemical environment, whereas charge stabilized particles are especially sensitive to changes, e.g., of ionic strength or pH. (Bucking and Nann 2006, Buecking 2006) How-

ever, also sterically stabilizing polymer coatings like polyvinyl alcohol (PVA) can show sensitivity to changes in specific the chemical environment due to chemical reactions like shifts in the cross-linking rate of the coating or functionalization components by hydrolyses equilibrium reactions. (Cajlakovic, Lobnik et al. 2002, Kittler 2009, Kittler, Greulich et al. 2009)

Even a dilution might cause a size change due to variations of the concentration ratio of coating or functionalization compounds bound to the core. (Frens 1973) Moreover, dilution can accelerate the dissolution of nanoparticles which could lead to a larger ionic fraction in the dissolved suspension. The differentiation between ionic and particulate fractions is still a challenging task to obtain. Determination of the total fraction by bulk analysis and the ionic fraction e.g. by ion-sensitive electrodes (Geranio, Heuberger et al. 2009) or ultracentrifugation with subsequent analysis (Hagendorfer, Kaegi et al. 2011, Hagendorfer, Kaegi et al. 2012) are proposed as suitable methods. The particulate fraction can be calculated by subtraction of the ionic fraction from the total amount. However, ion-sensitive electrodes show only moderate sensitivity with detection limits around 0.1 to 0.01 mg/l. Techniques like ultrafiltration or ultracentrifugation methods are time consuming and costly, but these two-step-methods provide better detection limits. Nevertheless, a centrifugation force which ensures a removal of nanoparticles down to about 1 nm might still not always ensure that the supernatant contains only ionic forms. Additionally, dissolved small metal complexes might also be present.

Besides composition, also structural details can influence the dissolution behaviour. Even ceramic nano-composite particles, which are usually supposed to be chemically stable, can show a preferential leaching. Metal doped titanium oxide-based nanoparticles for examples can form completely different structures, depending on the doping metal and the way of synthesis. Elements like chromium or tungsten are often embedded in the TiO₂ lattice replacing

Ti, (Akurati, Vital et al. 2008, Trenczek-Zajac, Radecka et al. 2009, Radecka, Rekas et al. 2010) when the nanoparticles are synthesized by flame synthesis, whereas elements like silver or platinum appear as discrete nobs on the top of the TiO₂ particles (Li, Xu et al. 2009, Selvam and Swaminathan 2011, Zhang 2011) and might be preferentially released in contact with water.

Next to sample preparation, also the analytical setup itself can influence analysis of nanoparticles. Hence, a basic knowledge about particle chemistry and their possible behaviour is essential to avoid false measurements caused by either sample handling or a non-optimum analytical setup. Since this knowledge is often not directly accessible, a fast and straight forward method to determine the influence of solution changes, e.g. on the agglomeration behaviour of nanoparticle samples based on kinetic studies with batch dynamic light scattering (DLS), is proposed. Three nanoparticle dispersions, representative for typical types of nanoparticle and coating or functionalization have been investigated: polyvinyl alcohol (Ag@PVA) and citrate (Ag@citrate) stabilized silver ENPs, and titanium oxide ENPs with poly-acrylate (TiO₂@PA). Kinetic studies of these differently coated or functionalized ENPs were performed using batch analysis with dynamic light scattering (DLS) to demonstrate the dependency e.g. of agglomeration on various influencing factors of the chemical environment such as dilution, or the change of pH, or ionic strength. This straight forward analytical approach allows a fast assessment of the behaviour of unknown ENP types or structures.

The second part of this study focus on the investigation of unspecific nanoparticle-membrane interactions which can have a negative influence on the nanoparticle fractionation efficiency and the recovery rates due to unspecific deposition on the membrane's surface in the field flow fractionation channel. Inadequate recovery rates of A4F for the analysis of nanoparticles

were reported in previous studies, (Hagendorfer 2011, Hagendorfer, Kaegi et al. 2011, Schmidt, Loeschner et al. 2011) but the causes are poorly investigated. A possible explanation for unspecific nanoparticle-membrane interactions based on zeta (ζ) potential investigations is being proposed. The investigation considers typically used A4F membrane materials as well as nanoparticle and coating or functionalization types to provide information for qualitative prediction of unwanted interactions and possible deposits of nanoparticles in the A4F channel.

7.1.2 Prospects and limitations of spICPMS and A4F-ICPMS

Degueldre *et al* introduced spICPMS for size distribution determinations of Zr, Th and Au nanoparticles in colloidal suspensions. (Degueldre and Favarger 2004, Degueldre, Favarger et al. 2004, Degueldre, Favarger et al. 2006, Degueldre, Favarger et al. 2006) Meanwhile the technique has been improved, e.g., by using micro-droplet sample introduction devices (Gschwind, Flamigni et al. 2011) to achieve better detection limits. The principle of spICPMS bases on transient signal spike counting statistics of highly diluted samples which requires a fast data acquisition. (Krystek, Ulrich et al. 2011) The big advantage of spICPMS is the relatively low instrumental effort, which makes the technique easily accessible in each ICPMS laboratory. However, spICPMS analyses are limited by the time resolution of the mass spectrometer used. Most of today's commercially available ICPMS instruments base on sequential mass filters which allow only single element analysis. Measurements of two or more isotopes during the very short transient signal events require much faster signal acquisition, e.g., by using instruments with continuous simultaneous mass analysers (Schilling, Andrade et al. 2007) like the newest development of a magnetic sector field mass spectrometer with CCD

array detector approach or a fast time-of-flight analyser. (Krystek, Ulrich et al. 2011) Another critical point in spICPMS is the number of measurements required to achieve an appropriate counting statistic of the highly diluted samples which are representative for the nanoparticle size distribution. Moreover, depending on the element the minimum detectable nanoparticle size in spICPMS mode ranges at 20 to 30 nm. The minimum detectable size limit is given by the relatively small number of atoms present in a single nanoparticle and the minimum element mass required to achieve ICPMS signals from the single particle event distinguishable from the background. (Gschwind, Flamigni et al. 2011, Laborda, Jimenez-Lamana et al. 2011) The upper size for direct particle analysis in ICPMS is mainly given by the sample introduction system, especially by the cut-off of the used spray chamber ranging typically between 1.5 and 2 μm , whereas the plasma power is usually sufficient to completely ionize even micro-meter particles introduced as slurries. (Krystek, Ulrich et al. 2011)

Field flow fractionation is more flexible in terms of the accessible lower size range down to about 1 nm. The injected sample volumes of typically 20 to 100 μl per run amount to a representative number of nanoparticles for each analysis. For example an injection volume of 50 μL of a 1 to 10 mg/L concentrated nanoparticle suspension amounts to 10^{14} to 10^8 particles (1-100nm) per replicate. For comparison it should be mentioned, that e.g. for image analysis in electron microscopy analysis typically only 150 to 2000 nanoparticles are counted for size determination. This nanoparticle fractionation allows exploiting also the multi-element capabilities of ICPMS. A further advantage of A4F is the possibility to couple the separation channel with several detectors in-line. Some recently published studies investigated the possibilities of A4F in a multi-detector approach coupled to UV/Vis, light scattering and ICPMS for size fractionation chemical analysis of gold and silver nanoparticles. (Hagendorfer 2011,

Hagendorfer, Kaegi et al. 2011, Schmidt, Loeschner et al. 2011, Hagendorfer, Kaegi et al. 2012) The flexibility to couple several different detectors and collect size-separated fractions via a fraction collector opens a lot of new prospects including the possibility to achieve not only information on size and the chemical composition of the nanoparticle core material but also information about the coating or functionalization e.g. via ICPMS or a fluorescence detector. However, highly disadvantageous for the A4F fractionation principle are the unwanted losses of nanoparticles in the separation channel. The mechanism is still not fully explained, but unspecific particle-membrane interactions due to repulsion or attraction forces between charged particles and membrane surface are most likely. Table 7.1 gives an overview of the two methods.

Appendix

Table 7.1: Comparison of single particle inductively coupled plasma mass spectrometry (spICPMS) versus asymmetric flow field flow fractionation coupled to plasma mass spectrometry ICPMS or used in a multi detector approach (A4F-ICPMS / MDA).

Analytical Method	spICPMS	A4F-ICPMS / MDA
Smallest detectable size in nm	ca. 20 nm [24, 31]	ca. 1 nm
Applicable size range	20 nm – ca. 1.5 μm	ca. 1 nm – 1 μm
Size resolution	10 nm	10 nm
Time for analysis	10 min/run	20 – 45 min per run
Advantages	<ol style="list-style-type: none"> 1. Size and elemental information 2. Low additional costs 3. Fast analyzing time per run 4. Flexible size range 	<ul style="list-style-type: none"> • Size and elemental information • Multi-element mode • Online approach • Highly flexible due to possibility to couple different detectors (e.g. UV, FLD, MALLS, DLS, RI, ICPMS) in line • sampling via fraction collector for other analysis like electron microscopy etc. • usual injection volumes of 20 – 100 μl containing representative atom and particle aliquots • possibility to achieve additional information on coating
Disadvantages	<ul style="list-style-type: none"> • usually only single element mode due to counting statistic • off-line (subsequent size analysis require time consuming calculation) • representative size analysis require multiple runs to achieve appropriate statistics • required dilution might change particle properties (e.g. due to dissolution, change of size) • two-particle-events cannot be distinguished from single-particle-events 	<ul style="list-style-type: none"> • high costs for A4F equipment • particle-membrane interactions due to different charges and resulting retention time shifts => impact on size calibration when size certified standard reference particles are used for size calibration • unpredictable particle losses due to depositions of particles on the membrane especially in the focus area and during the first injections after membrane exchange => sometimes poor recovery rates • dilution during size fractionation in the A4F channel might change particle properties (e.g. due to dissolution, change of size)
Application for ENP types	Th [20], Zr [21], U [22], Au [23], Ag [24, 26, 27, 30, 31],	Ag [8, 9, 18, 32, 33], Au [18, 40], poly styrene[1],
Other Applications		<ul style="list-style-type: none"> • aquatic colloids [19, 34, 36, 37] • macro-molecules, e.g. polymers, proteins [60]

Experimental

Chemicals: Nitric acid (65 % w/w), hydrochloric acid (30 % w/w) and 2-propanol were purchased in suprapur quality from Merck (Merck GmbH), sodium dodecyl sulfate (SDS) and dodecyl-trimethyl-ammonium bromide (DTAB) from Sigma Aldrich (Sigma Aldrich Chemie GmbH). A Milipore, Mili-Q A-10 water unit (Milipore AG) was used for the production of 18 M cm deionised water (DI-water). All solutions used as carrier for the A4F system were filtered prior to use through a 0.1 µm filter cartridge (PALL, Filtron) and degassed in an ultrasonic bath. ICPMS standards were prepared from single element standards in ICP quality from Merck (Merck GmbH). For A4F method validation, certified reference material Au particles purchased from National Institute of Standards and Technology (NIST SRM® 8011, 8012 and 8013) were used. After opening, the standards were transferred to nitrogen flushed and pre-cleaned (ethanol p.a.) PE-LD vessels and then stored in the dark. Before measurements, the standards were always freshly prepared, diluting from the stock with carrier solution directly in the 2 mL HPLC (PE-LD) vials. Details concerning synthesis and characterization of Au nanoparticles can be found elsewhere (Hagendorfer 2011, Hagendorfer, Kaegi et al. 2011, Hagendorfer, Kaegi et al. 2012) as well as details on the obtained size and concentration levels.

The silver nanoparticles with different coatings were provided by NanoSys GmbH - Fluids and Consulting, Switzerland. The titanium oxide nanoparticles originate from the European Research Project NanoHouse NMP-2009-1.3-1 & ENV.2009.3.1.3.2; Collaborative project n° 247810 (NanoHouse-Consortium 2010 - 2013) which focuses on the investigation of the release, environmental fate and toxicity of nanoparticles from paint products.

Batch DLS kinetic studies and ζ -potential for particles and A4F membranes: The influence of dilution, pH and ionic strength on the change in size distribution in a batch dynamic light scattering approach as well as the zeta (ζ) potentials for the above described titanium oxide and silver nanoparticles were monitored using a Zetasizer Nano ZS (Malvern Instruments Ltd., Germany). All samples were filtered prior to measurement using 0.22 μm PVDF syringe filters (BGB Analytik) and tempered for about 5 minutes to 20°C in the batch cell before analysis.

The streaming potentials of typical types of membranes for the A4F have been analysed using an electro-kinetic flow-through zeta potential analyser Mütek™ System Zeta Potential SZP-06 (BTG Instruments GmbH in Herrsching, Germany). Round membrane segments of 2 cm diameter (stationary phase) were placed in the flow through cell of the zeta potential analyser. The liquid phase streams through the membrane due to the applied pulsating vacuum (mechanical force). The electric potential (streaming potential) is measured from which the zeta potential is calculated. Each condition was measured in multiple determinations (5-times). Conductivity and pH were additionally determined using separate sensors.

Membrane materials were provided by Wyatt Technology (RC 10 kDa regenerated cellulose acetate, Alfa Laval, RC-70PP and the PES 100 kDa, Milipore, Biomax), and by GE Osmonics (PVDF 30 kDa, Sepa CF-PVDF-UF-JW). The streaming potentials of these membranes were determined over a large pH range and with different ionic strength.

Instrumental setup: A4F-UV/Vis-LS-ICP-MS: The A4F system is composed of a separation channel and a flow control unit (Eclipse®3) from Wyatt Technology Europe connected to a metal-free HPLC system from Shimadzu. It consists of a DGU-20A3 degasser, a LC-10Ai pump, a SIL-20AC autosampler, a CBM-20A control unit and a FRC-10A fraction collector. The

A4F system was coupled directly to an UV/Vis diode array detector (SPD-M20A, Shimadzu Germany GmbH) and an 18 angle MALS detector (DAWN Heleos® 2, Wyatt Technology Corporation), which operates at a laser wavelength of 658 nm. At an angle of 108° of the MALS detector, a DLS NanoStar® (Wyatt Technology Corporation) was connected via a glass fibre cord. Two Eclipse®3 channels of different dimension had been used: The longer with 275 mm and the shorter with 145 mm in length, and both of 50 mm in width and with a channel height of 350 µm given by a PEEK (Polyaryletherketone) spacer.

DI-water with a pH of 6.5 was applied as carrier flow, if not mentioned otherwise. The A4F separation consisted of 5 consecutive steps according to the description given in a previous paper. (Hagendorfer, Kaegi et al. 2011) A4F elugrams show the separation from the pre-separation step until beginning of the post separation step.

For online introduction of the samples to the ICPMS (Element 2, Thermo), the flow coming from the previous detectors (first UV/VIS, then MALS/DLS) was split by a factor of 200. To correct for non-spectral interferences an internal standard (flow rate of 10 µL/min, 10 µg/L Ir) in 10% aqua regia was added to the remaining flow. The sample introduction system consisted of a self-aspirating nebulizer (PFA-ST, Elemental Scientific) and a water-cooled Scott-type quartz spray chamber. A detailed description of the setup and the split design including operation conditions of the peristaltic pump (Gilson, M312)-and Tygon® tubing diameters are given in Hagendorfer *et al.* (Hagendorfer, Kaegi et al. 2011)

Data from the light scattering detector were processed with the ASTRA software (Wyatt, Version 5.3.4.20), UV/Vis data using the LC solution software (Shimadzu, Version 1.22 SP1), and ICPMS transient signals were evaluated applying the Element 2 software (Thermo, Version 3.1.0.236).

Each membrane was pre-cleaned, following a 3-phase procedure with a leaching, a cleaning, and an equilibration step. After 2 hours leaching in 25% 2-propanol, the membrane was thoroughly rinsed with DI water and equilibrated for 12 hours with carrier solution in the A4F channel. Recovery rates for different membranes were determined for a 30 kDa PVDF- (GE Osmonics, Sepa CF-PVDF-UF-JW), a 100 kDa PES- (Milipore, Biomax), a 10 kDa regenerated cellulose acetate (Alfa Laval, RC-70PP), and a series of ultra- and nanofiltration membranes purchased by GE Osmonics (DESAL UF 3.5 kDa GK, DESAL NF- DK, HL and 270). Recoveries for each membrane were determined in triplicates with Au nanoparticles of different sizes (20, 30 and 40 nm). Recovery rates were determined by a direct flow injection analysis of particles, followed by an A4F separation and comparison of the peak areas obtained by UV/Vis for both runs.

7.1.3 Results and Discussion

Selection of the nanoparticles for the study: Electrostatically and sterically stabilized nanoparticles as the two predominant ENP functionalization types are displayed in Figure 7. 2. Also the most interesting parameters as well as the influence factors of the chemical environment are summarized.

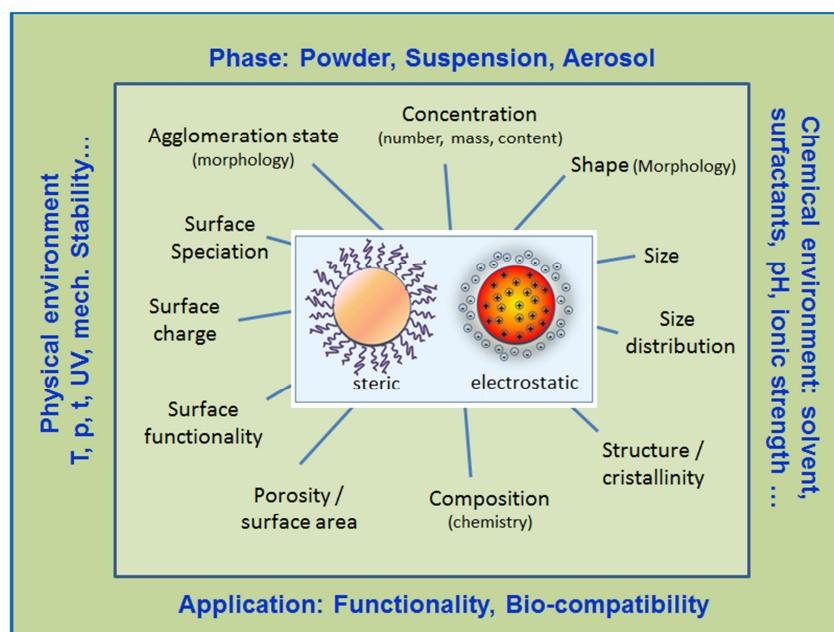


Figure 7. 2: The two predominant stabilization types of nanoparticles, the most important properties, and the relevant forms, influencing factors and applications.

Silver nanoparticles represent a wide spread type of nanoparticles, of which the citrate functionalization investigated here shall represent the electrostatic stabilization type and the polyvinyl alcohol (PVA) the steric type. Whereas Ag@citrate is easy accessible or self-synthesized, the polymeric functionalized Ag@PVA nanoparticle allow embedding e.g. in polymer materials proposed as dielectric elastomers. The third ENP class investigated here is a photo-catalytic active titanium oxide with a poly-acrylate functionalization (TiO₂@PA). Whereas non coated or functionalized titanium particles usually form aggregates, the poly-acrylate functionalization supports the homogeneous dispersion e.g. in paints. A dissolution of silver nanoparticles is often discussed (Hagendorfer, Lorenz et al. 2010, Hagendorfer, Kaegi et al. 2012) whereas titanium oxide nanoparticles is supposed to remain unaffected in aqueous environments. (Kaegi, Ulrich et al. 2008)

Effects of dilution, pH and ionic strength: As mentioned above, changes in the environment can have a significant impact on the analysis of nanoparticles. Dilution is required for most analysing procedures, especially for spICPMS, but also during A4F-ICPMS fractionation the sample is diluted due to the addition of channel and cross flow. Dilution is supposed to have an influence on electrostatic forces between coating or functionalization agent and nanoparticle and hence on the agglomeration state. Both silver nanoparticle types showed a slight increase of the size when the sample was diluted, whereas for TiO₂@PA nanoparticles no significant change in size was observed. Figure 7. 3 presents exemplarily the influence of dilution for the Ag@PVA nanoparticles.

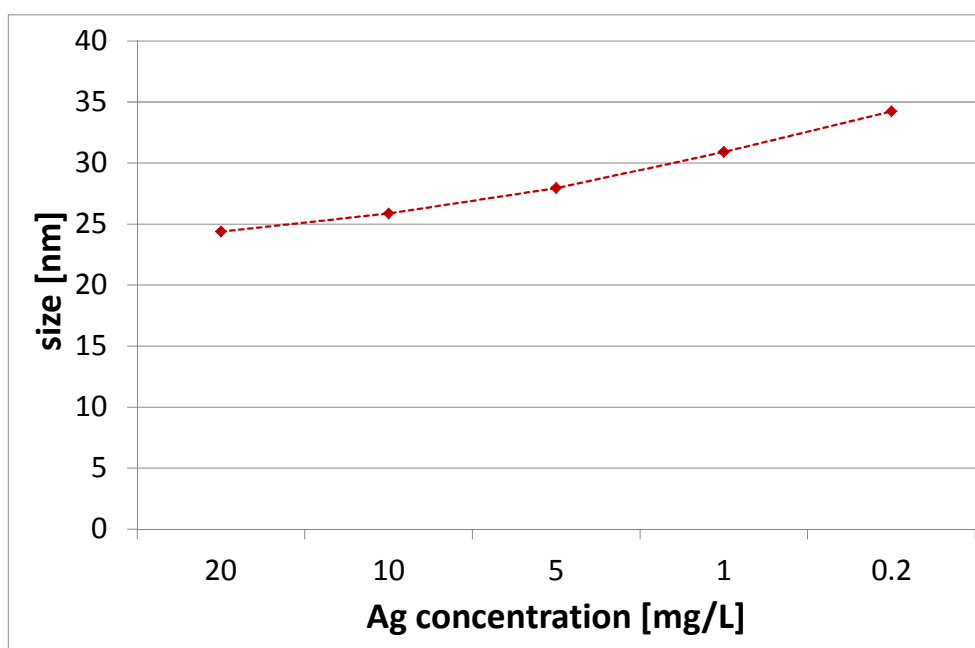


Figure 7. 3: Influence of dilution on the size of PVA stabilized silver nanoparticles for a 1000 mg/L nAg@PVA dispersion after dilution 1 : 50, 1 : 100, 1 : 500, 1 : 1000, and 1 : 5000 measured by batch DLS.

The small changes in size might be caused by a change of the ratio between nanoparticle and coating or functionalization agent bound to its surface. This assumption is supported by findings of Frens, who demonstrated a size dependency of gold nanoparticles in the presence of different coating or functionalization agent concentration. (Frens 1973) In the case of

Ag@PVA, the changes due to dilution were relatively small and in comparison to a given size resolution of about 10 nm e.g. for A4F the differences are small. However, the significance of possible changes for size-dependent analysis should be assessed for each specific case. Therefore, it is recommended to control for specific nanoparticle types, if a dilution effect occurs. A fast screening test using batch DLS prior time consuming analysis (e.g. by A4F-ICPMS/MDA or spICPMS) is therefore recommended.

In A4F-ICPMS analysis it is also sometimes recommended to add a surfactant or an electrolyte (e.g. Tween, SDS, etc.) to support the fractionation. However, an ionic surfactant or electrolyte can result in a change of ionic strength which might have a significant effect on nanoparticle properties. The agglomeration of the two silver nanoparticle types was significantly influenced by addition of sodium nitrate, whereas TiO₂@PA showed no significant size increase (Figure 7.4).

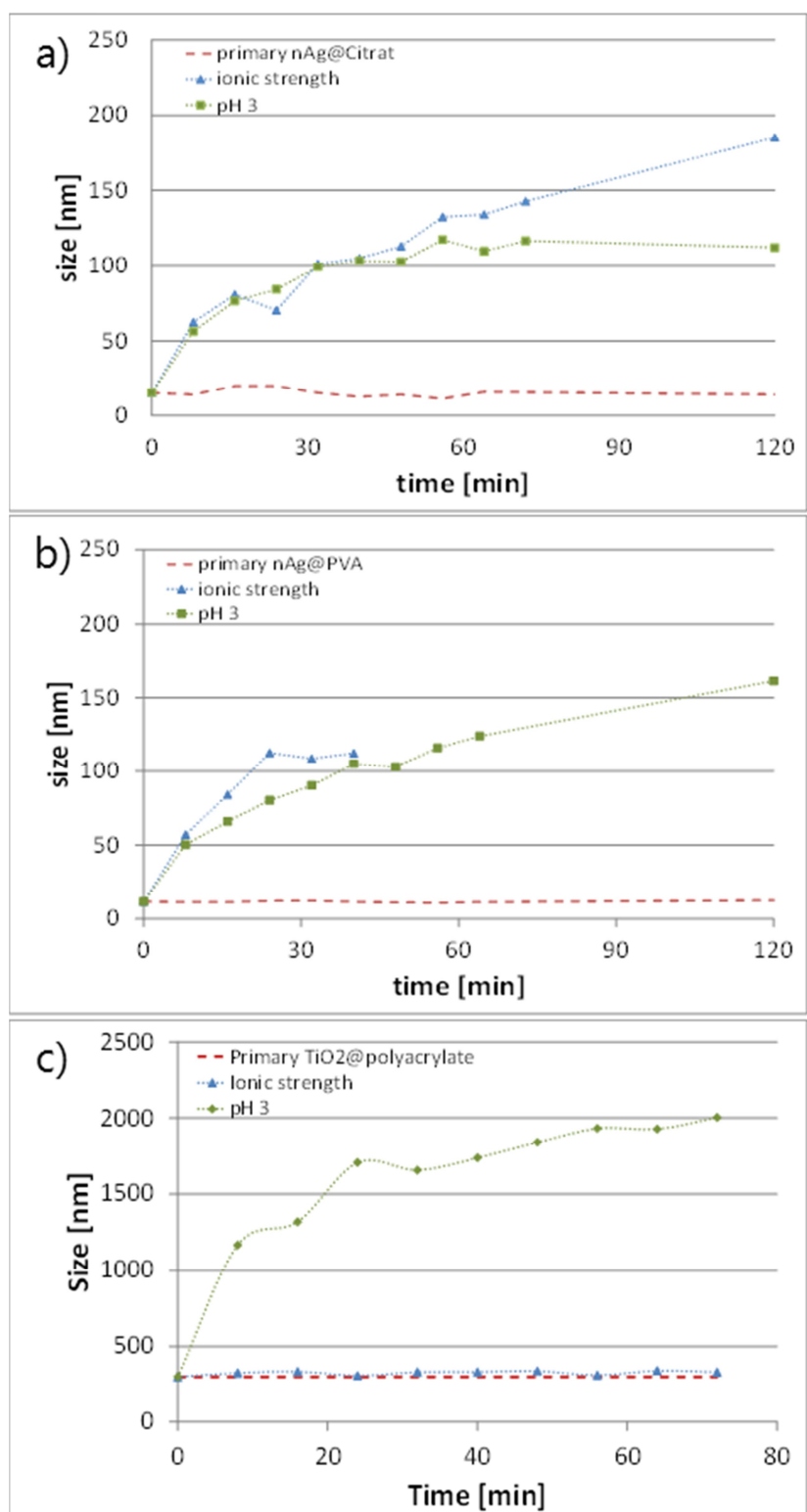


Figure 7.4: Time-dependent influence of a change in ionic strength (adjusted with NaNO₃) and pH (with HNO₃ acidified to pH 3) on the size of (a) TiO₂@, (b) Ag@PVA, and (c) Ag@citrate nanoparticles in comparison to the primary nanoparticle size (red line) measured by batch-DLS.

It is supposed that the addition of ions might change the electrostatic forces between coating or functionalization agent and nanoparticle core, which leads to the assumption that sterically stabilized nanoparticles are less sensitive to ion strength changes than electrostatically stabilized. However, specific salt types can also influence the pH of the environmental medium or even buffer the pH (e.g. phosphates).

The change of pH is also supposed to have more impact on electrostatically stabilizing coatings/functionalization than on steric ones. However, beside electrostatic forces there might be also additional chemical interactions, an influence on the cross-linking or binding between polymer coating/functionalization components of a steric type, e.g. due to hydrolysis or other chemical reactions like digestion.

This was also observed for the three coating/functionalization types investigated here. Figure 7.4 displays also the influence of a pH change on the size of the nanoparticles. The graph demonstrate exemplary, that also the sterically stabilizing types like the here investigated PA and PVA can be sensitive to pH changes. The time dependent curves give also hints on the kinetic in the agglomeration behaviour. For Ag@PVA a relatively steep increase was observed up to about 150 nm after 120 minutes, whereas Ag@citrate shows stabilization at about 120 nm after ca 60 minutes. A possible reason might be a protonation of the citrate and a change in the PVA by cross linking e.g. due to a shift in the hydrolysis balance equation which probably needs more time (slower kinetics).

It could be assumed, that for citrate a protonation of the functionalization agent occurs, for PVA possibly also a change in cross-linking of the polymeric stabilization agent. These changes probably lead to a significant change of the bonding strength between nanoparticle core and the stabilization agent. Therefore, fast batch-DLS measurements as screening tests

prior more sophisticated measurements are recommended to assess possible changes during sample preparation or analysis.

It could be concluded, that batch-DLS measurements represent a fast method (ca. 5 min/measurement) to detect significant changes in size of nanoparticles, even if the detection power is limited. It has to be taken into account that DLS shows more sensitivity for larger particles than for smaller ones, and provides average sizes only, which limits the applicability especially for samples with broad or multimodal size distributions. In these cases, the average size might be overestimated. (Hagendorfer, Kaegi et al. 2011, Hagendorfer, Kaegi et al. 2012) However, batch DLS could be very helpful to study the behaviour of unknown nanoparticles as well as the influence of added chemicals before more time consuming analysis are started.

Effects of surface charge: The change in the binding or electrostatic forces between coating or functionalization agent and core also influences the charge of the nanoparticles, which affects the so-called zeta potential. However, especially the charge of the nanoparticles could have an influence on the fractionation efficiency in A4F. Therefore both the charge of the membrane-material and the interactions with the particle charge were studied thoroughly here. According to the fractionation theory of Giddings (Giddings 1973) who is supposed to be the principle inventor of the field flow fractionation principle as well as Wahlund *et al* (Wahlund and Giddings 1987), the separation of components according to their sizes bases mainly on the cross flow in the fractionation channel and the diffusion which depends on the component size. This means that the size fractionation is only dependent on the size of the component but independent of the chemistry. However, newer studies, especially for the fractionation of nanoparticles, showed slight retention time shifts depending on the membrane material and the particle type which needs to be investigated more thoroughly.

(Hagendorfer, Kaegi et al. 2011) A second phenomenon observed in A4F fractionation is a sometimes significant particle loss, especially directly after replacement of the membrane. The recovery rates usually improve after several injections. An example for 6 replicates for Ag@citrate injected one after another directly after PVDF membrane replacement is displayed in Figure 7.5.

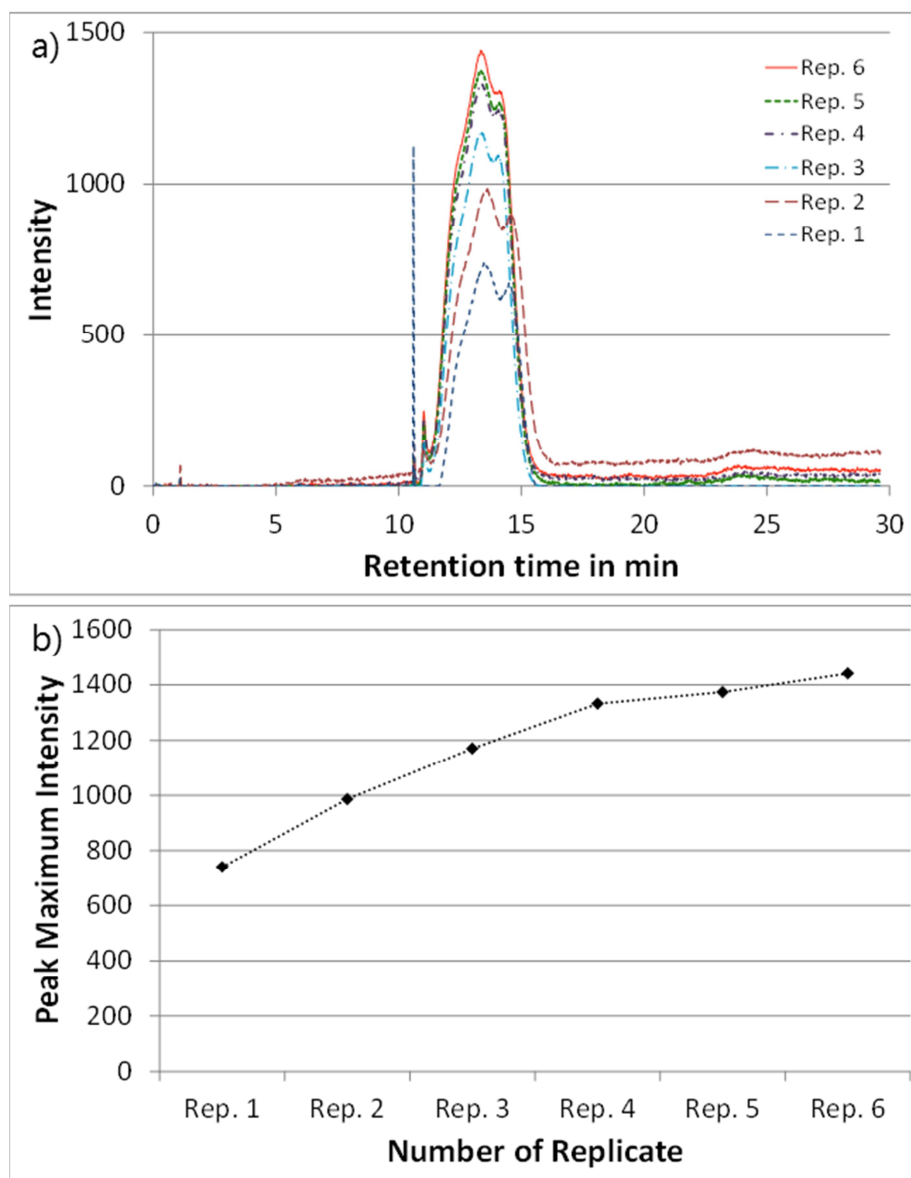


Figure 7.5: a) A4F fractograms of 6 successive injections for Ag@citrate measured directly after PVDF membrane replacement and b) the increase of the peak maxima of these replicates.

Even a slight shift in retention time is visible from the first to the last injection, but since the fractionation efficiency and size resolution capabilities of A4F is limited to about 10 nm for A4F, this small shift probably makes no visible influence in size determination. Anyway the particle loss due to deposition of nanoparticles especially in the focus zone area is nicely visible in particular for coloured nanoparticles such as gold nanocrystals (red). The increase of the signal and therefore also occurring improvement of the recovery rate after a few injections is probably caused by a deposition of the nanoparticles in the focus zone which later prevent further deposition of particles due to increasing repulsion forces. However, this assumption needs to be further investigated. Nevertheless, the unpredictable losses make quantification in A4F often difficult, so that alternative quantification strategies, such as batch analysis with prior ultracentrifugation procedure, are sometimes recommended. (Hagendorfer 2011, Hagendorfer, Kaegi et al. 2011, Hagendorfer, Kaegi et al. 2012)

However, it was recently discussed how much the different charges of particles and membrane materials influence the particle-membrane-interaction, but no investigations of the A4F membrane materials were available. (Hagendorfer 2011, Hagendorfer, Kaegi et al. 2011, Hagendorfer, Kaegi et al. 2012) Therefore, selected membrane materials are studied here. Regenerated cellulose (RC) and polyethersulfone (PES) are the mainly used membrane types in A4F. For nanoparticle analysis polyvinylidene fluoride (PVDF) is often recommended. (Hagendorfer, Kaegi et al. 2011, Hagendorfer, Kaegi et al. 2012) The zeta-potential of the three membrane materials were determined using a flow through zeta-potential device and are displayed in Figure 7.6.

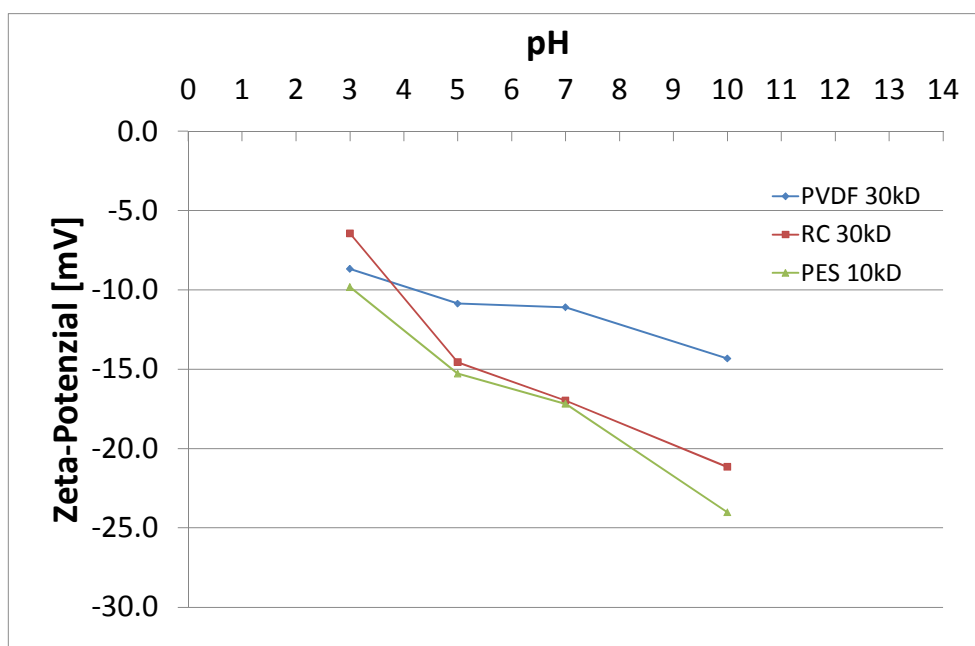


Figure 7.6: Influence of pH on the zeta potential of different membrane materials used for A4F measured by an electro-kinetic flow-through zeta potential analyser.

The curves demonstrate that a pH change results in a larger zeta potential value change for membrane materials with pH-sensitive functional groups such as OH, or COOH, whereas PVDF membrane with covalent Fluor-carbon bonds show less sensitivity against pH change.

Figure 7.7 displays the A4F fractograms of Ag@citrate with a diameter of ca. 15 nm and Ag@PVA with a diameter of ca. 12 nm using a PVDF membrane.

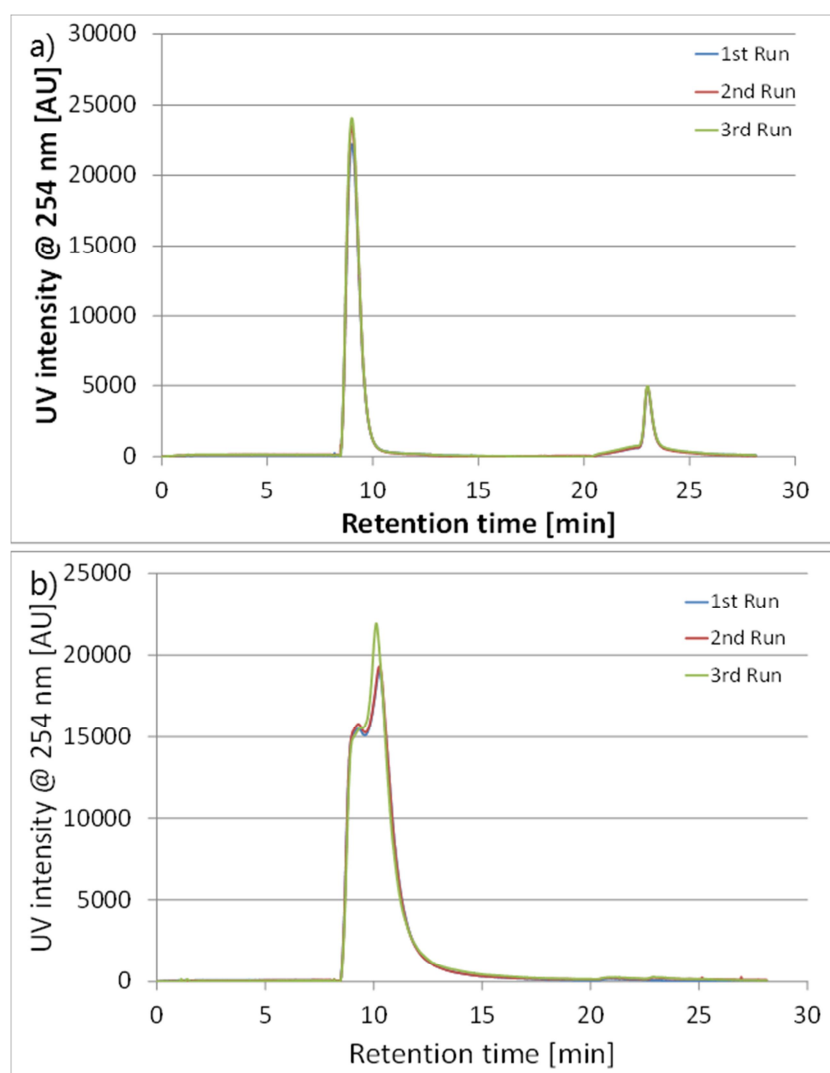


Figure 7.7: A4F fractograms of (a) Ag@citrate and (b) Ag@PVA using a PVDF membrane.

In the Ag@citrate the first peak appears after about 9 minutes and a second peak occurs after about 25 minutes. Since the A4F elugrams cover the separation from the pre-separation step until beginning of the post separation step, it can be assumed, that the second peak might be caused by retained particles which finally eluate after cross flow stop. The Ag@PVA fractogram shows only one slightly broader peak after about 10 minutes. The kink in the peak is not completely clear, but might be caused by unspecific interaction effects between the particle and the membrane or a slight polydispersity of the sample due to longer storage

time. However, according to the DLS measurements and the polydispersity index (PDI) the Ag@PVA nanoparticles were less polydisperse than the Ag@citrate nanoparticles.

The zeta potentials were determined to be -2.3 mV for Ag@PVA and -19.5 mV for Ag@citrate at neutral pH. Would the fractionation depend on size only, the retention time for the slightly smaller Ag@PVA should be a bit shorter than for the Ag@citrate, but the retention time until the peak maximum appears is with 8.99 to 9.01 minutes for Ag@citrate a bit shorter than with 10.25 to 10.26 minutes for Ag@PVA. Therefore, it is proposed that the charge of the separated particles as well as the membrane charge could have some influence on the size fractionation capabilities and retention time, especially when the particle sizes are in a similar size range with differences smaller than about 10 nm. In the following section a theory is proposed which can explain these effects.

7.1.4 Assumed theory of particle –particle and particle-membrane interaction

In general, two types of stabilization mechanism for nanoparticles can be distinguished: charge and steric stabilization (see Figure 7.1), which strongly depend on the type of the capping or coating / functionalization agent used. Charge stabilization is mainly dependent on surface charge, also called ζ -potential of a particle which can be described by a double layer model described elsewhere. (Parsegian 2006) Attractive forces between particles are usually calculated according to the microscopic theory of Hamaker, (Hamaker 1937, Parsegian 2006) and depend on the material which the particles are made of. On the other hand, repulsive interactions, such as steric and electrostatic interactions, depend primarily on the surface properties of the nanoparticles, which are strongly affected by the presence of coating agents. Hence silver particles with different coatings show different zeta potentials.

Also membranes show different surface charges, which depend on the material type. It can be assumed that van der Waals and electrostatic force are responsible for the particle-membrane interactions in the aqueous environment of an A4F channel. Electrostatic forces are active between charged particles and charged membrane surface whereas van der Waals forces as short-distance intermolecular dipole-dipole interactions are always present. (Leipert and Nirschl 2011) The attractive force between the membrane surface and the particle is determined by the membrane material, especially of the upper surface layer, the particle diameter, the distance between particle and membrane surface and the medium environment. The electrostatic forces F_{el} between charged particles and charged membrane surfaces depends on the charge of the membrane surface in comparison to the particle charge, which can either result in an attraction (surface load is different to the particle) or repulsion (same surface charge). The electrostatic force can be described by the sphere-plate model: (Bierman 1955, Leipert and Nirschl 2011)

$$F_{el} = \pi d 32 k T \rho_{\infty} \delta e^{(a_0 + a)\delta^{-1}} \tanh\left(\frac{z_i e \zeta_1}{4 k T}\right) \tanh\left(\frac{z_i e \zeta_2}{4 k T}\right)$$

- F_{el} electrostatic forces between charged particles and charged membrane surfaces
- T absolute temperature
- ρ_{∞} density of the media
- z ion valence
- ζ zeta potential of the substance i
- δ thickness of the diffusive layer
- a_0 Adhesion distance
- $a + a_0$ distance between the two interacting partners

The attractive Van der Waals force can be described by the sphere-plane model as follows:

$$F_{VdW} = -\frac{HR^3}{l^2(2R+l)^2} \cdot F_{VdW} \quad \text{Van der Waals force between a particles and a membrane surface}$$

H Hamaker constant for the solvent-mediated particle-membrane interactions

l Surface-to surface distance between particle and membrane

R Particle Radius

The attraction or repulsion force between particle and membrane, and hence a possible particle deposition (adhesion) is determined by the van-der-Waals force F_{VdW} , and the electrostatic force F_{el} . If the membrane surface and the particles are similarly charged, the resulting electrostatic repulsion between particle and surface can prevent that the particle moves close enough to the membrane surface that also van der Waals forces become active. Whereas in case of differently charged particle and membrane surface both electrostatic and van der Waals force are attractive. (Leipert and Nirschl 2011) In this case also depositions of particles on the membrane surface are possible, for example as observed for gold and silver nanoparticles. (Schmidt, Petersen et al. 2009, Hagendorfer, Kaegi et al. 2011, Hagendorfer, Kaegi et al. 2012) On the other hand, the stronger is the repulsion forces between particle and membrane, the larger is their distance, making the depositions less probable. However, especially during the focusing phase directly after injection is critical. During the focussing step flows from both sides of the channel are directed to the so-called focus point. A deposition in the focus point area is more likely for lower repulsion forces between a specific particle and the membrane surface. Hence, depositions of particles occur especially in the focus area, which is nicely visible e.g. for red coloured gold particles like the NIST certified standard reference na-

noparticles. During the relaxation phase particles experiencing weaker repulsion can remain closer to the surface whereas particles which experiencing stronger repulsion can reach faster field lines in the laminar channel flow, which results in a faster transport out of the channel and therefore to shorter retention times. Figure 7.8 displays these phenomena schematically.

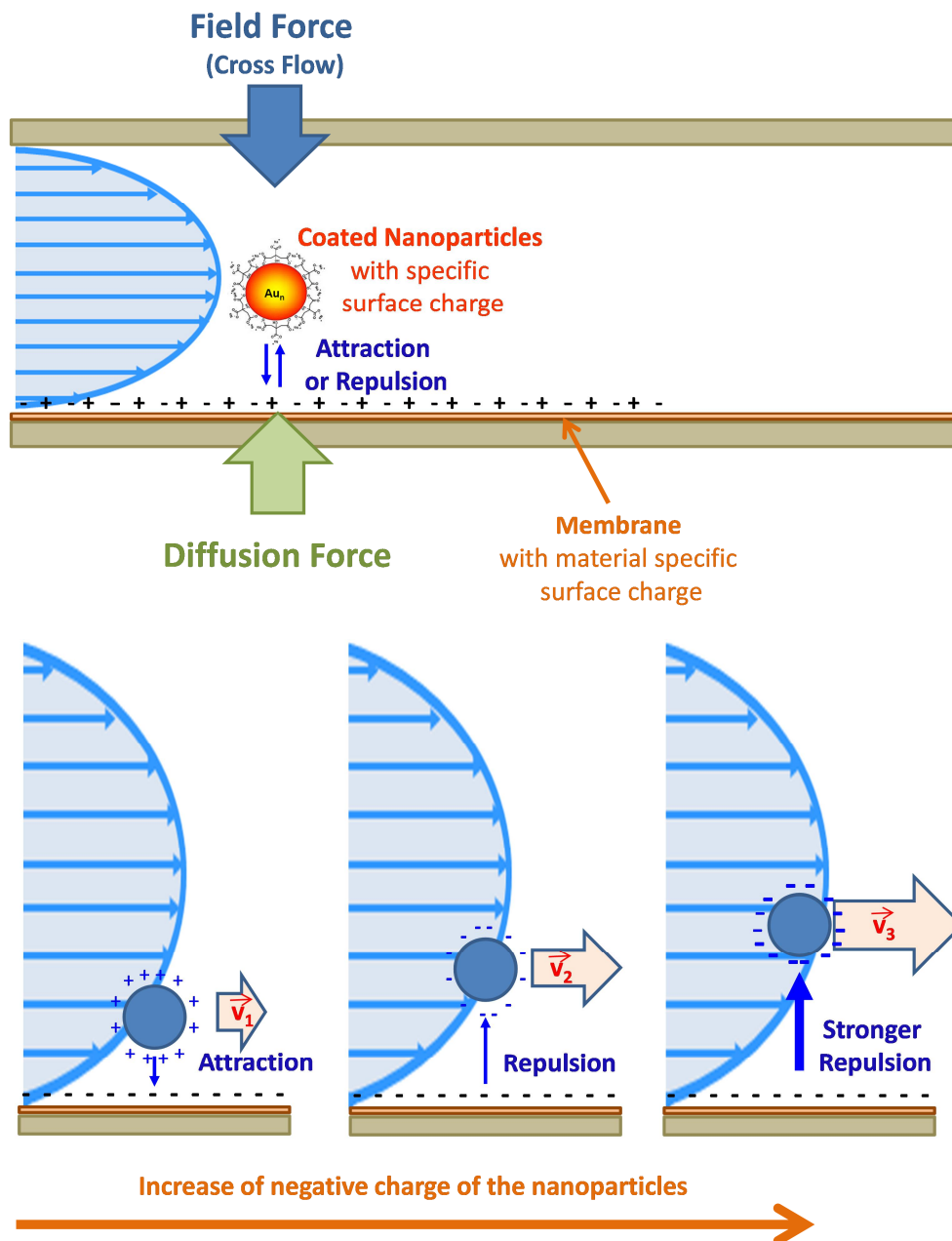


Figure 7.8: Scheme of nanoparticle-membrane-interaction in an A4F channel and attraction/ repulsion between membrane and nanoparticle depending on their different charges.

The proposed qualitative picture can explain the above mentioned results of Figure 7.7. It should be taken into consideration that the size difference between PVA and citrate functionalized silver nanoparticles is relatively small ($\Delta = 3$ nm). The zeta potential of Ag@PVA is with -2.3 mV less negative than -19.5 mV for Ag@citrate. Both measurements were performed with exactly the same flow conditions and membrane in the A4F fractionation channel. The zeta potential of the PVDF membrane at neutral pH was determined to be -11.1 mV. Since both, particles and membrane are negatively charged a repulsion force should be active between particles and membrane. However, the low zeta potential value of Ag@PVA indicates a weak repulsive force, whereas the repulsion force between Ag@citrate particles and PVDF membrane should be higher. Thus, the Ag@citrate particles reach slightly faster velocity lines of the laminar channel flow than the Ag@PVA nanoparticles which results in a slightly shorter retention time and faster elution. This hypothesis should be further evaluated with additional investigations.

7.1.5 Conclusion

Sample handling or changes in the chemical environment during analysis can have a significant impact on nanoparticle properties especially on size distribution or chemical transformation (e.g. dissolution). For example dilution can accelerate dissolution e.g. for specific silver nanoparticle types, and can even have a certain influence on agglomeration behaviour depending on the coating/functionalization agent type. However, changes in pH or ionic strength usually have a stronger influence. They can have an influence not only on charge but also on sterically stabilized ENPs due to chemical reactions like changes in the cross-linking or binding between the polymer functionalization agent and the nanoparticle core. Therefore,

it is recommended to check the behaviour of nanoparticles using a fast screening method like batch DLS prior analysis for size-classified, chemical analysis like spICPMS or A4F-ICPMS/MDA. Such a screening test allows the assessment of possible effects due to dilution, or other media changes (e.g. a change in ionic strength due to addition of surfactants or electrolytes, pH change, etc.) during sample preparation or analysing procedure and prevents erroneous results.

The charge of nanoparticles can also have an influence on the separation efficiency and recovery rate in A4F-ICPMS/MDA analysis. The charge of the particles and the membrane materials used in A4F fractionation can result in a slight retention time shift. These shifts are especially detectable for smaller size differences <10 nm between two particle types as shown here for PVA and citrate functionalized silver nanoparticles with a primary size of 12 and 15 nm respectively. However, for larger size differences between two particle fractions the effect is probably of minor importance. The here presented first results give probably good hints on the particle-membrane interactions in A4F, but further investigations are needed to fully understand the mechanisms. Therefore, the charges of different membrane materials and the interaction with different particle types should be studied more detailed in a future project to understand the mechanism of specific particle membrane interactions.

Media coverage for chapter 7.1 published as:

A. Ulrich, S. Losert, N. Bendixen, A. Al-Kattan, H. Hagendorfer, B. Nowack, C. Adlhart, J. Ebert, M. Lattuada, K. Hungerbühler, 2012, Critical aspects of sample handling for direct nanoparticle analysis and analytical challenges using asymmetric field flow fractionation in a multi-detector approach, *J. Anal. At. Spectrom.*, 27, 1120-1130.

7.2 Membrane-particle interactions in an asymmetric flow field flow fractionation channel studied with titanium dioxide nanoparticles

7.2.1 Introduction

Fast and proper analysis of nanoparticles is important for material sciences and product development as well as for safety and risk assessment. The current recommendation of the European Union, (2011/696/EU) (The_European_Commission 2011) which defines a substance as nanomaterial when 50 % of the particle number concentration is below 100 nm, requires suited analytical strategies to determine nanoparticles amount in materials and products. Therefore size and chemical composition are among the most important analytical properties of nanoparticles. (Ulrich, Losert et al. 2012)

Asymmetric flow field flow fractionation operated in a multi-detector approach (A4F-MDA) using several detectors inline such as UV/Vis, multi angle light scattering (MALS) and inductively coupled plasma mass spectrometry (ICPMS) is a powerful tool to derive size and elemental information simultaneously. (Hagendorfer, Kaegi et al. 2011, Krystek, Ulrich et al. 2011, Hagendorfer, Kaegi et al. 2012) A4F was first introduced by Wahlund and Giddings in 1987 (Wahlund and Giddings 1987) and proposed as a tool for the separation of macromolecules, colloids and particles according to their size. (Liu, Andya et al. 2006, Roda, Zattoni et al. 2009) The size fractionation principle of A4F is based on a parabolic laminar flow with a perpendicular cross-flow. Macromolecules or nanoparticles in the channel experience the cross-flow force towards the membrane and the diffusion force back into the channel. Depending on their size they are focused to a specific height in the separation channel. This results in a faster elution of smaller particles than for larger ones. (Wahlund and Giddings 1987) The follow-

ing equation describes the calculation of the retention time in asymmetric flow field flow fractionation (Roessner):

$$t_r = ((\pi\eta dw^2)/(2kT)) * (V_{cross}/V_{channel})$$

The retention time t_r depends on viscosity η [$\text{kg}\cdot\text{s}^{-1}\cdot\text{m}^{-1}$], the Stokes diameter d [m], the A4F channel height w [m], the Boltzmann constant k [$\text{m}^2\cdot\text{kg}\cdot\text{s}^{-2}\cdot\text{K}^{-1}$], the temperature T [K], as well as on the cross flow V_{cross} [$\text{L}\cdot\text{s}^{-1}$] and the channel flow $V_{channel}$ [$\text{L}\cdot\text{s}^{-1}$]. According to this equation the retention time of a particle should only depend on its size, whereas all other parameters can be kept constant during a separation.

Size determination of particles as a function of retention time (hydrodynamic diameter) with standardized NPs (e.g. Duke polystyrene particles or NIST gold nanoparticle standards SRM-8011, SRM-8012, SRM-8013) is easy and commonly used in A4F, especially if no size-determining detector is available. Besides, online detectors such as multi-angle light scattering (MALS) which provides the radius of gyration or dynamic light scattering (DLS) giving a hydrodynamic diameter are sometimes employed. However, some authors such as Hagendorfer *et al.* (Hagendorfer, Kaegi *et al.* 2011) reported incorrect size results using online MALS e.g. for gold nanoparticles – probably due to optical properties of the particles. As reported in their supporting information, they observed a non-typical angle-dependent scattering behavior e.g. for 60 nm gold NPs, whereas polystyrene particles of similar size behaved ideal. Thus, the applicability especially of MALS might be limited for the use of nanoparticle analysis. Therefore, an additional size determination via retention time is often necessary for validation. But particle size determination based on retention time using the above mentioned equation is only valid, as long as retention time and recovery rates in FFF were stable. However, in some recent publications insufficient recovery rates as well as retention time shifts were observed and explained by unspecific membrane-particle interactions.

Delay and Frimmel (Delay and Frimmel 2012) observed strong interactions of Ag NPs on A4F membranes. Hagendorfer *et al* (Hagendorfer, Kaegi et al. 2012) and Ulrich *et al* (Ulrich, Losert et al. 2012) reported varying recovery rates depending on the nanoparticle type and the used membrane material. (Hagendorfer, Kaegi et al. 2011, Hagendorfer, Kaegi et al. 2012, Ulrich, Losert et al. 2012) Also, Bolea *et al* (Bolea, Jiménez-Lamana et al. 2011) observed membrane-particle interactions resulting in quantification problems due to varying recovery rates. Schmidt *et al* (Schmidt, Loeschner et al. 2011) found an effect of the particle size in the case of gold NPs on the recovery rates and assumed that particles partially stuck to the membranes surface. Nischwitz and Goenaga-Infante (Nischwitz and Goenaga-Infante 2012) stated that particle-membrane interactions may alter the elution time and therefore reduce the accuracy of the size calculation. They propose an external size calibration with particle dispersions which show similar interactions like the particles in the sample. Loeschner *et al* (Loeschner, Navratilova et al. 2013) examined the retention times of Ag and Au NPs on different membranes and conclude that the FFF theory on the particle size calculation is not suitable when electrostatic or van der Waals interactions are present. Baalousha *et al* (Baalousha, Stolpe et al. 2011) observed membrane dependent interactions and state that van der Waals, hydrophobic and charge interaction forces may cause the membrane-particle interactions. Schachermeyer *et al* (Schachermeyer, Ashby et al. 2012) presented first investigations on the effect of the carrier on the membrane-particle interactions and stated that electrostatic repulsion might minimize the adsorption of particles on the membrane surface.

These observations indicate that the separation capacity in the A4F channel is not only dependent on the particle size but may also be influenced by the specific properties of the NPs and the membrane material. Recently Gigault and Hackley (Gigault and Hackley 2013) showed that the particle density has some influence on the retention time and they adapted

the equation for particle size determination in A4F accordingly. However, they stated in accordance to Loeschner *et al* (Loeschner, Navratilova et al. 2013) that retention time seemed to be influenced to a much higher degree by van der Waals forces (between NP and membrane) as well as interactions between different components in the mixture.

In a previous publication, (Ulrich, Losert et al. 2012) we proposed a theory to account for particle membrane interactions based on electrostatic forces between the particles and the membranes which occur in addition to repulsing and attracting forces among the particles themselves. During the injection phase, the usually charged particles are pushed towards the membrane surface and might therefore interact with the also charged membrane material. The more repulsive the force between the membrane and the particle is, the less probable is that deposition of particles occur and thus minimizing particle loss. Consequently, higher repulsion force compels the particles to find their equilibrium in a faster velocity zone of the laminar parabolic channel flow, and thus, the particle will elute with shorter retention times. On the other hand, if particles and membrane materials are oppositely charged, the likelihood for deposition will increase.

Based on this theory we are now questioning the importance of the ζ -potential in A4F: The ζ -potential of the membrane and the NPs may (A) determine the feasibility of an A4F method for a given sample type, (B) direct the optimization of an A4F method for better separation efficiency, (C) account for shifts in retention time that impede the correct calculation of the particle size, and (D) account for different recovery rates of different nanoparticle samples.

To test our hypothesis, we selected the most commonly used membrane materials in A4F i.e. regenerated cellulose (RC), polyethersulfone (PES), and polyvinylidene fluoride (PVDF) and we studied the influence of their ζ -potential on the separation of titanium dioxide nanoparticles. Titanium dioxide is one of the predominantly applied nanoparticles among the metal

and metal oxide nanoparticles. They are used in a large number of products, such as sun-screen, textiles, tooth paste, façade paint and in waste water treatment. (Allen 2008, Kaegi, Ulrich et al. 2008, Kwon, Fan et al. 2008, Robichaud, Uyar et al. 2009, Skocaj, Filipic et al. 2011) Moreover, TiO₂ (i.e. Aeroxide®P25, Evonik Degussa) was selected as representative material (EPA 2010) for the Nanoscale Materials Stewardship Program (NMSP) launched by the U.S. Environmental Protection Agency Office of Pollution Prevention and Toxics (EPA) (EPA 2009) as well as a master batch nanomaterial for OECD test procedures (OECD 2013). Thus, TiO₂ is a representative nanoparticle type, which makes it ideal as model substance for systematic method development for A4F-MDA analysis.

Furthermore the effect of different carrier media and additional surfactants on the surface charge of membranes and particles was systematically investigated. Additionally, the effect of different charging conditions on retention time and recovery rates of TiO₂ NPs with different membranes is studied. From this study, we were expecting increased knowledge on membrane-particle interactions, in particular, in how far the ζ-potential of membrane and particles would determine the outcome of A4F in terms of feasibility (A), separation efficiency (B), retention time (C), and recovery rate (D) or whether other factors such as membrane morphology and particle size were equally important. The findings of this work should help to minimize or make use of membrane-particle interactions during experimental work and to foster the discussion on correct calibration.

7.2.2 Material and Methods

Chemicals: Suspensions were prepared using commercially available titanium dioxide nanoparticle types from two different suppliers: TiO₂ powder (AEROXIDE® P25) from Evonik Degussa GmbH and a TiO₂ suspension (P/N 700347), 33 - 37 % in water containing 5 – 10 % [2-(2-Methoxyethoxy)ethoxy]acetic acid (MEAA) for stabilization, from Sigma-Aldrich. Both products consist of particles with a primary size of about 21 nm, whereas Sigma-Aldrich declares their particles to be present as agglomerates with a size < 150 nm To study the influence of sample preparation the AEROXIDE® P25 powder was dispersed in the following liquids: Deionized water from a Mili-Q A Gradient-10 water unit (Milipore AG), tap water, and solutions of deionized water and 0.01 % sodium dodecyl sulfate (SDS, from Sigma-Aldrich, 99.0 %), 0.1 mM SDS with 1 mM ammonia nitrate (Merck KGaA , pro analysi), 0.01 % Triton X-100 (Fisher Scientific, electrophoresis grade), 1 mM sodium hexametaphosphate (Alfa Aesar, technical grade), 1 mM disodium diphosphate (Merck KGaA, pro analysi) or 0.01 % 2-(2-Methoxyethoxy)ethoxy]acetic acid MEAA (Sigma Aldrich, tech. grade). Additionally monodisperse standard polystyrene nanoparticles (PS) with different sizes between 20 and 200 nm were used (Nanosphere Size Standard from Duke Scientific Corporation).

Suspensions: For the evaluation of the TiO₂ properties in different suspensions, 125 mg Aeroxide® TiO₂ powder was weighted into a 50 mL polypropylene tube and dispersed with the above mentioned media, resulting in a concentration of 2.5 g/L. This initial suspension got further diluted in the corresponding media to a concentration of 0.1 g/L. To minimize agglomeration all samples were probe sonicated for 2 minutes with 9 cycles and 25 % power

(Sonopuls HD2200, Bandelin) before analysis. Precipitation of large agglomerates occurred within hours in all suspensions. Therefore only the supernatant was used for experiments.

For the membrane-particle interaction test suspensions of the Aeroxide®P25 TiO₂ and of the Sigma-Aldrich TiO₂ in 1 mM sodium hexametaphosphate were used. They were centrifuged for 60 min at 5000 rpm (cutoff at around 110 nm) and the supernatant was characterized and used for the tests. The final Aeroxide®P25 suspension had a concentration of 32 mg/L TiO₂ (validated by batch analysis using inductively coupled plasma mass spectrometry ICPMS), a ζ -potential of -45.2 ± 1.2 mV (determined with a Malvern Zetasizer) and a diameter of 86.6 ± 3.4 nm (A4F-MALS). For the final Sigma-Aldrich TiO₂ suspension a concentration of 57 mg/L TiO₂, a ζ -potential of -44.9 ± 1.5 mV and a diameter of 63 ± 1.6 nm was determined. As these suspensions were used during a period of around 8 months, further precipitation occurred over time and the size characterization given in section 3.2.3 results in smaller diameters.

Zeta-Potential and Diameter Measurement: The characterization of the hydrodynamic diameter and the ζ -potential of the TiO₂ suspensions were carried out using a Malvern Zetasizer NanoZS (Malvern Instruments Ltd., Germany). The samples were tempered to 20°C for 5 minutes in a batch cell prior to analysis and the hydrodynamic diameter as well as the ζ -potential were determined in triplicates for each sample. For the ζ -potential measurement the Smoluchowski model was used with 30 repetitions per measurement. For the size determination the general purpose model (defined in the software, no further details available) was used with 10 repetitions per measurement.

Membranes: As most commonly used membrane materials regenerated cellulose (RC) with cutoffs of 10 kDa and 30 kDa (Wyatt Technology Europe GmbH, Germany), polyethersulfone

(PES) with a cutoff of 10 kDa (Wyatt Technology Europe GmbH, Germany) and polyvinylidene difluoride (PVDF) with a cutoff of 30 kDa (GE Healthcare, Switzerland) were selected. The characterization of the ζ -potential was carried out on a streaming potential analyzer Müttek™SZP-06 (BTG Instruments GmbH, Germany). By application of the formula below, the ζ -potential can get derived from the streaming potential:

$$\zeta = (\Delta U \cdot \Delta P^{-1}) \cdot \kappa_B \cdot \eta \cdot (\epsilon_r - 1 \cdot \epsilon_0^{-1})$$

The ζ -potential depends on the slope of the streaming potential ΔU [V], the pressure difference ΔP [$\text{kg} \cdot \text{m}^{-1} \cdot \text{s}^{-2}$], the conductivity κ_B [$\text{A} \cdot \text{V}^{-1} \cdot \text{m}^{-1}$], the viscosity of the solvent η [$\text{kg} \cdot \text{m}^{-1} \cdot \text{s}^{-1}$], the dielectric constant ϵ_r and the permittivity ϵ_0 [$\text{A} \cdot \text{s} \cdot \text{m}^{-1} \cdot \text{V}^{-1}$].

The measurements were performed with tap water, DI water, 0.01 % SDS, 0.1 % MEAA, and 1 mM sodium hexametaphosphate. Each experiment was performed in 10 repetitions. The conductivity and pH were determined using a MultiLine P3 instrument (WTW, Germany).

The surface morphology of the membranes was analyzed using a XL30 ESEM-FEG (Philips). Before analysis the membranes were covered with about 1 nm of platinum coating (MED 020 Coating System, BAL-TEC).

A4F-UV/Vis-MALS: The asymmetric flow field flow fractionation instrument used for this work was an Eclipse 3 from Wyatt Technology Europe GmbH (Dernbach, Germany) equipped with a LC pump LC-10Ai and an autosampler SIL-20AC from Shimadzu (Reinach, Switzerland). The A4F was online connected to an UV/Vis-Detector SPD-M20A from Shimadzu, followed by a MALS-Detector DAWN Heleos II from Wyatt. The A4F was operated using a long A4F channel (275 mm) with the above mentioned membrane materials (specification depending on the experiment) and a spacer of 350 μm thickness. For the finally optimized A4F procedure, a

mobile phase consisting of 1 mM sodium hexametaphosphate in deionized water was used. Best separation for the given TiO₂ nanoparticles were achieved with a channel flow of 1.5 mL/min and a gradient cross-flow from 1.5 to 0.0 mL/min. The UV/Vis signal was analyzed at 254 nm, the 18 angles MALS was operated at 658 nm and the Zimm model was applied.

Recovery Rate: For the evaluation of the recovery rate injections were done without channel and without a cross flow applied. Therefore the A4F channel got replaced by a 4 port cross piece. The area of the eluting peak was treated as the set point. To evaluate the recovery rate the area of the UV/Vis signal when using an A4F channel with a membrane was compared to this set point.

7.2.3 Results and Discussion

Investigation of the A4F Conditions: The selected A4F conditions were based on a literature study on the most widely applied A4F conditions for the analysis of TiO₂ suspensions in terms of membrane materials, cutoffs, typical separation conditions, and surfactants. As membrane material regenerated cellulose (RC) was predominantly used. (Nischwitz and Goenaga-Infante 2012) For other nanoparticle types e.g. silver or gold, also polyethersulfone (PES) and polyvinylidene fluoride (PVDF) was proposed. (Hagendorfer, Kaegi et al. 2011, Hagendorfer, Kaegi et al. 2012) Therefore, we selected these materials with commonly used cutoffs. Regarding the surfactants, both ultrapure water only as well as the usage of specific surfactants for the preparation of nanoparticle suspensions or as supporting agents for improved A4F separation are reported. (Dulog and Schauer 1996, Dubascoux, Von Der Kammer et al. 2008, Nischwitz and Goenaga-Infante 2012) Therefore, we selected the following typical suspension

agents and surfactants for all the experiments: DI water, sodium dodecyl sulfate (SDS), SDS with ammonia nitrate, Triton X-100, sodium hexametaphosphate, disodium diphosphate, and 2-(2-methoxyethoxy)ethoxy]acetic acid (MEAA). Tap water was used as one possible representative for typical aquatic ionic strength and pH conditions and is often used to simulate washing or leaching processes of products. It was already stated elsewhere that the resulting pH and the final ionic strength can have a significant influence on the stability of nanoparticles. (von der Kammer, Ottofuelling et al. 2010, Ottofuelling, Von Der Kammer et al. 2011, Ulrich, Losert et al. 2012)

To evaluate the optimum A4F conditions for the analysis of titanium dioxide nanoparticles, the ζ -potential of the membranes and of the particles was measured evaluating different carrier solutions. Further optimizations were also performed concerning the flow rates and durations of the steps. The results for the membrane potentials are presented in Figure 7.9.

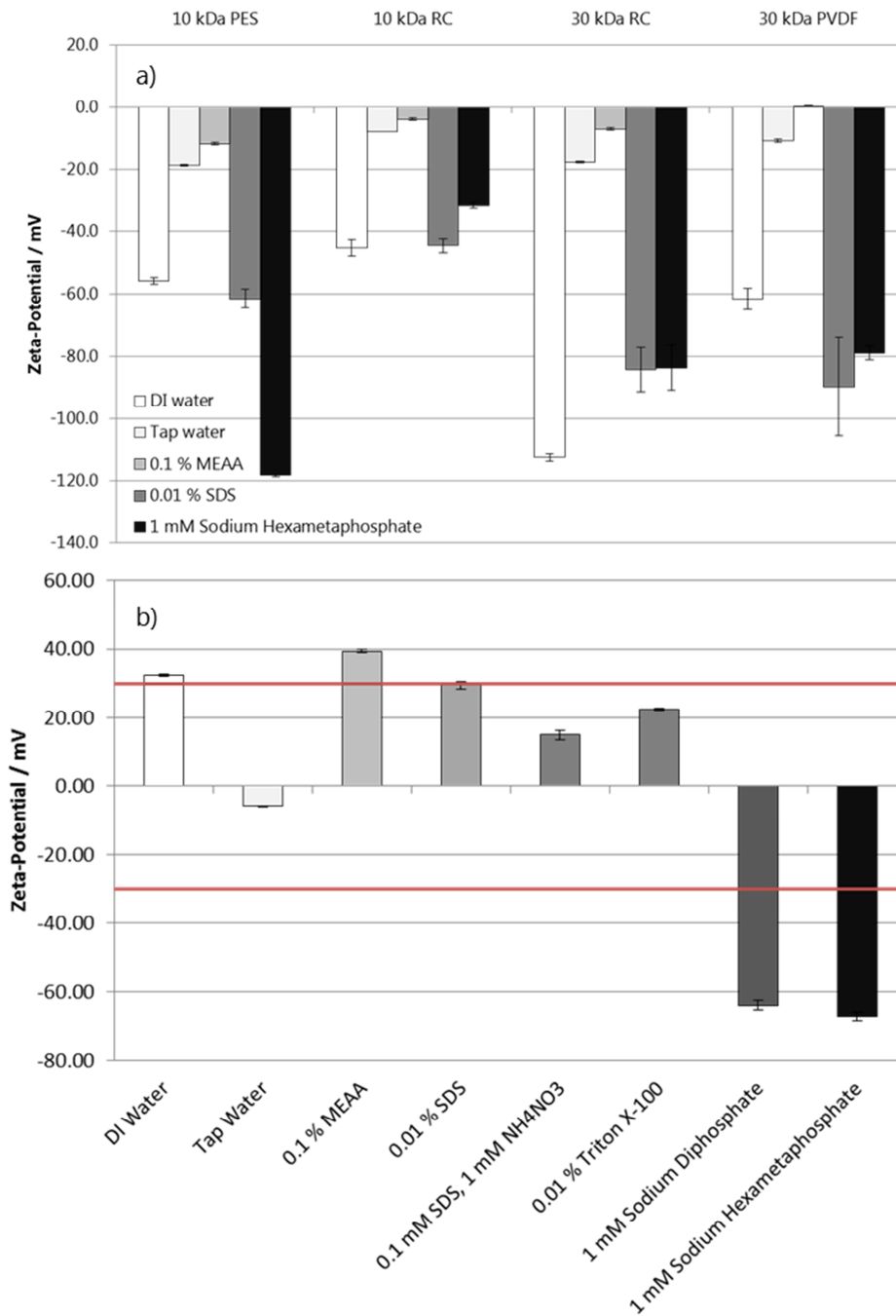


Figure 7.9: Influence of different surfactants and the type of water on the ζ -potential of a) different membrane materials and b) of TiO₂ NPs (Aeroxide®P25). The straight red lines indicate the critical ζ -potentials concerning stable conditions (higher than ± 30 mV).

All membrane materials showed negative ζ -potential for the given solutions. The absolute values of the measurements in DI water and in 0.01 % SDS solution have to be considered carefully, due to the low conductivity which was below the recommended minimum for the

used instrument. However, it still can be seen that the values are clearly negative. Tap water, 1 mM hexametaphosphate and 0.1 % MEAA met perfectly the required conductivity criterion which makes the absolute values reliable. Hexametaphosphate is a multiply charged ion which probably attaches to the membrane surface. This effect increases the surface charge which results in the observed highly negative ζ -potential indicating a strong electrostatic repulsion for negatively charged particles. SDS is an anionic surfactant which is often recommended for A4F analysis. It might also attach to the membrane surface with its alkyl chain and introduce negative charges by its anionic head. This effect should also increase the electrostatic repulsion for negatively charged particles. The effect of MEAA is presumably not due to attachment to the surface of the membrane, but due to a more acidic pH-value of around pH 3.1. Some of the results of this study got previously published (Ulrich, Losert et al. 2012, Bendixen, Losert et al. 2014) and they show that a decrease in the pH results in a less negatively charged membrane. Depending on the isoelectric point of a membrane material the potential might even turn positive. Surprisingly, PVDF showed the strongest variation in the ζ -potential, although the chemical groups should be insensitive to pH changes. It should be mentioned that similar membrane materials provided by other manufacturers may vary due to different surface finishing (chemical functionality, layered constructions, and roughness). (Kassalainen 2012) Thus such a finishing might be an explanation for the reaction of the PVDF membrane on pH variations. However, details on the processing of the membrane materials are rarely accessible from the established distributors of field flow fractionation equipment. Thus, careful consideration of membrane materials for A4F is highly recommended to improve reliability during method development.

Figure 7.9b demonstrates the effect of suspending agents or surfactants on the surface charge of the studied TiO₂ NPs. Different agents change the ζ -potential of the TiO₂ NPs (Aer-

oxide®P25) significantly from positive to negative ζ -potentials. The tests did not get performed with Sigma-Aldrich NPs.

However, only DI water, 0.1 % MEAA, 0.01 % SDS, 1 mM sodium hexametaphosphate and 1 mM sodium diphosphate resulted in a ζ -potential higher or lower than ± 30 mV and should therefore prevent agglomeration according to the DLVO theory [30]. The other tested carrier liquids are thus not appropriate for the stabilization of TiO₂ NPs. MEAA, DI water and SDS result in a pH below 6, which corresponds to the isoelectric point of TiO₂. Below pH 6 the surface of titanium dioxide is protonated and this results in a positive ζ -potential. (Jiang, Oberdörster et al. 2009, Suttiponparnit, Jiang et al. 2011)

The strong negative ζ -potential observed for polyphosphates correlates with literature: Jiang *et al* measured a ζ -potential of -53 mV for TiO₂ particles dispersed in sodium pyrophosphate. (Jiang, Oberdörster et al. 2009)

Assuming that positively charged particles would lead to a more pronounced deposition due to increasing attracting forces between negatively charged membrane and positively charged particles, only sodium hexametaphosphate and sodium diphosphate are appropriate agents because they give rise to a negative ζ -potential. To focus on only one agent it was decided to use sodium hexametaphosphate for all further investigations. Only for the evaluation of the influence of opposite charged membrane and particle surfaces also 0.01 % SDS was used.

Hexametaphosphate gave also rise to similar negative ζ -potential between - 40 and -50 mV for other TiO₂ NP types such as the TiO₂ suspension provided by Sigma-Aldrich, or a photocatalytically active TiO₂ NP type with polyacrylate stabilization used e.g. in paints to generate a self-cleaning effect (Sachtleben HOMBİKAT UV 100 WP). Even the investigated polystyrene nanoparticles (PS 20 nm) showed a negative surface charge. Furthermore the in-

fluence of the pH on ζ -potential using hexametaphosphate was studied and showed little effect on the particle size or the ζ -potential of the Aeroxide® P25 NPs as shown in Figure 7.10 (the Sigma-Aldrich NPs did not get tested). The pH was adjusted by NaOH or HNO₃. The measurements were performed using a Zetasizer instrument. This makes sodium hexametaphosphate as a polyphosphate surfactant being supposed to be beneficial to achieve stable and reliable A4F conditions independent of the sample.

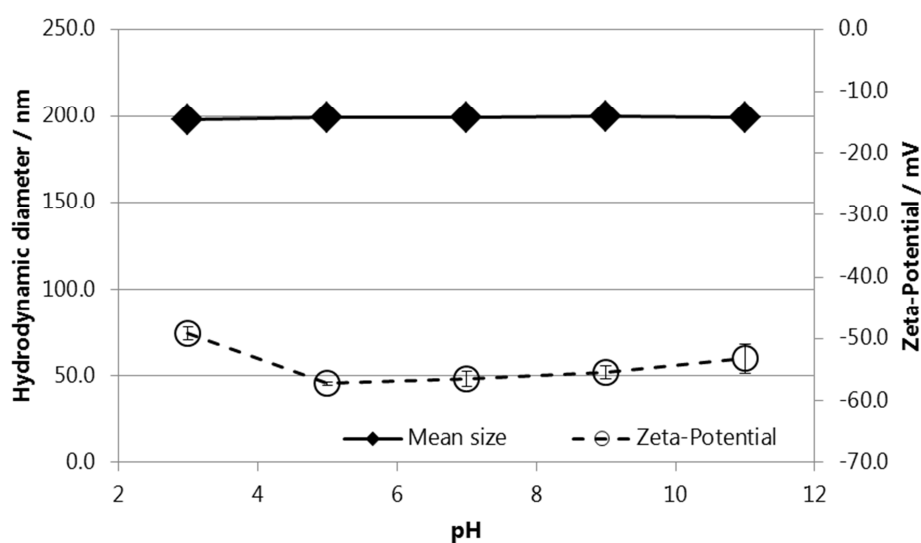


Figure 7.10: Stabilizing effect of sodium hexametaphosphate on the size and the ζ -potential of Aeroxide® P25 TiO₂ particles at different pH values.

Membrane-Particle Interactions: Based on the results from above an A4F method was developed using 1 mM sodium hexametaphosphate as suspension and as carrier medium. However, for a thorough evaluation of the proposed membrane-particle interactions, a 0.01 % SDS suspension was employed.

Adsorption of positively charged particles on negatively charged membranes: As mentioned above it is supposed that positively charged particles strongly attach to the negatively charged membrane. To examine this assumption titanium dioxide (Aeroxide® P25) was diluted either in 1 mM sodium hexametaphosphate or in 0.01 % SDS. The addition of these surfactants gave rise to a positive ζ -potential (30 mV) for the suspension in SDS with a TiO_2 concentration of 176 mg/L and a negative ζ -potential (- 45 mV) for the hexametaphosphate with a TiO_2 concentration of 32 mg/L. Both suspensions were injected into the A4F channel equipped with a RC 10 kDa membrane. As carrier fluid the same liquid was used as the sample was diluted in, resulting in a negative ζ -potential of the membrane for both sodium hexametaphosphate and SDS (see Figure 7.9a). The mean recovery rate of titanium dioxide analyzed in sodium hexametaphosphate is $23.5 \pm 4.7 \%$ ($n=3$). However the measurement in SDS resulted in a complete particle loss with a mean recovery rate of $0.03 \pm 0.02 \%$ ($n=3$). As the concentrations of the injected particles were rather high the results cannot be attributed to a sensitivity problem of the UV/Vis detector. Instead the findings support the interaction hypothesis and show that positively charged particles are likely to adsorb on a negatively charged membrane. As all the blanks measured did not show any signal at all, a remobilization of the particles after some runs can be excluded. On the contrary, the negatively charged TiO_2 NPs suspended in hexametaphosphate seem to experience enough repulsion force to prevent a strong interaction with the membrane and thus a deposition. Nevertheless, the low recovery rate of 23.5 % is attributed to the presence of large particles. Based on these results it is highly recommended to perform a ζ -potential screening for unknown samples and the membrane prior to measurements. Otherwise false-negative results might occur. Thus the hypothesis (A) is true: The A4F feasibility can be predicted based on the ζ -potential of the membrane and the NPs.

Modification of the separation based on the ζ -potential: The effect of the membrane's ζ -potential on the retention time of TiO_2 NPs was investigated to characterize the influence of the membrane material on the retention time. Aeroxide®P25 particles suspended in a 1 mM hexametaphosphate solution were investigated with different membrane materials (the Sigma-Aldrich NPs did not get tested). The resulting comparison of the retention times is displayed in Figure 7.11a demonstrates the effect of the membrane cutoff for regenerated cellulose membranes.

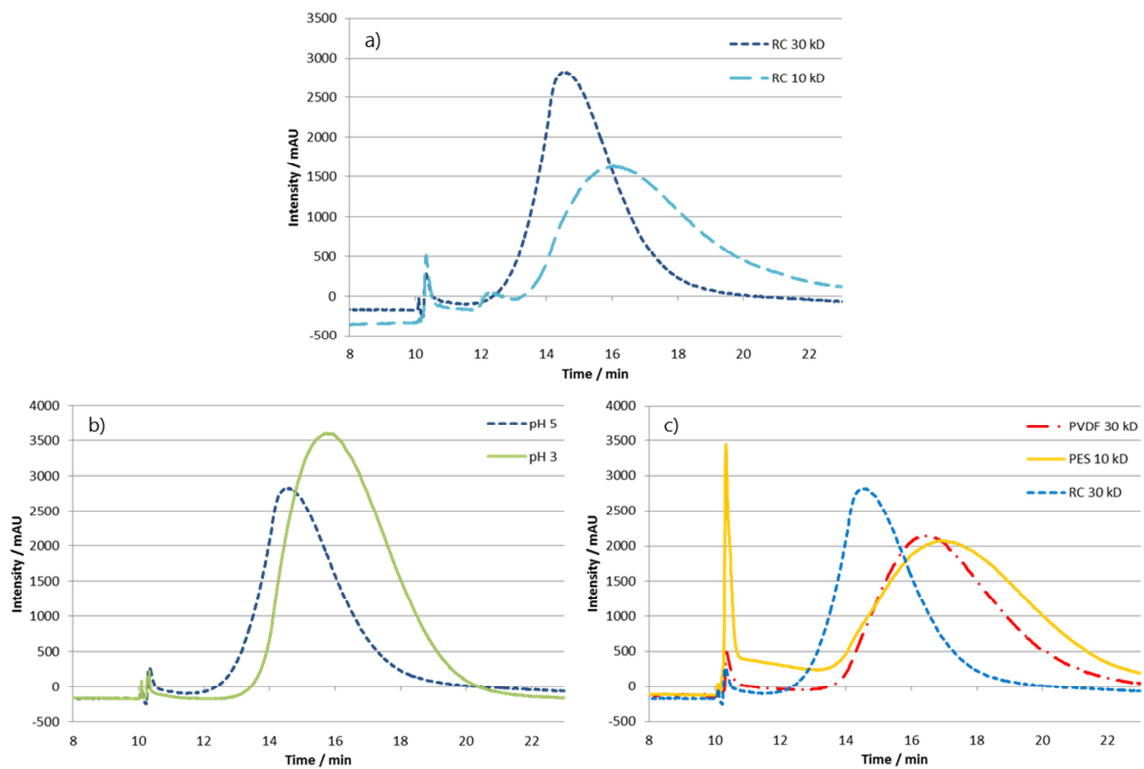


Figure 7.11: UV/Vis signals of retention time modification of TiO_2 NPs (Aeroxide® P25) on membranes. a) Effect of membrane cutoff (RC 10 kDa and RC 30 kDa, 1 mM sodium hexametaphosphate. b) Effect of pH (RC 10 kDa, pH 3 = 0.1 % MEAA, pH 5 = 1 mM sodium hexametaphosphate. c) Retention time of TiO_2 on different membrane materials with 1 mM sodium hexametaphosphate as carrier. The corresponding ζ -potentials are indicated.

As Fievet *et al* (Fievet, Szymczyk *et al.* 2000) already showed, the smaller the cutoff the less negatively charged the membrane. According to the theory proposed by Ulrich *et al*, (Ulrich, Losert *et al.* 2012) this should result in less repulsion and thus in a longer retention time which perfectly correlates with our findings. In Figure 7.11b the effect of the pH on the membrane ζ -potential is demonstrated. The lower the pH the less negatively charged is a membrane. This too correlates with the hypothesis and the findings of Fievet *et al* and Ulrich *et al.* (Fievet, Szymczyk *et al.* 2000, Ulrich, Losert *et al.* 2012)

Figure 7.11c presents the overlaid UV/Vis signals of TiO₂ on different membrane materials under identical conditions. The corresponding ζ -potentials show that no prediction of the retention time can be made based on these potentials. Obviously, some other membrane specific effects seem to influence the retention time of the NPs in the A4F channel. Most of the membrane materials currently used in A4F is mainly manufactured for other purposes, e.g. ultrafiltration. However, in A4F an ideal, parabolic, laminar flow profile is required to get a perfect separation of particles. Thus, the demand for a smooth and flat surface finishing of the membrane material is probably a critical task. But also the swelling behavior of the membranes might have a significant influence: The more a membrane expands in the liquid, the smaller the channel height gets which results in shorter elution time of the particles. Baalousha *et al* (Baalousha, Stolpe *et al.* 2011) state that also van der Waals, hydrophobic and charge interaction forces may cause the membrane-particle interactions and thus lead to shifted retention times on different membrane materials. Therefore, additional morphology investigations are planned.

Thus the hypothesis (B) that tuning of the separation efficiency can be directed by the ζ -potential is only partly true. The ζ -potential can be used for separation modifications within a given membrane material (cutoff, pH). But by changing the membrane material it cannot get

concluded from the ζ -potential on the separation efficiency. Obviously some membrane specific properties (e.g. swelling behavior, roughness, hydrophobicity) are then more dominant.

Size calculation based on the retention time: According to the A4F theory the retention time of a particle is solely dependent on the particle size. Assuming that some membrane-particle interactions take place in the channel this would probably also influence the retention time. To evaluate this hypothesis three particle types (Aeroxide® P25 TiO₂, Sigma-Aldrich TiO₂, PS 80 nm) were investigated with four different membrane materials (PES 10 kDa, RC 10 kDa, RC 30 kDa and PVDF 30 kDa). The measurement conditions were identical for all runs to allow a direct comparison of the retention behavior. The UV/Vis signals are plotted in Figure 7.12.

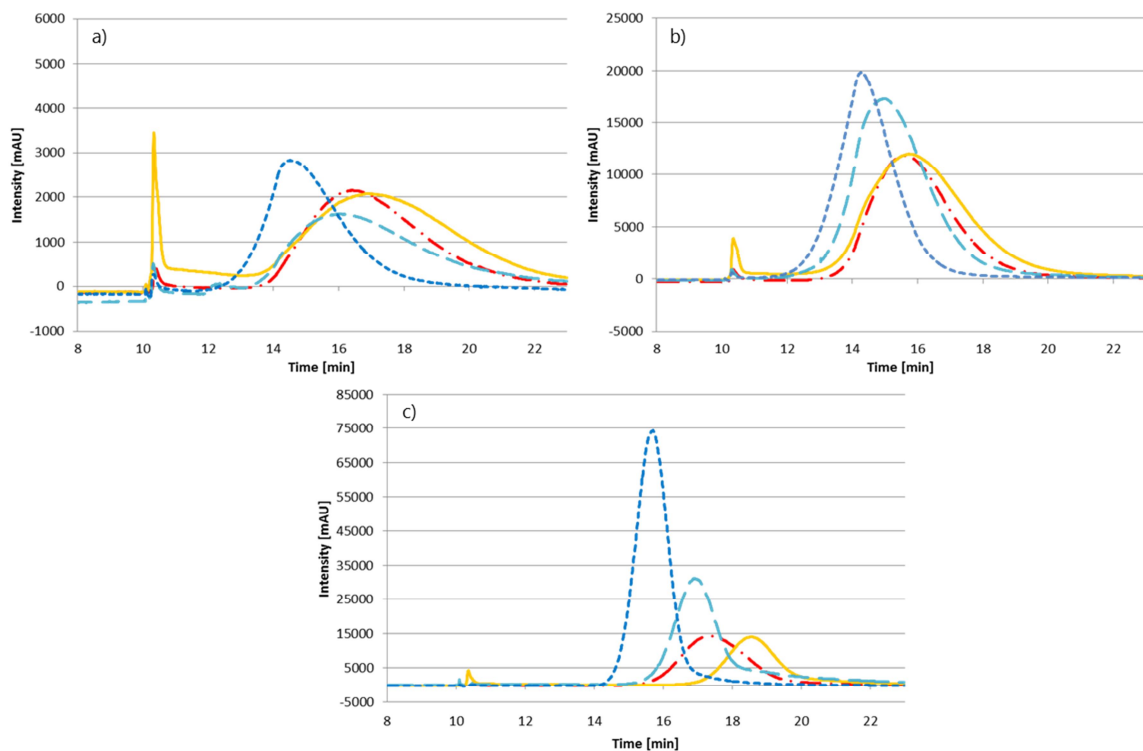


Figure 7.12: Overlaying UV/Vis signals for the injections of a) Aeroxide® P25 TiO₂, b) Sigma-Aldrich TiO₂ and c) a 80 nm PS standard for four different membrane types. All measurement conditions were identical.

Appendix

Depending on the membrane type the retention time for a specific particle type can vary within up to 3 minutes. This clearly indicates that the membrane material influences the behavior of the particle in the channel and thus the retention time. Therefore determining the particle size solely based on the retention time is questionable, especially when different particle types are used.

This effect has already been mentioned in the literature and several publications propose to perform a size calibration with particles of known diameters. (Dubascoux, Von Der Kammer et al. 2008, Nischwitz and Goenaga-Infante 2012) To check the applicability PS 20 nm, 80 nm, and 200 nm were injected on each of the membrane types and a quadratic regression (due to non-linear flow profile) was applied. With this calibration the particle sizes of TiO₂ NPs was calculated and compared to the measured diameters. The results are shown in Table 7.2.

Table 7.2: Summary on the measured and the calculated particle diameters (with MALS the radius of gyration and with DLS the hydrodynamic radius was analyzed).

Particle	Measured (n=3)		Calculated (n=1)			
	A4F-MALS / nm	DLS / nm	PES 10 kDa /nm	RC 10 kDa / nm	RC 30 kDa / nm	PVDF 30 kDa / nm
Aeroxide® P25	66.3 ± 5.2	99.8 ± 1.5	58	62	64	66
Sigma- Aldrich	48.6 ± 3.6	69 ± 1.0	48	47	55	49

The sizes calculated for the different membrane materials based on a polystyrene size calibration fit well with the measured size by MALS. As the elution program uses a non-linear gradient instead of an isocratic elution, the retention time of the particle sizes also shows a non-

linear relationship. Therefore it seems as if a size calibration with PS standard was appropriate to evaluate the particle sizes of TiO₂ NPs. Nevertheless, this has to be applied carefully. When adapting this size calibration on another type of nanoparticle the validity of the model should get checked prior to application. Further, a variation of 0.4 minutes of the elution times on different membrane batches was observed. Therefore, a size calibration should be performed daily to minimize the effect of these variations. As Gigault and Hackley (Gigault and Hackley 2013) showed, the particle density can also cause retention time shifts, especially in mixtures of different particle types. Although the effect is rather small it has to be taken into account for a correct size calibration. Hence, an additional size-determining method like light scattering techniques is recommended to avoid daily size calibration and to avoid the possible problem that other particle types may behave different to the size calibration standards. However, as already mentioned in the introduction chapter, the sensitivity ranges is in the mg/L range and especially static light scattering sometimes seems to show odd behavior for specific nanoparticle types. As Hagendorfer *et al* showed, Au NP's size cannot get determined by MALS as the particles show a strong scattering behavior which falsifies the diameter. (Hagendorfer, Kaegi et al. 2011)

The hypothesis (C) that the ζ -potential accounts for shifts in retention time was only partly evaluated. Since the ζ -potentials of the NPs were in a narrow range, their influence on retention time was not experimentally accessible. But the membranes used showed massive retention time shifts which impede the correct calculation of the particle size based on the retention time only. It remains unclear to which extend the retention times shifts are caused by different ζ -potential or other membrane specific properties.

Recovery Rate: Not only the retention time but also the recovery rate of NPs is potentially influenced by membrane-particle interactions. To evaluate this effect the influence of the particle size and the particle concentration on the recovery rate was evaluated. This was done by comparing the resulting area of the UV/Vis signal with the area of an injection without A4F channel. PS standards (20, 30, 40, 60, 100, 200 nm) at comparable concentrations were investigated with two different RC 10 kDa membrane types. All standards were injected separately and in triplicates. In Figure 7.13a the resulting recovery rates are plotted.

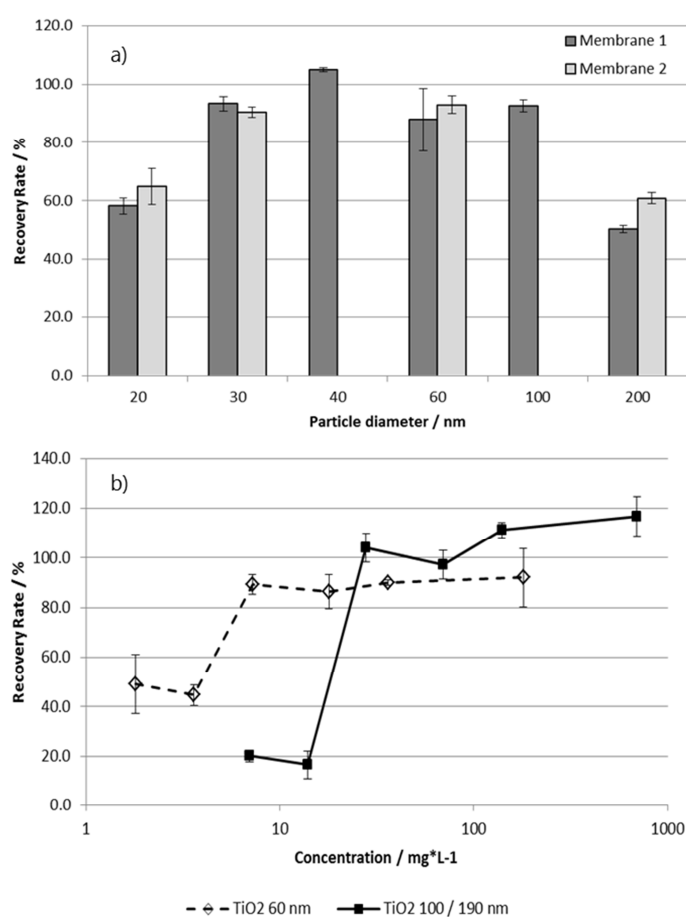


Figure 7.13: a) Recovery rate of PS particles of different sizes (20, 30, 40, 60, 100, 200 nm), measured on two RC membranes (same batch, but two different samples analyzed at two different days). b) Recovery rate of TiO₂ (Aeroxide® P25) for different dilutions. The size of the smaller TiO₂ particle sample was 60 nm (MALS) ◇ and the large sized sample ■ a polydisperse sample in a size range of 100 to 190 nm (MALS).

Especially the largest particles show a reduced recovery rate: This can be explained by the fact that the larger particles accumulate closest to the membrane and are thus more prone to interactions. To minimize this effect a reduction of the cross flow could be applied and would probably lead to an accumulation of larger particles in regions of the channel with higher flow and should result in a better recovery rate. Additionally, the smallest particles also show a reduced recovery rate. This can be explained by a non-ideal focusing of smaller particles due to a larger diffusion which may lead to a broadening of the peak and to some loss in the system.

To evaluate the concentration dependency of the recovery rate TiO_2 (Aeroxide® P25) samples of different diameters and concentrations were investigated. The TiO_2 sample was first centrifuged to obtain two size fractions: A small fraction with a main signal at a diameter of 60 nm and a large fraction with two main signals, one at 100 nm and one at 190 nm (analyzed by MALS) were recovered. These two fractions were investigated for 6 different dilution levels and the recovery rates were calculated. The results are displayed in Figure 7.13b. The recovery rates for the lower concentrations are poor, but it is worth mentioning that the lower signals may be attributed to the fact, that the dilution factor was relatively high and thus the resulting concentrations were close to the limits of detection of the UV/Vis instrument (estimated limit of detection is around 5 mg/L). Whether the probability of particle loss also increases for smaller concentrations needs to be further investigated. A certain size dependence on the recovery rate can be observed in this graph: The larger sized TiO_2 fraction shows a higher particle loss which correlates with the hypothesis that larger particles will equilibrate closer to the membrane. This is also consistent with the previous findings. The also achieved MALS signals support these observations.

When varying the injection volume of a sample the loss of large particles can be observed as well. An injection volume of 10 μL of the Aeroxide® P25 sample results in a size distribution of 45 – 100 nm, an injection volume of 50 μL of the same sample shows a size distribution of 41 – 158 nm (evaluated by A4F-MALS). This may on the one hand be attributed to the detection limit of the MALS, on the other hand it seems as if a fixed amount of the larger particles gets lost in the system. This makes the correct characterization of a sample challenging.

A comparison of the recovery rate for the two different TiO_2 NP types is displayed in Figure 7.14.

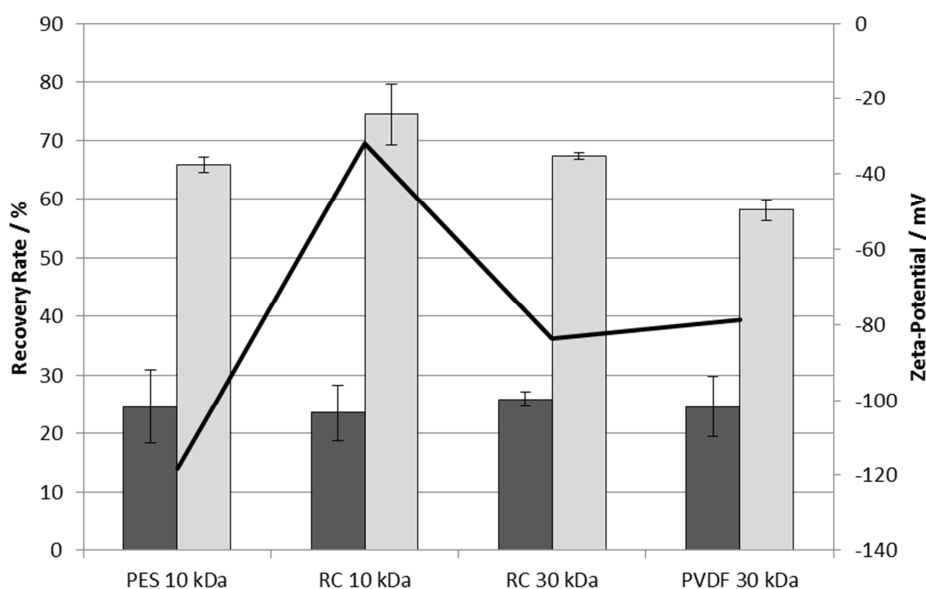


Figure 7.14: Recovery rate of TiO_2 NPs from different producers (suspended in 1 mM sodium hexametaphosphate). Injected on different membrane materials using 1 mM sodium hexametaphosphate as carrier fluid.

It is obvious, that the Aeroxide® P25 particles show consistently lower recovery rates than the Sigma-Aldrich particles independent from the used membrane material. As both samples show a similar ζ -potential, the electrostatic repulsion does not provide full explanation for the difference in the recovery rate. Also the ζ -potential of the membranes shows no obvious cor-

relation with the recovery rate of the different particle types. Whether a different surface chemistry or functionality is present could not be evaluated as no data were available from the manufacturer. The previously reported size depending recovery rate may give an explanation for this observation instead. The mean hydrodynamic diameter of the Aeroxide® P25 sample is larger than the one of the Sigma-Aldrich sample, same is the poly-dispersity determined in batch DLS (Aeroxide® P25 particles are 99.8 ± 1.5 nm with a PDI of 0.132, Sigma-Aldrich particles are 69 ± 1.0 nm with a PDI of 0.11). Therefore the larger particles present in the Aeroxide® P25 sample are possibly easier to adsorb on the membrane, resulting in a lower recovery rate whereas the smaller sized and more mono-disperse Sigma-Aldrich sample shows a better recovery rate.

Thus it was not possible to evaluate hypothesis (D) that the ζ -potential would determine the recovery rate: The varying recovery rates between different sample types tends to correlate with their particle size. Since the ζ -potential of the NPs was in a narrow range, their influence on the recovery rate was not experimentally accessible.

7.2.4 Summary and Conclusion

This study presents a systematic investigation of the membrane-particle interactions occurring in an A4F channel. Based on the hypothesis that the ζ -potential might be responsible for the attraction or repulsion between particles and the membrane, different aspects were evaluated. The findings can be used for a more straight-forward method development.

- All of the tested membrane materials under the tested conditions showed a negative ζ -potential.

- The TiO₂ NPs can show an either positive or negative ζ -potential depending on the suspending agent. When injecting a positively charged NP on a negatively charged membrane a total particle loss occurs: The A4F conditions must be selected carefully especially when developing multi-methods for different particle types.
- The retention time of a TiO₂ NP may vary within several minutes on different membrane materials. A prediction based on the ζ -potential is not applicable as no correlation between the magnitude of the potential and the retention time shift could be observed.
- These retention time shifts prevent the calculation of the size based on the retention time as usually applied in FFF. Instead a size calibration or even more the use of an online-MALS is highly recommended.
- The retention time behavior of the TiO₂ NPs within the same membrane material but with different conditions applied (cut-off, pH) can get predicted based on the ζ -potential.
- The recovery rate of a TiO₂ NP shows no correlation to the ζ -potential of a membrane. Instead the particle size is more determining: The larger the diameter the bigger the particle loss. This can also explain the different recovery rates found for two different TiO₂ NP samples.
- This size dependent particle loss has severe consequences for the particle characterization: Depending on the concentration and the injection volume a different size range might get obtained, as the large particles seem to get lost to a fixed amount.

Thus it can be concluded that the ζ -potential can be used to explain a part of the membrane-particle interactions, but not all of them. Other studies state that van der Waals forces, the

hydrophobicity of the membranes or the particle density also contribute to the effect (Baalousha, Stolpe et al. 2011, Gigault and Hackley 2013, Loeschner, Navratilova et al. 2013).

7.2.5 Outlook

Future studies should focus on the one hand on varying retention time depending on the membrane material and on the particle type. Morphological studies of the membranes could help to identify some of the effects. In particular the swelling behavior and the surface roughness, as well as the hydrophobicity of the membrane are worth being investigated. As first results (Gigault and Hackley 2013) show the particle density and the van der Waals forces contribute to the shifts as well and only by clearly knowing their role, the formula for the size calculation based on retention time can be adapted accordingly.

On the other hand future studies may focus on the varying recovery rates for different NPs, which tend to correlate with their particle size. Therefore the sink for the larger particles has to be determined. This could either be the irreversible adsorption on the membrane at the focus point or adsorption could happen on the entire surface of the membrane. The surface chemistry of the membrane and the particles could have an influence as well. Another important aspect for further studies to extent these findings to other particle types, too.

Media coverage for chapter 7.2 published as:

N. Bendixen, S. Losert, C. Adlhart, M. Lattuada, A. Ulrich, 2014, Membrane–particle interactions in an asymmetric flow field flow fractionation channel studied with titanium dioxide nanoparticles, *J. Chrom. A.*, 1334, 92–100.

7.3 General supplementary material

Media coverage for chapter 2, published as: S. Losert, N. von Goetz, C. Bekker, W. Fransman, S. W.P. Wijnhoven, C. Delmaar, K. Hungerbühler, A. Ulrich, 2014, Human exposure to conventional and nanoparticle containing sprays – a critical review, *Environ. Sci. Tech.*, 48 (10) 5366-5378.

Media coverage for chapter 3, published as: S. Losert, N. Bendixen, T. V. Ashworth, K. Hungerbühler, H. Hagendorfer, 2014, Evaluation of membrane zeta-potential and morphology on particle-membrane interaction in field-flow-fractionation analysis, *JAAS*, submitted.

Media coverage for chapter 5, published as: S. Losert, A. Hess, G. Ilari, N. von Goetz, K. Hungerbühler, 2014, Online characterization of the nano-aerosol released by commercial spray products using SMPS-ICPMS coupling, *J. Nanopart. Res.*, submitted.

Chapter 8

8 References

Akurati, K. K., A. Vital, J. P. Dellemann, K. Michalow, T. Graule, D. Fetti and A. Baiker (2008). "Flame-made WO₃/TiO₂ nanoparticles: Relation between surface acidity, structure and photocatalytic activity." Applied Catalysis B-Environmental **79**(1-2): 53-62.

Al-Kattan, A., A. Wichser, R. Vonbank, S. Brunner, A. Ulrich, S. Zuin and B. Nowack (2013). "Release of TiO₂ from paints containing pigment-TiO₂ or nano-TiO₂ by weathering." Environmental Sciences: Processes and Impacts **15**(12): 2186-2193.

Allen, N. S. E., Michele; Verran, Joanne; Stratton, John; Maltby, Julie; Bygott, Claire (2008). Photocatalytic Surfaces: Antipollution and Antimicrobial Effects. Nanotechnology. Volume 2: Environmental Aspects. H. F. Krug. Weinheim, Wiley-VCH: 317. 978-3-527-31735-6

Aschberger, K., H. J. Johnston, V. Stone, R. J. Aitken, C. L. Tran, S. M. Hankin, S. A. K. Peters and F. M. Christensen (2010). "Review of fullerene toxicity and exposure – Appraisal of a human health risk assessment, based on open literature." Regulatory Toxicology and Pharmacology **58**(3): 455-473.

ASTM (2010). "ASTM D4336-054 : Standard test method for determination of the output per strokes of a mechanical pump dispenser."

ASTM (2010). "ASTM Designation: D4532 – 10: Standard Test Method for Respirable Dust in Workplace Atmospheres Using Cyclone Samplers."

ASTM (2012). "ASTM 2456-06 Standard Terminology Relating to Nanotechnology."

ASTM (2012). "ASTM D6062 – 07: Standard Guide for Personal Samplers of Health-Related Aerosol Fractions."

Baalousha, M., B. Stolpe and J. R. Lead (2011). "Flow field-flow fractionation for the analysis and characterization of natural colloids and manufactured nanoparticles in environmental systems: A critical review." Journal of Chromatography A **1218**(27): 4078-4103.

Bammes, G. (2001). Studien zur Gestalt des Menschen : eine Zeichenschule zur Künstleranatomie mit Arbeiten von Laienkünstlern, Kunstpädagogen und Kunststudenten. Leipzig Seemann

References

Bekker, C., Brouwer, D.H., van Duuren-Stuurman, B., Tuinman, I.L., Tromp, P., and Fransman, W. (2014). "Airborne manufactured nano-objects released from commercially available spray products: Temporal and spatial influences." Journal of Exposure Science and Environmental Epidemiology **24**: 74-81.

Bendixen, N., S. Losert, C. Adlhart, M. Lattuada and A. Ulrich (2014). "Membrane-Particle Interactions in an Asymmetric Flow Field Flow Fractionation Channel Studied With Titanium Dioxide Nanoparticles." Journal of Chromatography A(1334): 92-100.

Benn, T., B. Cavanagh, K. Hristovski, J. D. Posner and P. Westerhoff (2010). "The Release of Nanosilver from Consumer Products Used in the Home." Journal of Environmental Quality **39**(6): 1875-1882.

Berger-Preiß, E., A. Boehncke, G. Könnecker, I. Mangelsdorf, D. Holthenrich and W. Koch (2005). "Inhalational and dermal exposures during spray application of biocides." International Journal of Hygiene and Environmental Health **208**(5): 357-372.

Berger-Preiß, E., S. Gerling, H. Kock and K. E. Appel (2006). "Investigations in the passenger cabin during application of biocides for disinsection." Gefahrstoffe, Reinhaltung der Luft **66**(3): 116-119.

Berger-Preiß, E., W. Koch, W. Behnke, S. Gerling, H. Kock, L. Elflein and K. E. Appel (2004). "In-flight spraying in aircrafts: Determination of the exposure scenario." International Journal of Hygiene and Environmental Health **207**(5): 419-430.

Berger-Preiß, E., W. Koch, S. Gerling, H. Kock and K. E. Appel (2009). "Use of biocidal products (insect sprays and electro-vaporizer) in indoor areas - Exposure scenarios and exposure modeling." International Journal of Hygiene and Environmental Health **212**(5): 505-518.

Berger-Preiß, E., W. Koch, S. Gerling, H. Kock, J. Klasen, G. Hoffmann and K. E. Appel (2006). "Aircraft disinsection: Exposure assessment and evaluation of a new pre-embarkation method." International Journal of Hygiene and Environmental Health **209**(1): 41-56.

Berlin, K., et al. (2011). "Endbericht zu den Forschungsprojekten NanoExpo und NanoGesund."

BgVV (2000). "Organozinnverbindungen in Imprägniermitteln für Lederwaren und Textilien." Bundesinstitut für gesundheitlichen Verbraucherschutz und Veterinärmedizin. Retrieved 03.09.2014, from http://www.bfr.bund.de/cm/343/organozinnverbindungen_in_impraegniermitteln_fuer_lederwaren_und_textilien.pdf.

References

Bierman, A. (1955). "Electrostatic forces between nonidentical colloidal particles." Journal of Colloid Science **10**(3): 231-245.

Bolea, E., J. Jiménez-Lamana, F. Laborda and J. R. Castillo (2011). "Size characterization and quantification of silver nanoparticles by asymmetric flow field-flow fractionation coupled with inductively coupled plasma mass spectrometry." Analytical and Bioanalytical Chemistry: 1-10.

Brzeziński, S., G. Malinowska, D. Kowalczyk, A. Kaleta, B. Borak, M. Jasiorski, K. Dabek, A. Baszczuk and A. Tracz (2012). "Antibacterial and fungicidal coating of textile-polymeric materials filled with bioactive nano-and submicro-particles." Fibres and Textiles in Eastern Europe **90**(1): 70-77.

Bucking, W. and T. Nann (2006). "Electrophoretic analysis of gold nanoparticles: size-dependent electrophoretic mobility of nanoparticles." IEE Proceedings - Nanobiotechnology **153**(3): 47-53.

Buecking, W. (2006). Untersuchung von mesoskopischen Eigenschaften von Nanopartikeln mit elektroanalytischen Methoden. Dissertation zur Erlangung des Doktorgrades der Fakultät für Angewandte Wissenschaften. Freiburg im Breisgau, Albert-Ludwigs-Universität Freiburg im Breisgau. **PhD thesis**.

Cajlakovic, M., A. Lobnik and T. Werner (2002). "Stability of new optical pH sensing material based on cross-linked poly(vinyl alcohol) copolymer." Analytica Chimica Acta **455**(2): 207-213.

Causserand, C., M. Nyström and P. Aimar (1994). "Study of streaming potentials of clean and fouled ultrafiltration membranes." Journal of Membrane Science **88**(2-3): 211-222.

Chen, B. T., A. Afshari, S. Stone, M. Jackson, D. Schwegler-Berry, D. G. Frazer, V. Castranova and T. A. Thomas (2010). "Nanoparticles-containing spray can aerosol: Characterization, exposure assessment, and generator design." Inhalation Toxicology **22**(13): 1072-1082.

Chen, X. and H. J. Schluesener (2008). "Nanosilver: A nanoproduct in medical application." Toxicology Letters **176**(1): 1-12.

Class, T. J. and J. Kintrup (1991). "Pyrethroids as household insecticides: analysis, indoor exposure and persistence." Fresenius' Journal of Analytical Chemistry **340**(7): 446-453.

Contado, C. and A. Pagnoni (2008). "TiO₂ in commercial sunscreen lotion: Flow field-flow fractionation and ICP-AES together for size analysis." Analytical Chemistry **80**(19): 7594-7608.

References

Dang, Y., Y. Zhang, L. Fan, H. Chen and M. Roco (2010). "Trends in worldwide nanotechnology patent applications: 1991 to 2008." Journal of Nanoparticle Research **12**(3): 687-706.

Degueldre, C. and P. Y. Favarger (2004). "Thorium colloid analysis by single particle inductively coupled plasma-mass spectrometry." Talanta **62**(5): 1051-1054.

Degueldre, C., P. Y. Favarger and C. Bitea (2004). "Zirconia colloid analysis by single particle inductively coupled plasma-mass spectrometry." Analytica Chimica Acta **518**(1-2): 137-142.

Degueldre, C., P. Y. Favarger, R. Rossé and S. Wold (2006). "Uranium colloid analysis by single particle inductively coupled plasma-mass spectrometry." Talanta **68**(3): 623-628.

Degueldre, C., P. Y. Favarger and S. Wold (2006). "Gold colloid analysis by inductively coupled plasma-mass spectrometry in a single particle mode." Analytica Chimica Acta **555**(2): 263-268.

Delay, M. and F. H. Frimmel (2012). "Nanoparticles in aquatic systems." Analytical and Bioanalytical Chemistry **402**(2): 583-592.

DIN (2012). DIN 33899-1: Workplace exposure – Guide for the use of direct-reading instruments for aerosol monitoring – Part 1: Choice of monitor for specific applications (Draft)

DIN (2012). "DIN 33899-2: Workplace exposure – Guide for the use of direct-reading instruments for aerosol monitoring – Part 2: Evaluation of airborne particle concentrations using optical particle counters (Draft)."

Dubascoux, S., I. Le Hecho, M. Hasselov, F. Von der Kammer, M. P. Gautier and G. Lespes (2010). "Field-flow fractionation and inductively coupled plasma mass spectrometer coupling: History, development and applications." Journal of Analytical Atomic Spectrometry **25**(5): 613-623.

Dubascoux, S., F. Von Der Kammer, I. Le Hécho, M. P. Gautier and G. Lespes (2008). "Optimisation of asymmetrical flow field flow fractionation for environmental nanoparticles separation." Journal of Chromatography A **1206**(2): 160-165.

Dulog, L. and T. Schauer (1996). "Field flow fractionation for particle size determination." Progress in Organic Coatings **28**(1): 25-31.

References

ECHA (2008). "Guidance on information requirements and chemical safety assessment " Consumer exposure estimation: Version 1.1 Chapter R.15 http://guidance.echa.europa.eu/docs/guidance_document/information_requirements_en.htm.

EPA (2009). Nanoscale Materials Stewardship Program Interim Report of the U.S. Environmental Protection Agency Office of Pollution Prevention and Toxics (EPA).

EPA (2010). State of the Science Literature Review: Nano Titanium Dioxide Environmental Matters.

EU (2009). "Kosmetik-Verordnung " (EG) No. 1223/2009. Retrieved 12.06.2014, from <http://eur-lex.europa.eu/LexUriServ/LexUriServ.do?uri=OJ:L:2009:342:0059:0209:DE:PDF>.

Fierz, M., M. G. C. Vernooij and H. Burtcher (2007). "An improved low-flow thermodenuder." Journal of Aerosol Science **38**(11): 1163-1168.

Fievet, P., A. Szymczyk, B. Aoubiza and J. Pagetti (2000). "Evaluation of three methods for the characterisation of the membrane-solution interface: Streaming potential, membrane potential and electrolyte conductivity inside pores." Journal of Membrane Science **168**(1-2): 87-100.

FORS (2007). "COMPASS, Swiss Health Survey 2007 (SHS)." Retrieved 08.12.2014, from http://compass-data.unil.ch/webview/index/en/compass/Data-from-the-swiss-public-statistic.c.COMPASS/Health-Survey.d.11/Swiss-Health-Survey-2007-SHS-.s.ESSSGB-2007-072012/Gesundheitszustand.h.7/K-rpermasse- -Schwanger.h.29/K-rpergr-sse-cm- /fVariable/ESSSGB-2007-072012_V760.

Frens, G. (1973). "Controlled nucleation for regulation of particle-size in monidisperse gold suspensions." Nature-Physical Science **241**(105): 20-22.

Fujitani, Y., T. Kobayashi, K. Arashidani, N. Kunugita and K. Suemura (2008). "Measurement of the physical properties of aerosols in a fullerene factory for inhalation exposure assessment." Journal of occupational and environmental hygiene **5**(6): 380-389.

Ganguly, K., et al. (2011). "Impaired resolution of inflammatory response in the lungs of JF1/Msf mice following carbon nanoparticle instillation." Respiratory Research **12**.

Geranio, L., M. Heuberger and B. Nowack (2009). "The Behavior of Silver Nanotextiles during Washing." Environmental Science & Technology **43**(21): 8113-8118.

References

Giddings, J. C. (1973). "The conceptual basis of field-flow fractionation." Journal of Chemical Education **50**(10): 667-null.

Gigault, J. and V. A. Hackley (2013). "Observation of size-independent effects in nanoparticle retention behavior during asymmetric-flow field-flow fractionation." Analytical and Bioanalytical Chemistry **405**(19): 6251-6258.

Gold, R. E., T. Holcslaw, D. Tupy and J. B. Ballard (1984). "Dermal and respiratory exposure to applicators and occupants of residences treated with dichlorvos (DDVP)." Journal of Economic Entomology **77**(2): 430-436.

Gold, R. E., J. R. C. Leavitt, T. Holcslaw and D. Tupy (1982). "Exposure of urban applicators to carbaryl." Archives of Environmental Contamination and Toxicology **11**(1): 63-67.

González-Domínguez, R., T. García-Barrera and J. L. Gómez-Ariza (2014). "Characterization of metal profiles in serum during the progression of Alzheimer's disease." Metallomics **6**(2): 292-300.

Gottschalk, F. and B. Nowack (2011). "The release of engineered nanomaterials to the environment." Journal of Environmental Monitoring **13**(5): 1145-1155.

Graf, B. W., E. J. Chaney, M. Marjanovic, M. De Lisio, M. C. Valero, M. D. Boppart and S. A. Boppart (2013). "In vivo imaging of immune cell dynamics in skin in response to zinc-oxide nanoparticle exposure." Biomedical Optics Express **4**(10): 1817-1828.

Grieneisen, M. L. and M. Zhang (2011). "Nanoscience and nanotechnology: Evolving definitions and growing footprint on the scientific landscape." Small **7**(20): 2836-2839.

Gschwind, S., L. Flamigni, J. Koch, O. Borovinskaya, S. Groh, K. Niemax and D. Gunther (2011). "Capabilities of inductively coupled plasma mass spectrometry for the detection of nanoparticles carried by monodisperse microdroplets." Journal of Analytical Atomic Spectrometry **26**(6): 1166-1174.

Hagendorfer, H. (2011). New analytical methods for size fractionated-, quantitative-, and element specific analysis of metallic engineered nanoparticles in aerosols and dispersions (PhD thesis) La faculté de l'environnement naturel, architectural et construit (ENAC). Lausanne Empa Swiss Federal Laboratories for Material Science and Technology and EPFL **PHD**.

References

Hagendorfer, H., R. Kaegi, M. Parlinska, B. Sinnet, C. Ludwig and A. Ulrich (2012). "Characterization of silver nanoparticle products using asymmetric flow field flow fractionation with a multidetector approach - A comparison to transmission electron microscopy and batch dynamic light scattering." Analytical Chemistry **84**(6): 2678-2685.

Hagendorfer, H., R. Kaegi, J. Traber, S. F. Mertens, R. Scherrers, C. Ludwig and A. Ulrich (2011). "Application of an asymmetric flow field flow fractionation multi-detector approach for metallic engineered nanoparticle characterization - Prospects and limitations demonstrated on Au nanoparticles." Analytica Chimica Acta **706**(2): 367-378.

Hagendorfer, H., C. Lorenz, R. Kaegi, B. Sinnet, R. Gehrig, N. Goetz, M. Scheringer, C. Ludwig and A. Ulrich (2010). "Size-fractionated characterization and quantification of nanoparticle release rates from a consumer spray product containing engineered nanoparticles." Journal of Nanoparticle Research **12**(7): 2481-2494.

Hall, B., W. Steiling, B. Safford, M. Coroama, S. Tozer, C. Firmani, C. McNamara and M. Gibney (2011). "European consumer exposure to cosmetic products, a framework for conducting population exposure assessments Part 2." Food and Chemical Toxicology **49**(2): 408-422.

Hall, B., S. Tozer, B. Safford, M. Coroama, W. Steiling, M. C. Leneuve-Duchemin, C. McNamara and M. Gibney (2007). "European consumer exposure to cosmetic products, a framework for conducting population exposure assessments." Food and Chemical Toxicology **45**(11): 2097-2108.

Hamaker, H. C. (1937). The London-van der Waals Attraction between Spherical Particles. Physica, Nr. 4, : 1058–1072.

Hartmann, R. L. and S. K. R. Williams (2002). "Flow field-flow fractionation as an analytical technique to rapidly quantitate membrane fouling." Journal of Membrane Science **209**(1): 93-106.

Hassellöv, M., J. W. Readman, J. F. Ranville and K. Tiede (2008). "Nanoparticle analysis and characterization methodologies in environmental risk assessment of engineered nanoparticles." Ecotoxicology **17**(5): 344-361.

Hess, A., M. Tarik and C. Ludwig (2014). "A Hyphenated SMPS-ICPMS Coupling Setup: Size-Resolved Element-Specific Analysis of Airborne Nanoparticles." Journal of Aerosol Science: submitted.

References

Hirn, S., et al. (2011). "Particle size-dependent and surface charge-dependent biodistribution of gold nanoparticles after intravenous administration." European Journal of Pharmaceutics and Biopharmaceutics **77**(3): 407-416.

Hueglin, C., L. Scherrer and H. Burtscher (1997). "An accurate, continuously adjustable dilution system (1:10 to 1:104) for submicron aerosols." Journal of Aerosol Science **28**(6): 1049-1055.

ISO (2008). "ISO/TS 27687: Nanotechnologies - Terminology and definitions for nano objects - nanoparticle, nanofibre and nanoplate."

ISO, D. E. (2010). "DIN EN ISO 10808:2010: Nanotechnologies – Characterization of nanoparticles in inhalation exposure chambers for inhalation toxicity testing."

ISO/TR (2007). "ISO/TR 27628:Workplace atmospheres – Ultrafine, nanoparticle and nanostructured aerosols – Inhalation exposure characterization and assessment ".

Jankovic, J. T., M. A. Hall, T. L. Zontek, S. M. Hollenbeck and B. R. Ogle (2010). "Particle loss in a scanning mobility particle analyzer sampling extension tube." International Journal of Occupational and Environmental Health **16**(4): 429-433.

Jiang, J., G. Oberdörster and P. Biswas (2009). "Characterization of size, surface charge, and agglomeration state of nanoparticle dispersions for toxicological studies." Journal of Nanoparticle Research **11**(1): 77-89.

Kaegi, R., B. Sinnet, S. Zuleeg, H. Hagendorfer, E. Mueller, R. Vonbank, M. Boller and M. Burkhardt (2010). "Release of silver nanoparticles from outdoor facades." Environmental Pollution **158**(9): 2900-2905.

Kaegi, R., et al. (2008). "Synthetic TiO₂ nanoparticle emission from exterior facades into the aquatic environment." Environmental Pollution **156**(2): 233-239.

Kammer, F. V. D., M. Baborowski and K. Friese (2005). "Field-flow fractionation coupled to multi-angle laser light scattering detectors: Applicability and analytical benefits for the analysis of environmental colloids." Analytica Chimica Acta **552**(1-2): 166-174.

Kammer, F. v. d., S. Legros, T. Hofmann, E. H. Larsen and K. Loeschner (2011). "Separation and characterization of nanoparticles in complex food and environmental samples by field-flow fractionation." TrAC Trends in Analytical Chemistry **30**(3): 425-436.

References

Kassalainen, G. E. (2012). "Assessing Protein-Ultrafiltration Membrane Interactions Using Flow Field-Flow Fractionation." 23-36.

Kittler, S. (2009). Synthese, Löslichkeit und biologische Aktivität von Silber-Nanopartikeln. Institut für Anorganische Chemie, Universität Duisburg-Essen. **PhD**.

Kittler, S., C. Greulich, M. Köller and M. Epple (2009). "Synthesis of PVP-coated silver nanoparticles and their biological activity towards human mesenchymal stem cells." Materialwissenschaft und Werkstofftechnik **40**(4): 258-264.

Koch, W., W. Dunkhorst and H. Lodding (1999). "Design and performance of a new personal aerosol monitor." Aerosol Science and Technology **31**(2-3): 231-246.

Kreyling, W. G., M. Semmler-Behnke and W. Möller (2006). "Ultrafine particle - Lung interactions: Does size matter?" Journal of Aerosol Medicine: Deposition, Clearance, and Effects in the Lung **19**(1): 74-83.

Krug, H. F. and P. Wick (2011). "Nanotoxicology: An interdisciplinary challenge." Angewandte Chemie - International Edition **50**(6): 1260-1278.

Krystek, P., A. Ulrich, C. C. Garcia, S. Manohar and R. Ritsema (2011). "Application of plasma spectrometry for the analysis of engineered nanoparticles in suspensions and products." Journal of Analytical Atomic Spectrometry **26**(9): 1701-1721.

Kuhlbusch, T., C. Asbach, H. Fissan, D. Gohler and M. Stintz (2011). "Nanoparticle exposure at nanotechnology workplaces: A review." Particle and Fibre Toxicology **8**(1): 22.

Kuhlbusch, T. A. J. and H. Fissan (2006). "Particle characteristics in the reactor and pelletizing areas of carbon black production." Journal of occupational and environmental hygiene **3**(10): 558-567.

Kuhlbusch, T. A. J., S. Neumann and H. Fissan (2004). "Number size distribution, mass concentration, and particle composition of PM1 PM2.5, and PM10 in bag filling areas of carbon black production." Journal of occupational and environmental hygiene **1**(10): 660-671.

Kwon, S., M. Fan, A. T. Cooper and H. Yang (2008). "Photocatalytic applications of micro- and nano-TiO₂ in environmental engineering." Critical Reviews in Environmental Science and Technology **38**(3): 197-226.

References

Laborda, F., J. Jimenez-Lamana, E. Bolea and J. R. Castillo (2011). "Selective identification, characterization and determination of dissolved silver(I) and silver nanoparticles based on single particle detection by inductively coupled plasma mass spectrometry." Journal of Analytical Atomic Spectrometry **26**(7): 1362-1371.

Leipert, C. and H. Nirschl (2011). "Untersuchung der Reinigungsfähigkeit von Filtergeweben aus Polymeren." F & S Filtrieren und Separieren **25** (5): 270-277.

Li, J. X., J. H. Xu, W. L. Dai and K. N. Fan (2009). "Dependence of Ag Deposition Methods on the Photocatalytic Activity and Surface State of TiO₂ with Twistlike Helix Structure." Journal of Physical Chemistry C **113**(19): 8343-8349.

Lioy, P. J., Y. Nazarenko, T. W. Han, M. J. Lioy and G. Mainelis (2010). "Nanotechnology and exposure science: What is needed to fill the research and data gaps for consumer products." International Journal of Occupational and Environmental Health **16**(4): 378-387.

Liu, J., J. Andya and S. Shire (2006). "A critical review of analytical ultracentrifugation and field flow fractionation methods for measuring protein aggregation." The AAPS Journal **8**(3): E580-E589.

Llewellyn, D. M., A. Brazier, R. Brown, J. Cocker, M. L. Evans, J. Hampton, B. P. Nutley and J. White (1996). "Occupational exposure to permethrin during its use as a public hygiene insecticide." Annals of Occupational Hygiene **40**(5): 499-509.

Loeschner, K., J. Navratilova, C. Købler, K. Mølhave, S. Wagner, F. Von Der Kammer and E. H. Larsen (2013). "Detection and characterization of silver nanoparticles in chicken meat by asymmetric flow field flow fractionation with detection by conventional or single particle ICP-MS." Analytical and Bioanalytical Chemistry **405**(25): 8185-8195.

Loeschner, K., J. Navratilova, S. Legros, S. Wagner, R. Grombe, J. Snell, F. von der Kammer and E. H. Larsen (2013). "Optimization and evaluation of asymmetric flow field-flow fractionation of silver nanoparticles." Journal of Chromatography A **1272**: 116-125.

Lorenz, C. (2010). Human Exposure to Engineered Nanoparticles in Consumer Products; Diss ETH No. 19195, ETH ZURICH.

Lorenz, C., H. Hagendorfer, N. von Goetz, R. Kaegi, R. Gehrig, A. Ulrich, M. Scheringer and K. Hungerbühler (2011). "Nanosized aerosols from consumer sprays: experimental analysis and exposure modeling for four commercial products." Journal of Nanoparticle Research **13**(8): 3377-3391.

References

Lorenz, C., L. Windler, N. von Goetz, R. P. Lehmann, M. Schuppler, K. Hungerbühler, M. Heuberger and B. Nowack (2012). "Characterization of silver release from commercially available functional (nano)textiles." Chemosphere **89**(7): 817-824.

Losert, S., N. von Goetz, C. Bekker, W. Fransman, S. W. P. Wijnhoven, C. Delmaar, K. Hungerbuhler and A. Ulrich (2014). "Human Exposure to Conventional and Nanoparticle-Containing Sprays—A Critical Review." Environmental Science & Technology **48**(10): 5366-5378.

Madaeni, S. S. and Y. Mansourpanah (2004). "Chemical cleaning of reverse osmosis membranes fouled by whey." Desalination **161**(1): 13-24.

Malvern (2004). "Zetasizer Nano Series User Manual." Malvern Instruments.

Methner, M., L. Hodson, A. Dames and C. Geraci (2010). "Nanoparticle Emission Assessment Technique (NEAT) for the identification and measurement of potential inhalation exposure to engineered nanomaterials--Part B: Results from 12 field studies." Journal of occupational and environmental hygiene **7**(3): 163-176.

Mitrano, D. M., E. K. Leshner, A. Bednar, J. Monserud, C. P. Higgins and J. F. Ranville (2012). "Detecting nanoparticulate silver using single-particle inductively coupled plasma-mass spectrometry." Environmental Toxicology and Chemistry **31**(1): 115-121.

NanoHouse-Consortium (2010 - 2013). "NanoHouse EU FP7 Project No. 247810." Retrieved 01.09.2012, from <http://www-nanohouse.cea.fr/>.

Nazarenko, Y., T. W. Han, P. J. Liroy and G. Mainelis (2011). "Potential for exposure to engineered nanoparticles from nanotechnology-based consumer spray products." Journal of Exposure Science and Environmental Epidemiology **21**(5): 515-528.

Neubauer, E., F. V.d. Kammer and T. Hofmann (2011). "Influence of carrier solution ionic strength and injected sample load on retention and recovery of natural nanoparticles using Flow Field-Flow Fractionation." Journal of Chromatography A **1218**(38): 6763-6773.

Nischwitz, V. and H. Goenaga-Infante (2012). "Improved sample preparation and quality control for the characterisation of titanium dioxide nanoparticles in sunscreens using flow field flow fractionation on-line with inductively coupled plasma mass spectrometry." J. Anal. At. Spectrom.

References

NIST (2010). "NIST PCC-7: Measuring the size of nanoparticles using transmission electron microscopy (TEM) ".

NIST (2011). "NIST PCC-15: Measuring the size of colloidal gold nanoparticles using high-resolution scanning electron microscopy ".

Nørgaard, A. W., C. Janfelt, M. Benassi, P. Wolkoff and F. R. Lauritsen (2011). "Nebulization ionization and desorption ionization analysis of reactive organofunctionalized silanes in nanofilm products." Journal of Mass Spectrometry **46**(4): 402-410.

Nørgaard, A. W., K. A. Jensen, C. Janfelt, F. R. Lauritsen, P. A. Clausen and P. Wolkoff (2009). "Release of VOCs and particles during use of nanofilm spray products." Environmental Science and Technology **43**(20): 7824-7830.

Nørgaard, A. W., S. T. Larsen, M. Hammer, S. S. Poulsen, K. A. Jensen, G. D. Nielsen and P. Wolkoff (2010). "Lung damage in mice after inhalation of nanofilm spray products: The role of perfluorination and free hydroxyl groups." Toxicological Sciences **116**(1): 216-224.

Nørgaard, A. W., P. Wolkoff and F. R. Lauritsen (2010). "Characterization of nanofilm spray products by mass spectrometry." Chemosphere **80**(11): 1377-1386.

Nyström, M., A. Pihlajamäki and N. Ehsani (1994). "Characterization of ultrafiltration membranes by simultaneous streaming potential and flux measurements." Journal of Membrane Science **87**(3): 245-256.

OECD (2009). "OECD 403: Test Guideline 403: Acute Inhalation Toxicity ".

OECD (2009). "OECD 412: Test Guideline 412: Subacute Inhalation toxicity: 28-Day Study."

OECD (2009). "OECD 413: Test Guideline 413: Subchronic inhalation toxicity: 90-Day Study ".

OECD (2013). "OECD Website related to nanomaterials <http://www.oecd.org/env/ehs/>." from <http://www.oecd.org/env/ehs/>.

Oomen, A., M. Bennink, J. v. Engelen and A. Sips (2011, 2011). "Nanomaterials in consumer products - Detection, characterization and interpretation." Retrieved 12.06.2013, from <http://www.rivm.nl/bibliotheek/rapporten/320029001.html>.

References

Ottofuelling, S., F. Von Der Kammer and T. Hofmann (2011). "Commercial Titanium Dioxide Nanoparticles in Both Natural and Synthetic Water: Comprehensive Multidimensional Testing and Prediction of Aggregation Behavior." Environmental Science & Technology **45**(23): 10045-10052.

Park, J., B. K. Kwak, E. Bae, J. Lee, Y. Kim, K. Choi and J. Yi (2009). "Characterization of exposure to silver nanoparticles in a manufacturing facility." Journal of Nanoparticle Research **11**(7): 1705-1712.

Parsegian, V. A. (2006). Van Der Waals Forces. A Handbook for Biologists, Chemists, Engineers, and Physicists, Cambridge University Pr., Cambridge

Poda, A. R., A. J. Bednar, A. J. Kennedy, A. Harmon, M. Hull, D. M. Mitrano, J. F. Ranville and J. Steevens (2011). "Characterization of silver nanoparticles using flow-field flow fractionation interfaced to inductively coupled plasma mass spectrometry." Journal of Chromatography A **1218**(27): 4219-4225.

Quadros, M. E. and L. C. Marr (2011). "Silver nanoparticles and total aerosols emitted by nanotechnology-related consumer spray products." Environmental Science and Technology **45**(24): 10713-10719.

Radecka, M., M. Rekas, E. Kusior, K. Zakrzewska, A. Heel, K. A. Michalow and T. Graule (2010). "TiO₂-Based Nanopowders and Thin Films for Photocatalytical Applications." Journal of Nanoscience and Nanotechnology **10**(2): 1032-1042.

Ricq, L., A. Pierre, S. Bayle and J. C. Reggiani (1997). "Electrokinetic characterization of polyethersulfone UF membranes." Desalination **109**(3): 253-261.

Robichaud, C. O., A. E. Uyar, M. R. Darby, L. G. Zucker and M. R. Wiesner (2009). "Estimates of upper bounds and trends in nano-TiO₂ production as a basis for exposure assessment." Environmental Science and Technology **43**(12): 4227-4233.

Roda, B., A. Zattoni, P. Reschiglian, M. H. Moon, M. Mirasoli, E. Michelini and A. Roda (2009). "Field-flow fractionation in bioanalysis: A review of recent trends." Analytica Chimica Acta **635**(2): 132-143.

Roessner, D. Field Flow Fractionation - Basics and Method Development, Wyatt Technology Europe.

References

Rothe, H., R. Fautz, E. Gerber, L. Neumann, K. Rettinger, W. Schuh and C. Gronewold (2011). "Special aspects of cosmetic spray safety evaluations: Principles on inhalation risk assessment." Toxicology Letters **205**(2): 97-104.

Rühli, F., M. Henneberg and U. Woitek (2008). "Variability of height, weight, and body mass index in a Swiss armed forces 2005 census." American Journal of Physical Anthropology **137**(4): 457-468.

SCENIHR (2010). "Scientific Basis for the Definition of the Term "nanomaterial"." Retrieved 12.12.2014, from http://ec.europa.eu/health/scientific_committees/emerging/docs/scenih_r_032.pdf.

Schachermeyer, S., J. Ashby, M. Kwon and W. Zhong (2012). "Impact of carrier fluid composition on recovery of nanoparticles and proteins in flow field flow fractionation." Journal of Chromatography A **1264**(0): 72-79.

Scheuch, G. and J. Heyder (1990). "Dynamic Shape Factor of Nonspherical Aerosol Particles in the Diffusion Regime." Aerosol Science and Technology **12**(2): 270-277.

Schilling, G. D., F. J. Andrade, J. H. Barnes, R. P. Sperline, M. B. Denton, C. J. Barinaga, D. W. Koppelaar and G. M. Hieftje (2007). "Continuous simultaneous detection in mass Spectrometry." Analytical Chemistry **79**(20): 7662-7668.

Schmidt, B., K. Loeschner, N. Hadrup, A. Mortensen, J. J. Sloth, C. Bender Koch and E. H. Larsen (2011). "Quantitative characterization of gold nanoparticles by field-flow fractionation coupled online with light scattering detection and inductively coupled plasma mass spectrometry." Analytical Chemistry **83**(7): 2461-2468.

Schmidt, B., J. H. Petersen, C. B. Koch, D. Plackett, N. R. Johansen, V. Katiyar and E. H. Larsen (2009). "Combining asymmetrical flow field-flow fractionation with light-scattering and inductively coupled plasma mass spectrometric detection for characterization of nanoclay used in biopolymer nanocomposites." Food Additives and Contaminants Part a-Chemistry Analysis Control Exposure & Risk Assessment **26**(12): 1619-1627.

Schneider, T., D. H. Brouwer, I. K. Koponen, K. A. Jensen, W. Fransman, B. Van Duuren-Stuurman, M. Van Tongeren and E. Tielemans (2011). "Conceptual model for assessment of inhalation exposure to manufactured nanoparticles." Journal of Exposure Science and Environmental Epidemiology **21**(5): 450-463.

References

Seipenbusch, M., A. Binder and G. Kasper (2008). "Temporal evolution of nanoparticle aerosols in workplace exposure." Annals of Occupational Hygiene **52**(8): 707-716.

Selvam, K. and M. Swaminathan (2011). "Cost effective one-pot photocatalytic synthesis of quinaldines from nitroarenes by silver loaded TiO₂." Journal of Molecular Catalysis a-Chemical **351**: 52-61.

Semmler-Behnke, M., W. G. Kreyling, H. Schulz, S. Takenaka, J. P. Butler, F. S. Henry and A. Tsuda (2012). "Nanoparticle delivery in infant lungs." Proceedings of the National Academy of Sciences of the United States of America **109**(13): 5092-5097.

Shimada, M., et al. (2009). "Development and Evaluation of an Aerosol Generation and Supplying System for Inhalation Experiments of Manufactured Nanoparticles." Environmental Science & Technology **43**(14): 5529-5534.

Skocaj, M., M. Filipic, J. Petkovic and S. Novak (2011). "Titanium dioxide in our everyday life; Is it safe?" Radiology and Oncology **45**(4): 227-247.

Soppimath, K. S., T. M. Aminabhavi, A. R. Kulkarni and W. E. Rudzinski (2001). "Biodegradable polymeric nanoparticles as drug delivery devices." Journal of Controlled Release **70**(1-2): 1-20.

Statistisches_Bundesamt (2009). "Ergebnisse des Mikrozensus 2009." Körpermaße nach Altersgruppen. Retrieved 08.12.2014, from <https://www.destatis.de/DE/ZahlenFakten/GesellschaftStaat/Gesundheit/Gesundheitszustand/RelevantesVerhalten/Tabellen/Koerpermasse.html?nn=50798>.

Sung, J. H., et al. (2008). "Lung function changes in Sprague-Dawley rats after prolonged inhalation exposure to silver nanoparticles." Inhalation Toxicology **20**(6): 567-574.

Suttiponparnit, K., J. Jiang, M. Sahu, S. Suvachittanont, T. Charinpanitkul and P. Biswas (2011). "Role of Surface Area, Primary Particle Size, and Crystal Phase on Titanium Dioxide Nanoparticle Dispersion Properties." Nanoscale Research Letters **6**(1): 1-8.

The_European_Commission (2011). 2011/696/EU - Commission recommendation of 18 October 2011 on the definition of nanomaterial, Official Journal of the European Union **L 275/38**.

Toyokuni, S. (2013). "Genotoxicity and carcinogenicity risk of carbon nanotubes." Advanced Drug Delivery Reviews **65**(15): 2098-2110.

References

Trenczek-Zajac, A., et al. (2009). "Influence of Cr on structural and optical properties of TiO₂:Cr nanopowders prepared by flame spray synthesis." Journal of Power Sources **194**(1): 104-111.

Tuoriniemi, J. and M. Hasselov (2010). "Detection of nanoparticles in the environment using field flow fractionation coupled to single particle ICP-MS." Geochimica Et Cosmochimica Acta **74**(12): A1060-A1060.

Ulrich, A. and H. Hagendorfer (2009) Final Report NanoSpray Project - Release of nanoparticles from spray products

Ulrich, A., et al. (2012). "Critical aspects of sample handling for direct nanoparticle analysis and analytical challenges using asymmetric field flow fractionation in a multi-detector approach." Journal of Analytical Atomic Spectrometry **27**(7): 1120-1130.

UNECO (2007). "Working papers of the 22nd session of the Informal group on the Particle Measurement Programme (PMP) 13 December 2007." Retrieved 12.12.2014, from <http://www.unece.org/trans/main/wp29/wp29wgs/wp29grpe/pmp22.html>.

Vernez, D., R. Bruzzi, H. Kupferschmidt, A. De-Batz, P. Droz and R. Lazor (2006). "Acute respiratory syndrome after inhalation of waterproofing sprays: A posteriori exposure-response assessment in 102 cases." Journal of occupational and environmental hygiene **3**(5): 250-261.

Von der Kammer, F., M. Baborowski, S. Tadjiki and W. Von Tumpling (2004). "Colloidal particles in sediment pore waters: Particle size distributions and associated element size distribution in anoxic and re-oxidized samples, obtained by FFF-ICP-MS coupling." Acta Hydrochimica Et Hydrobiologica **31**(4-5): 400-410.

von der Kammer, F., S. Ottofuelling and T. Hofmann (2010). "Assessment of the physico-chemical behavior of titanium dioxide nanoparticles in aquatic environments using multi-dimensional parameter testing." Environmental Pollution **158**(12): 3472-3481.

von Goetz, N., L. Fabricius, R. Glaus, V. Weitbrecht, D. Günther and K. Hungerbühler (2013). "Migration of silver from commercial plastic food containers and implications for consumer exposure assessment." Food Additives and Contaminants - Part A Chemistry, Analysis, Control, Exposure and Risk Assessment **30**(3): 612-620.

References

Wahlund, K. G. and J. C. Giddings (1987). "Properties of an asymmetrical flow field-flow fractionation channel having one permeable wall." Analytical Chemistry **59**(9): 1332-1339.

Wang, J., C. Asbach, H. Fissan, T. Hülser, T. A. J. Kuhlbusch, D. Thompson and D. Y. H. Pui (2011). "How can nanobiotechnology oversight advance science and industry: Examples from environmental, health, and safety studies of nanoparticles (nano-EHS)." Journal of Nanoparticle Research **13**(4): 1373-1387.

Wiedensohler, A. (2010). "Particle mobility size spectrometers: harmonization of technical standards and data structure to facilitate high quality long term observations of atmospheric particle number size distribution." Atmospheric Measurement Techniques Discussion **3**: 5521-5587.

Windler, L., C. Lorenz, N. Von Goetz, K. Hungerbühler, M. Amberg, M. Heuberger and B. Nowack (2012). "Release of titanium dioxide from textiles during washing." Environmental Science and Technology **46**(15): 8181-8188.

Woodrow_Wilson (2008). "Project on Emerging Nanotechnologies." Retrieved 04.10.2012, from <http://www.nanotechproject.org>.

Wu, Y., Y. Sun, H. D. Chen and X. H. Gao (2011). "Nanotechnology for topical application in cosmetic dermatology." Journal of Applied Cosmetology **29**(1): 3-15.

Xue, C. H., J. Chen, W. Yin, S. T. Jia and J. Z. Ma (2012). "Superhydrophobic conductive textiles with antibacterial property by coating fibers with silver nanoparticles." Applied Surface Science **258**(7): 2468-2472.

Yeganeh, B., C. M. Kull, M. S. Hull and L. C. Marr (2008). "Characterization of airborne particles during production of carbonaceous nanomaterials." Environmental Science and Technology **42**(12): 4600-4606.

Zhang, D. F. (2011). "Photocatalytic oxidation of organic dyes with nanostructured zinc dioxide modified with silver metals." Russian Journal of Physical Chemistry A **85**(8): 1416-1422.

Zhang, R., Y. Bai, B. Zhang, L. Chen and B. Yan (2012). "The potential health risk of titania nanoparticles." Journal of Hazardous Materials **211-212**(0): 404-413.

References

Zhu, R., W. Zhao, M. Zhai, F. Wei, Z. Cai, N. Sheng and Q. Hu (2010). "Molecularly imprinted layer-coated silica nanoparticles for selective solid-phase extraction of bisphenol A from chemical cleansing and cosmetics samples." *Analytica Chimica Acta* **658**(2): 209-216.



Curriculum Vitae

Born on 04.03.1987 in Marktredwitz, Germany

sabrina.losert@googlemail.com

EDUCATION

ETH Zürich 2011-2015

Institute for Chemical and Bioengineering

PhD student in the Safety and Environmental Technology Group/Analytical Chemistry Lab at EMPA (Swiss Federal Laboratories for Materials Science and Technology)

Technical University of Munich 2010-2011

Department of Chemistry

Master of Science in Chemistry with honors in analytical and inorganic chemistry

Technical University of Munich 2006-2010

Department of Chemistry

Bachelor of Science in Chemistry

PROFESSIONAL EXPERIENCE

Schott Rohrglas AG July/August 2006

Intern

Dispensary clinical center "Fichtelgebirge" August 2006

Intern

PUBLICATIONS

S. Losert, N. von Goetz, C. Bekker, W. Fransman, S. W.P. Wijnhoven, C. Delmaar, K. Hungerbühler, A. Ulrich, 2014, Human exposure to conventional and nanoparticle containing sprays – a critical review, *Environ.Sci.Tech.*, 48 (10) 5366-5378.

S. Losert, N. Bendixen, T. V. Ashworth, K. Hungerbühler, H. Hagendorfer, 2014, Evaluation of membrane zeta-potential and morphology on particle-membrane interaction in field-flow-fractionation analysis, *JAAS*, submitted.

S. Losert, A. Hess, G. Ilari, N. von Goetz, K. Hungerbühler, Online characterization of nano-aerosols re-released by commercial spray products using SMPS-ICPMS coupling, *J. Nanopart. Res.*, submitted.